THE

LONDON, EDINBURGH, AND DUBLIN

PHILOSOPHICAL MAGAZINE

AND

JOURNAL OF SCIENCE.

[SEVENTH SERIES.]

SEPTEMBER 1936.

XXXIII. *The Hall Effect and some other Physical Constants of Alloys.*—Part V. *The Antimony-Silver Series.*

By W. G. JOHN, *B.Sc.*, *and* Prof. E. J. EVANS, *D.Sc.*, *Physics Department, University College of Swansea* *.

THIS investigation of the physical properties of the antimony-silver system of alloys is a continuation of previous work † which has been carried out at the Physics Department of the University College of Swansea.

The present experiments were undertaken with the object of throwing further light on the structure of the alloys, which were carefully annealed down to room-temperature.

The resistivities, temperature coefficients of resistance, thermoelectric powers, densities, and the Hall coefficients of the alloys were measured, and the experimental results will be considered later in relation to the equilibrium diagrams and to the conclusions deduced from the X-ray analysis of the system.

The alloys, containing more than 40 per cent. of antimony by weight, were brittle, and great care in handling was necessary when carrying out measurements of the physical constants.

* Communicated by the Authors.

† Phil. Mag. xvi. p. 329 (1933).

The equilibrium diagram of this system of alloys was first determined by Gautier *. He found that the melting-point curve consisted of two branches, which met at the eutectic point corresponding to 55 per cent. silver by weight. Charpy † examined the alloys microscopically, and discovered the probable existence of the two compounds Ag_3Sb and Ag_4Sb.

Heycock and Neville ‡ showed that the melting-point curve consisted of three branches, and that the bends

Graph I. (A).

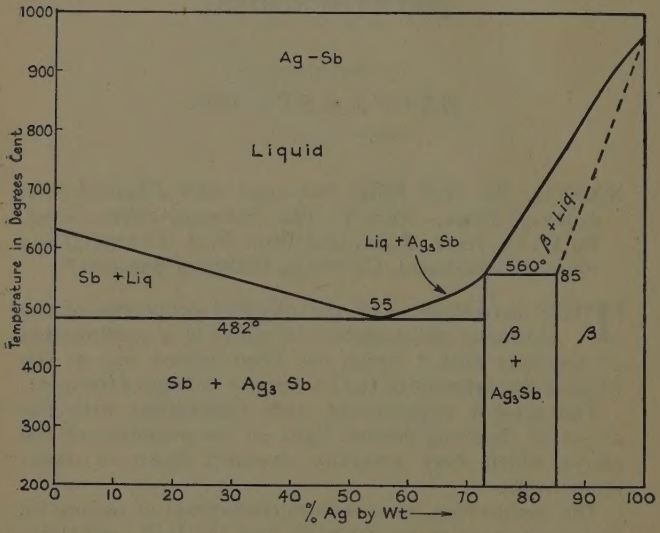

in the curve were situated at points corresponding to about 25 and 40 atoms per cent. of antimony.

In 1906 the system was again investigated by Petrenko §, who completed and confirmed the work of Heycock and Neville. The equilibrium diagram || (graph I. (A)), which is a slight modification of Petrenko's,

* (i.) Bull. Soc. d'Encour (5) i. p. 1309 (1896); (ii.) Phil. Trans. clxxxix. A, p. 37 (1897).

† 'Contributions à l'étude des alliages'; Paris, p. 149 (1901).

‡ Phil. Trans. clxxxix. A, p. 27 (1897).

§ *Zeits. Inorg. Chem.* l. p. 139 (1906).

|| International Critical Tables, ii. p. 422.

shows a solid solution of antimony in silver extending to 15 per cent. of antimony by weight. Between 15 and 27·07 per cent. antimony there exists a mixture phase of the compound Ag_3Sb and the solid solution referred to above, while the remaining compositions consist of a mixture of Ag_3Sb and antimony.

A diagram given by Guertler * agrees in the main with that due to Pentrenko. The latter, however, did not find any evidence for the 5 per cent. solid solution of silver in antimony which is indicated in Guertler's diagram.

Maey † measured the specific volumes of the alloys, and came to the conclusion that there was only one compound, Ag_3Sb, in the silver-antimony system.

More recently Raeder ‡ investigated the system by measuring the hydrogen overvoltage of the alloys, and Westgren, Hägg, and Eriksson § studied the crystal structure of the system by means of X-rays.

The positions of the phase boundaries as determined by Raeder are in good agreement with the results of the crystal structure investigation. According to the X-ray analysis there are three homogeneous phases, α, ϵ, and ϵ', as shown in graph I. (B).

The α phase has a face-centred cubic structure and extends from the silver end of the series to the composition corresponding to 94·47 per cent. silver by weight. The ϵ phase has a close-packed hexagonal structure and extends from 89·0 per cent. silver to 82·5 per cent. silver, while the ϵ' phase, having a slightly deformed close-packed hexagonal or more probably a rhombohedral structure, extends from 78·2 per cent. silver to the compound Ag_3Sb at the composition 72·93 per cent. silver. Between the α and ϵ and the ϵ and ϵ' phases occur the $\alpha+\epsilon$ and the $\epsilon+\epsilon'$ mixture phases, and between 100 per cent. antimony and the ϵ' phase there is a mixture phase of antimony $+\epsilon'$.

Dupuy ‖ measured the magnetic susceptibilities of the alloys and Haken ¶ determined their thermoelectric

* 'Metallographie,' B. D. 1. t. 1, p. 769.
† *Zeit. Phys. Chem.* l. p. 203 (1905).
‡ (i.) *Zeit. f. Phys. Chem.* cxxxiii. p. 15 (1928); (ii.) *Zeit. f. Phys. Chem.* 6 Abt. B. 1, pp. 40–42 (Nov. 1929).
§ *Zeit. f. Phys. Chem.* (B) iv. p. 453 (1929).
‖ *Rev. de Met.* p. 651 (Août 1915).
¶ *Ann. der Physik*, (4) xxxii. p. 325 (1910).

powers and electrical conductivities. Both observers found evidence for the existence of the compound Ag_3Sb, a solid solution of 15 per cent. by weight of antimony in silver, and a solid solution of 5 per cent. by weight of silver in antimony.

Later E. von Aubel * redetermined the thermoelectric powers of the alloys, and found no evidence for the existence of a solid solution at the antimony end of the series.

Graph I. (B).

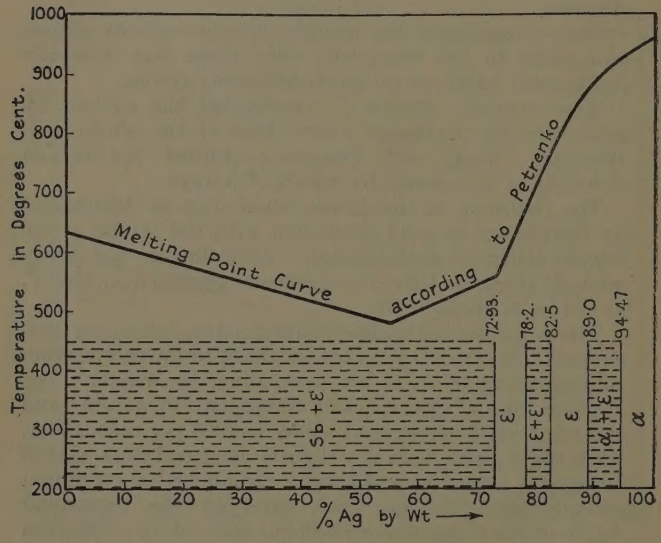

Preparation and Annealing of the Alloys.

Silver and antimony alloy in all proportions and satisfactory plates of the alloys can be readily prepared if care be taken to avoid oxidation and the formation of blow holes.

The pure metals were weighed out in the required proportions and placed in a salamander crucible. The metals were then covered with a layer of carbon to prevent

* Bull. Sci. Acad. Roy. Belg. (5) xii. pp. 559–570 (1926).

oxidation as far as possible, and the crucible was heated in an electric furnace. When molten the alloy was well stirred with a graphite rod and allowed to cool. On remelting the alloy was cast into an iron mould which had been treated with graphite. For alloys of composition ranging from 0 to 70 per cent. silver it was found satisfactory to cast the plates from a melt whose temperature did not exceed that of the melting-point of the particular alloy by too great a margin. Unless this precaution was taken blowholes were liable to form in the plates.

For the high percentage antimony alloys the plates were chill cast, but for the silver rich ones the mould was heated to a white heat in a special heater.

When cold the plates were trimmed and the surfaces and edges polished. The length, breadth, and thickness of the plates were approximately 12 cm., 2·3 cm., and ·25 cm. respectively. The variation in thickness over any plate did not exceed 0·3 per cent. and the variation in breadth did not exceed 0·2 per cent.

After preparation the resistivity of each alloy was measured at the temperature of melting ice. All the plates were then subjected to a process of annealing in a vacuum electric furnace.

The complete series of alloys was annealed in two batches. Those alloys of composition ranging from 0 to 70 per cent. silver were annealed at 450° C., and all the others were in the first place annealed at 550° C. At the end of a fortnight the furnace was cooled down slowly to room-temperature and the resistivities of the alloys at the temperature of melting ice were remeasured.

This process was continued until further annealing produced no change in the resistivity. The temperature of the annealing furnace was then reduced by steps of approximately 100° C. to room-temperature, and at each stage the annealing was continued until the resistivity was constant.

The whole period of annealing in the case of each alloy occupied about six weeks. When the physical constants of the alloys had been measured it was decided to reanneal four alloys containing 92·07, 94·6, 96·4, and 98 per cent. of silver at higher temperatures. These plates had not been fully annealed at the lower temperature, and the effect of further annealing on the values of the various physical constants will be discussed later.

Analysis of the Alloys.

In order to estimate accurately the concentration of silver in a plate a sample of the alloy was dissolved in nitric acid. The silver nitrate formed was titrated with potassium thiocyanate in the presence of ferric sulphate. The thiocyanate precipitated white silver thiocyanate from the solution, the end of the reaction being indicated by a red coloration. The potassium thiocyanate of approximately decinormal strength had been previously standardized with a silver nitrate solution of known strength.

TABLE I.

Percentage Composition by Weight of Alloys.

Silver.	Antimony.	Silver.	Antimony.
0	100	72·70	27·30
2·25	97·75	72·96	27·04
4·43	95·57	74·85	25·15
5·00	95·00	78·20	21·80
8·03	91·97	80·77	19·23
13·78	86·22	81·90	18·10
17·32	82·68	85·00	15·00
31·70	68·30	88·08	11·92
50·07	49·93	89·20	10·80
55·03	44·97	92·07	7·93
65·38	34·62	94·60	5·40
70·74	29·26	96·40	3·60
72·00	28·00	98·00	2·00
72·50	27·50	100	0

Samples of the alloys were taken from each end of the plates, and it was found that the composition of the plates was uniform as far as could be detected by the analysis. It is estimated that the error in the analysis is on the average not greater than 0·2 per cent. The percentage composition by weight of the various alloys is given in Table I.

Measurement of the Physical Constants.

In a previous communication * the methods employed in the determination of the Hall coefficients and the other physical constants of the alloys have been discussed in detail, and here it is only necessary to give a brief account of the measurements undertaken.

* Phil. Mag. xvi. *loc. cit.*

Resistivity.

The resistivity of each alloy was measured at 0° C., and the experimental results are given in Table II. and graph II. It is estimated that the error of measurement is on the average not greater than 0·3 per cent.

TABLE II.

Composition by weight of Ag.	Resistivities at 0° C. in microhms per cm.³.	
	Before annealing.	After annealing.
Per cent.		
0	37·09	36·12
2·25	45·27	36·27
4·43	41·37	37·47
5·00	41·80	38·10
8·03	42·47	38·72
13·78	43·36	41·31
17·32	46·46	43·47
31·70	56·58	57·02
50·07	77·30	78·07
55·03	80·13	86·37
65·38	95·33	101·80
70·74	117·50	122·7
72·00	135·00	138·0
72·50	130·70	163·0
72·70	177·2	177·2
72·96	166·5	179·5
74·85	165·5	154·0
78·20	142·6	135·7
80·77	129·2	128·3
81·90	104·4	116·9
85·00	89·44	88·60
88·08	76·60	79·40
89·20	68·71	76·00
92·07	63·60	51·21
94·60	30·72	23·17
96·40	21·62	15·74
98·00	20·90	12·81
100·00	1·49	1·51

Temperature Coefficient of Resistance.

The mean temperature coefficient of resistance of each alloy was determined over the temperature range 0–100° C., and the values are given in Table III. and plotted in graph III. The estimated experimental error is not greater than $\frac{1}{2}$ per cent.

Graph II.

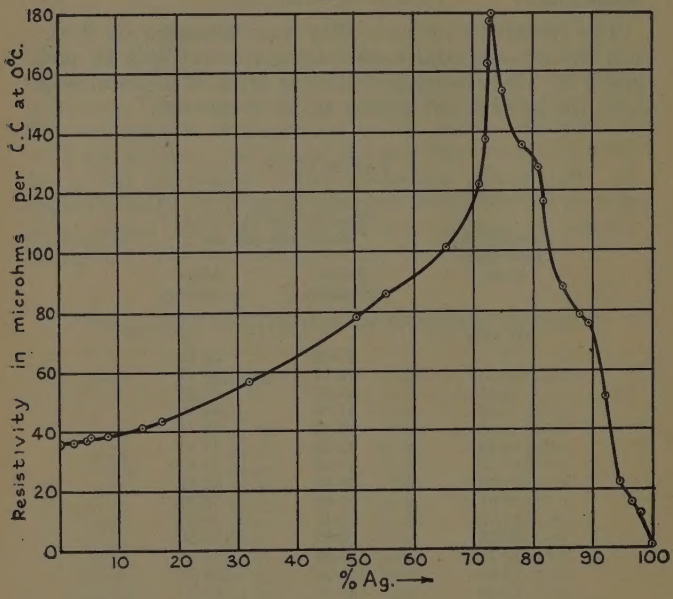

TABLE III.

Composition by weight of Ag.	Mean temperature coefficient of resistance between 0° and 100° C. × 10⁴.	Composition by weight of Ag.	Mean temperature coefficient of resistance between 0° and 100° C. × 10⁴.
Per cent.		Per cent.	
0	51·5	72·70	2·44
2·25	51·01	72·96	1·70
4·43	50·18	74·85	·74
5·00	50·0	78·20	·408
8·03	48·1	80·77	1·91
13·78	47·18	81·90	2·68
17·32	44·60	85·00	2·70
31·70	35·3	88·08	2·78
50·07	23·15	89·20	2·82
55·03	18·02	92·07	4·83
65·38	13·00	94·60	11·03
70·74	7·69	96·40	13·55
72·00	5·01	98·00	15·29
72·50	3·44	100·00	40·50

Graph III.

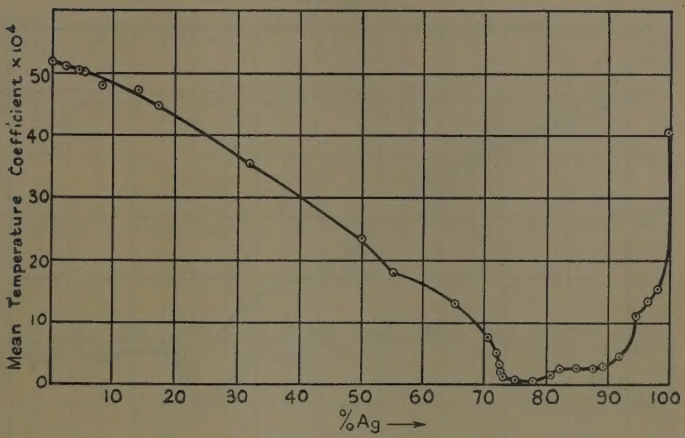

Thermoelectric Power.

The mean thermoelectric power of each alloy with respect to a plate of pure electrolytic copper was determined over the range 0–100° C., and the results are shown in Table IV. and plotted in graph IV. The experimental error is estimated to be on the average not greater than 0·4 per cent.

TABLE IV.

Composition by weight of Ag.	Thermoelectric power with reference to copper in microvolts per degree C.	Composition by weight of Ag.	Thermoelectric power with reference to copper in microvolts per degree C.
Per cent.		Per cent.	
0	+38·41	72·70	−2·55
2·25	+38·13	72·96	−1·99
4·43	+37·00	74·85	−1·68
5·00	+36·50	78·20	−1·49
8·03	+35·68	80·77	−1·77
13·78	+33·78	81·90	−1·92
17·32	+32·83	85·00	−2·56
31·70	+25·61	88·08	−2·41
50·07	+10·44	89·20	−2·41
55·03	+ 9·94	92·07	−2·49
65·38	+ 2·46	94·60	−2·57
70·74	− 5·25	96·40	−2·53
72·00	− 6·31	98·00	−2·34
72·50	− 4·25	100·00	− ·29

Graph IV.

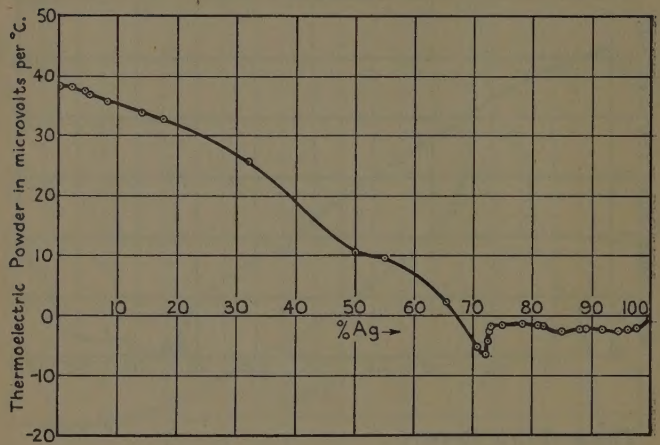

Density.

The densities are given in Table V. and plotted in graph V. The density determinations are estimated to be accurate to within 0·1 per cent.

TABLE V.

Composition by weight of Ag.	Density in grams per c.c. at 18° C.	Composition by weight of Ag.	Density in grams per c.c. at 18° C.
Per cent.		Per cent.	
0	6·68	72·70	9·69
2·25	6·72	72·96	9·70
4·43	6·81	74·85	9·80
5·00	6·83	78·20	9·87
8·03	6·90	80·77	9·88
13·78	7·10	81·90	9·89
17·32	7·23	85·00	9·96
31·70	7·82	88·08	10·01
50·07	8·63	89·20	10·02
55·03	8·72	92·07	10·10
65·38	9·24	94·60	10·24
70·74	9·46	96·40	10·31
72·00	9·63	98·00	10·33
72·50	9·66	100·00	10·49

Graph V.

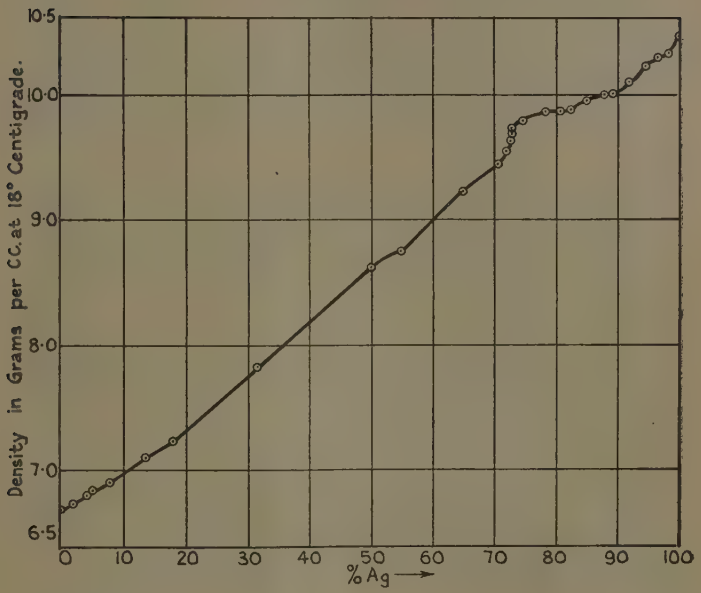

Hall Effect.

The Hall coefficient of each alloy was measured for six different field strengths of magnitudes 3089, 4641, 5797, 6740, 7535, and 8346 gauss. The Hall coefficient of antimony has a large positive value, whilst that of silver has a comparatively small negative value. For the antimony rich alloys the determinations are considered to be accurate to within 0·5 per cent., as the Hall E.M.F. deflexions are large, and the error is due to inaccuracy in the measurements of the magnetic field. At the silver end of the series the deflexions are much smaller and the accuracy of the values is less. The value of the Hall coefficient in the case of pure silver is in good agreement with that obtained by Zahn *.

The experimental results are given in Table VI. and plotted in graphs VI., VII, and VIII. Graphs VI. and VII.

* Campbell, 'Galvanomagnetic and Thermomagnetic Effects,' p. 124.

Table VI.

Composition by weight of Ag.	Hall coefficients in absolute units. (Magnetic fields in gauss.) 3089.	4641.	5797.	6740.	7535.	8346.	Temp. in °C.
Per cent.							
0	$2{\cdot}26 \times 10^{-1}$	$2{\cdot}24 \times 10^{-1}$	$2{\cdot}22 \times 10^{-1}$	$2{\cdot}22 \times 10^{-1}$	$2{\cdot}15 \times 10^{-1}$	$2{\cdot}14 \times 10^{-1}$	15
2·25	$2{\cdot}25 \times 10^{-1}$	$2{\cdot}22 \times 10^{-1}$	$2{\cdot}21 \times 10^{-1}$	$2{\cdot}19 \times 10^{-1}$	$2{\cdot}18 \times 10^{-1}$	$2{\cdot}13 \times 10^{-1}$	15
4·43	$2{\cdot}21 \times 10^{-1}$	$2{\cdot}21 \times 10^{-1}$	$2{\cdot}20 \times 10^{-1}$	$2{\cdot}17 \times 10^{-1}$	$2{\cdot}15 \times 10^{-1}$	$2{\cdot}12 \times 10^{-1}$	13
5·00	$2{\cdot}196 \times 10^{-1}$	$2{\cdot}192 \times 10^{-1}$	$2{\cdot}19 \times 10^{-1}$	$2{\cdot}16 \times 10^{-1}$	$2{\cdot}12 \times 10^{-1}$	$2{\cdot}11 \times 10^{-1}$	16
8·03	$2{\cdot}19 \times 10^{-1}$	$2{\cdot}18 \times 10^{-1}$	$2{\cdot}18 \times 10^{-1}$	$2{\cdot}15 \times 10^{-1}$	$2{\cdot}13 \times 10^{-1}$	$2{\cdot}10 \times 10^{-1}$	14
13·78	$2{\cdot}19 \times 10^{-1}$	$2{\cdot}16 \times 10^{-1}$	$2{\cdot}15 \times 10^{-1}$	$2{\cdot}13 \times 10^{-1}$	$2{\cdot}11 \times 10^{-1}$	$2{\cdot}09 \times 10^{-1}$	13
17·32	$2{\cdot}18 \times 10^{-1}$	$2{\cdot}15 \times 10^{-1}$	$2{\cdot}13 \times 10^{-1}$	$2{\cdot}11 \times 10^{-1}$	$2{\cdot}10 \times 10^{-1}$	$2{\cdot}08 \times 10^{-1}$	16
31·70	$2{\cdot}08 \times 10^{-1}$	$2{\cdot}04 \times 10^{-1}$	$2{\cdot}03 \times 10^{-1}$	$2{\cdot}02 \times 10^{-1}$	$2{\cdot}02 \times 10^{-1}$	$1{\cdot}99 \times 10^{-1}$	16·5
50·07	$1{\cdot}69 \times 10^{-1}$	$1{\cdot}66 \times 10^{-1}$	$1{\cdot}64 \times 10^{-1}$	$1{\cdot}63 \times 10^{-1}$	$1{\cdot}63 \times 10^{-1}$	$1{\cdot}62 \times 10^{-1}$	17
55·03	$1{\cdot}56 \times 10^{-1}$	$1{\cdot}55 \times 10^{-1}$	$1{\cdot}54 \times 10^{-1}$	$1{\cdot}53 \times 10^{-1}$	$1{\cdot}53 \times 10^{-1}$	$1{\cdot}51 \times 10^{-1}$	18·5
65·38	$\cdot 809 \times 10^{-1}$	$\cdot 807 \times 10^{-1}$	$\cdot 804 \times 10^{-1}$	$\cdot 803 \times 10^{-1}$	$\cdot 801 \times 10^{-1}$	$\cdot 793 \times 10^{-1}$	18
70·74	$-11{\cdot}97 \times 10^{-4}$	$-12{\cdot}13 \times 10^{-4}$	$-12{\cdot}11 \times 10^{-4}$	$-12{\cdot}09 \times 10^{-4}$	$-12{\cdot}10 \times 10^{-4}$	$-12{\cdot}23 \times 10^{-4}$	16·5
72·00	$-133{\cdot}6 \times 10^{-4}$	$-133{\cdot}4 \times 10^{-4}$	$-134{\cdot}0 \times 10^{-4}$	$-133{\cdot}9 \times 10^{-4}$	$-134{\cdot}8 \times 10^{-4}$	$-134{\cdot}1 \times 10^{-4}$	15
72·50	$-64{\cdot}1 \times 10^{-4}$	$-64{\cdot}1 \times 10^{-4}$	$-64{\cdot}5 \times 10^{-4}$	$-63{\cdot}9 \times 10^{-4}$	$-64{\cdot}2 \times 10^{-4}$	$-63{\cdot}9 \times 10^{-4}$	17
72·70	$-14{\cdot}36 \times 10^{-4}$	$-14{\cdot}37 \times 10^{-4}$	$-14{\cdot}30 \times 10^{-4}$	$-14{\cdot}44 \times 10^{-4}$	$-14{\cdot}38 \times 10^{-4}$	$-14{\cdot}50 \times 10^{-4}$	16
72·96	$-9{\cdot}89 \times 10^{-4}$	$-9{\cdot}84 \times 10^{-4}$	$-9{\cdot}83 \times 10^{-4}$	$-9{\cdot}79 \times 10^{-4}$	$-9{\cdot}75 \times 10^{-4}$	$-9{\cdot}77 \times 10^{-4}$	15
74·85	$-7{\cdot}31 \times 10^{-4}$	$-7{\cdot}29 \times 10^{-4}$	$-7{\cdot}33 \times 10^{-4}$	$-7{\cdot}33 \times 10^{-4}$	$-7{\cdot}31 \times 10^{-4}$	$-7{\cdot}30 \times 10^{-4}$	17
78·20	$-5{\cdot}86 \times 10^{-4}$	$-6{\cdot}10 \times 10^{-4}$	$-5{\cdot}91 \times 10^{-4}$	$-5{\cdot}92 \times 10^{-4}$	$-5{\cdot}88 \times 10^{-4}$	$-5{\cdot}85 \times 10^{-4}$	16·5
80·77	$-7{\cdot}03 \times 10^{-4}$	$-6{\cdot}94 \times 10^{-4}$	$-7{\cdot}10 \times 10^{-4}$	$-6{\cdot}93 \times 10^{-4}$	$-6{\cdot}98 \times 10^{-4}$	$-6{\cdot}95 \times 10^{-4}$	17
81·90	$-9{\cdot}02 \times 10^{-4}$	$-8{\cdot}97 \times 10^{-4}$	$-9{\cdot}03 \times 10^{-4}$	$-9{\cdot}06 \times 10^{-4}$	$-8{\cdot}86 \times 10^{-4}$	$-8{\cdot}99 \times 10^{-4}$	18
85·00	$-9{\cdot}10 \times 10^{-4}$	$-9{\cdot}03 \times 10^{-4}$	$-8{\cdot}96 \times 10^{-4}$	$-8{\cdot}89 \times 10^{-4}$	$-8{\cdot}96 \times 10^{-4}$	$-8{\cdot}86 \times 10^{-4}$	17
88·08	$-8{\cdot}79 \times 10^{-4}$	$-8{\cdot}72 \times 10^{-4}$	$-8{\cdot}70 \times 10^{-4}$	$-8{\cdot}80 \times 10^{-4}$	$-8{\cdot}82 \times 10^{-4}$	$-8{\cdot}80 \times 10^{-4}$	16·5
89·20	$-8{\cdot}70 \times 10^{-4}$	$-8{\cdot}64 \times 10^{-4}$	$-8{\cdot}69 \times 10^{-4}$	$-8{\cdot}64 \times 10^{-4}$	$-8{\cdot}64 \times 10^{-4}$	$-8{\cdot}56 \times 10^{-4}$	16·5
92·07	$-10{\cdot}01 \times 10^{-4}$	$-10{\cdot}09 \times 10^{-4}$	$-10{\cdot}11 \times 10^{-4}$	$-10{\cdot}15 \times 10^{-4}$	$-10{\cdot}09 \times 10^{-4}$	$-10{\cdot}21 \times 10^{-4}$	17
94·60	$-19{\cdot}90 \times 10^{-4}$	$-19{\cdot}73 \times 10^{-4}$	$-19{\cdot}72 \times 10^{-4}$	$-19{\cdot}78 \times 10^{-4}$	$-19{\cdot}83 \times 10^{-4}$	$-19{\cdot}78 \times 10^{-4}$	18·5
96·40	$-18{\cdot}67 \times 10^{-4}$	$-18{\cdot}87 \times 10^{-4}$	$-18{\cdot}77 \times 10^{-4}$	$-18{\cdot}75 \times 10^{-4}$	$-18{\cdot}66 \times 10^{-4}$	$-18{\cdot}61 \times 10^{-4}$	18·0
98·00	$-17{\cdot}93 \times 10^{-4}$	$-18{\cdot}08 \times 10^{-4}$	$-18{\cdot}08 \times 10^{-4}$	$-18{\cdot}18 \times 10^{-4}$	$-18{\cdot}16 \times 10^{-4}$	$-17{\cdot}95 \times 10^{-4}$	18·6
100·00	$-8{\cdot}97 \times 10^{-4}$	$-8{\cdot}98 \times 10^{-4}$	$-8{\cdot}93 \times 10^{-4}$	$-8{\cdot}91 \times 10^{-4}$	$-8{\cdot}85 \times 10^{-4}$	$-8{\cdot}89 \times 10^{-4}$	16

Graph VI.

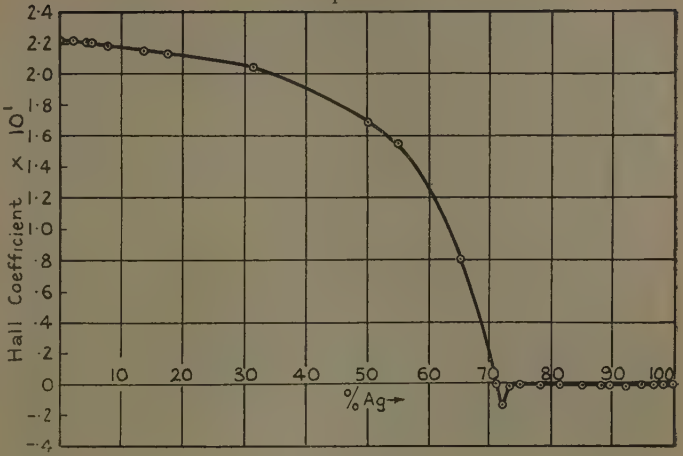

Graph VII.

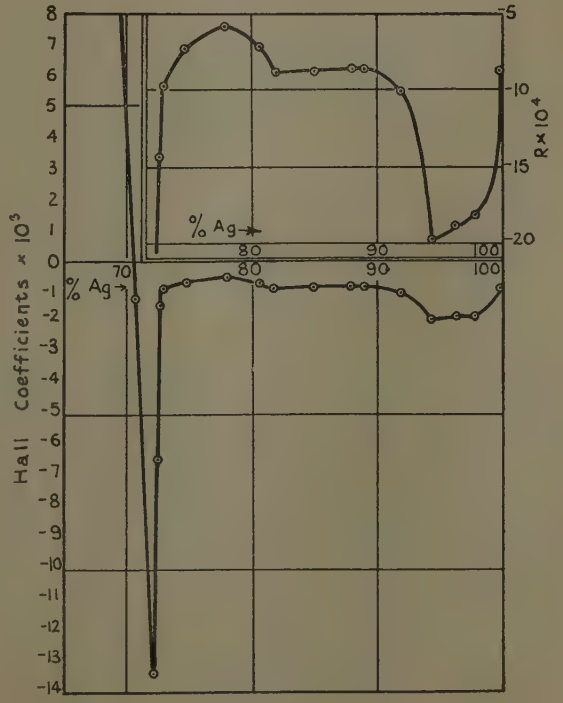

show the variation of the Hall coefficient with composition for a field of 5797 gauss. In graph VII. the variation of the Hall coefficient with composition at the silver end of the series is represented on a larger scale. Graph VIII. gives the variation of the Hall E.M.F. for alloys of definite compositions with field strength.

Graph VIII.

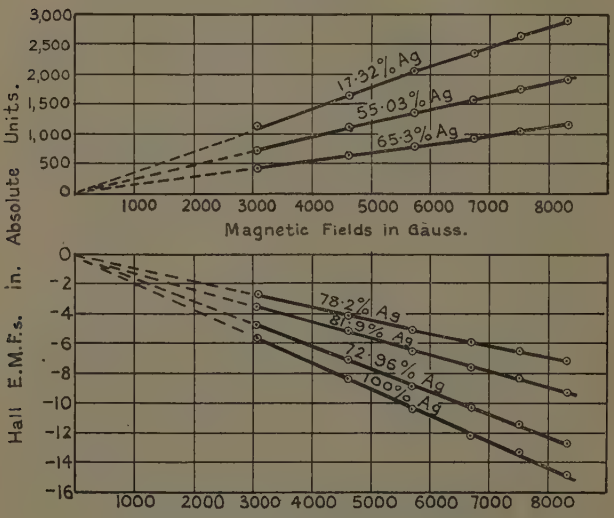

Discussion.

It is seen from graph I. (B), which represents the results obtained by Raeder * and by Westgren †, Hägg, and Eriksson, that the most interesting portion of the equilibrium diagram is to be found at the silver end of the series. Between the alloy containing about 73 per cent. silver and the silver end of the series five different phases have been identified by the above investigators. According to their work only one phase, a mixture phase of Sb and Ag_3Sb, exists in the region extending from 0 to 72·93 per cent. silver.

* Raeder, *loc. cit.*
† Westgren, Hägg, and Eriksson, *loc. cit.*

The positions of the phase boundaries are indicated on a curve giving the variation of a physical property with composition by changes of slope at various points of the curve.

The variation of the specific resistance with composition is given in graph II. As the concentration of silver in the alloy increases the curve rises gradually at first, then much more rapidly in the neighbourhood of the composition 70 per cent silver, and reaches a maximum at 72·9 per cent. silver. This composition marks the boundary between the $Sb+\epsilon'$ and ϵ' phases, and corresponds to the compound Ag_3Sb. The resistivity curve then descends rapidly until the silver end of the series is reached. The descending portion of the curve shows changes of slope in the neighbourhood of the compositions 78, 82, 89, and 94·6 per cent. by weight of silver. These compositions correspond to the boundaries between the ϵ' and $\epsilon'+\epsilon$, the $\epsilon'+\epsilon$ and ϵ, the ϵ and $\epsilon+\alpha$, and the $\epsilon+\alpha$ and α phases respectively.

The resistivity experiments show that the solid solution at the silver end of the series extends to 94·47 per cent. silver, and not to 85 per cent. silver as stated by some earlier observers. The effect of annealing on the resistivity of the alloys (Table II.) is rather irregular and depends on the conditions of casting.

The variation of the temperature coefficient of resistance with composition is given in graph III. This curve again indicates that only a 5·5 per cent. solid solution of antimony in silver exists at the silver end of the series. The various phase boundaries are also indicated on this graph. In all phases, with the exception of the ϵ' and ϵ phases, a decrease of temperature coefficient corresponds to an increase in resistivity. In the ϵ' phase a slight decrease in temperature coefficient with increasing silver content accompanies a considerable decrease in resistivity, and in the ϵ phase the temperature coefficient remains sensibly constant whilst the resistivity falls rapidly.

At the composition corresponding to 55·03 per cent. silver a slight discontinuity occurs in the temperature coefficient composition curve. A similar discontinuity appears in the other curves at this composition, which corresponds to the eutectic point as given by Petrenko.

The densities of the various alloys are situated on a curve which lies in the neighbourhood of the straight

line joining the densities of antimony and silver. The greatest deviation from this straight line is found in the region between 70 and 80 per cent. silver. The density composition curve (graph V.) shows slight changes of slope at the phase boundaries. The density of the compound Ag_3Sb, calculated from the dimensions of the lattice, is in good agreement with the value given in the graph.

The variation of the thermoelectric power of the alloys with composition is shown in graph IV. On adding silver to antimony the thermoelectric power falls until it reaches a zero value at the composition corresponding to about 67 per cent. silver, and after crossing the concentration axis attains a negative maximum at 72 per cent. silver. From this point the curve rises fairly rapidly until the composition corresponding to the compound Ag_3Sb (72·93 per cent. Ag) is reached. From this composition to pure silver at the end of the series the curve remains on the negative side of the concentration axis, and shows slight changes of slope at points near the phase boundaries, except possibly at the point corresponding to the end of the solid solution of antimony in silver.

In its general form the curve agrees with that obtained by Haken *, who also found that the negative maximum occurred at 72 per cent. silver and not at the phase boundary corresponding to the compound Ag_3Sb. There is, however, a change of slope in the curve at this point also.

There is a marked similarity between the curve connecting thermoelectric power with composition and that showing the relation between the Hall coefficient and composition. This relation has been plotted in graph VI., and on a much larger scale in graph VII. The Hall coefficient of antimony, which has a high positive value, decreases with the addition of silver, and finally reaches a negative maximum value at the composition corresponding to 72 per cent. silver. The curve then rises until the composition corresponding to the compound Ag_3Sb is reached, and from this point to the silver end of the series it remains below the concentration axis, showing variations in slope (graph VII.) at points corresponding to the phase boundaries.

* Haken, *loc. cit.*

Graph VIII. shows the variation of the Hall E.M.F. with magnetic field strength for alloys of different compositions. In the case of alloys containing over 65 per cent. of silver the curve connecting the E.M.F. with field strength is sensibly linear and the Hall coefficient is practically independent of field strength.

Pure antimony and the other alloys containing from 0 to 55 per cent. silver show a diminution in the value of the Hall coefficient with increasing field strength. In this connexion it is interesting to note that the rapid fall in the Hall coefficient as the concentration of silver is increased commences in the neighbourhood of the composition corresponding to 55 per cent. silver.

It was stated early in this paper that certain alloys near the silver end of the series after being initially annealed at 550° C. for a period of six weeks were finally annealed at higher temperatures. It was considered possible that the rate of annealing at 550° C. was too slow to bring the alloys to their equilibrium state even in six weeks.

The alloys containing 96·4 and 98 per cent. silver were then annealed at 800° C. for several hours, and afterwards cooled down slowly to room-temperature. Their resistivities at 0° C. were then measured. The process of annealing at 800° C. was then continued until the resistivities at 0° C. remained constant.

The two alloys were then annealed down to room-temperature by stages, and it was found that their resistivities at 0° C. did not change.

Similar treatment was also given to the plates containing 92·07 and 94·6 per cent. silver, but in this case the highest annealing temperature was 650° C. The comparatively large effect of the second annealing on the values of the physical constants is shown in Table VII. It is seen from the table that the resistivities and the thermoelectric powers decreased, whilst the temperature coefficients of resistance and the Hall coefficients increased.

The results of this investigation strongly support the conclusions deduced by Raeder * from his hydrogen overvoltage experiments, and by Westgren †, Hägg, and Eriksson from the X-ray crystal analysis of the system.

* Raeder, *loc. cit.*
† Westgren, Hägg, and Eriksson, *loc. cit.*

TABLE VII.

Composition by weight of silver.	Resistivity at 0° C. in microhms per cm.³ after initial annealing at 550° C.	Resistivity at 0° C. in microhms per cm.³ after final annealing at higher temperatures.
92·07	65·8	51·21
94·60	33·4	23·17
96·40	27·3	15·74
98·0	22·9	12·81

Composition by weight of silver.	Temperature coefficient of resistance between 0° and 100° C. $\times 10^4$ after initial annealing at 550° C.	Temperature coefficient of resistance between 0° and 100° C. $\times 10^4$ after final annealing at higher temperatures.
92·07	3·30	4·83
94·60	3·51	11·03
96·40	6·95	13·55
98·0	9·30	15·29

Composition by weight of silver.	Thermoelectric power in microvolts per degree with respect to copper after initial annealing at 550° C.	Thermoelectric power in microvolts per degree with respect to copper after final annealing at higher temperatures.
92·07	−2·49	−2·49
94·60	−3·26	−2·57
96·40	−3·30	−2·53
98·0	−3·39	−2·34

Composition by weight of silver.	Hall coefficient in absolute units after initial annealing at 550° C.	Hall coefficient in absolute units after final annealing at higher temperatures.
92·07	$-10{\cdot}14\times10^{-4}$	$-10{\cdot}11\times10^{-4}$
94·60	$-12{\cdot}62\times10^{-4}$	$-19{\cdot}72\times10^{-4}$
96·40	$-11{\cdot}14\times10^{-4}$	$-18{\cdot}77\times10^{-4}$
98·0	$-\ 9{\cdot}44\times10^{-4}$	$-18{\cdot}08\times10^{-4}$

The present experiments show no indication of a solid solution at the antimony end of the series. Evidence for this solid solution has been given by Haken *, who measured the thermoelectric powers of the alloys, and by Dupuy †, who determined their magnetic susceptibilities.

The X-ray analysis of the system shows no indication of a phase change at 72 per cent. silver, the concentration at which sharp negative maxima occur in the thermoelectric power composition, and the Hall coefficient composition curves. There may possibly be a slight solid solution of antimony in Ag_3Sb, but the other physical properties, with the possible exception of the density, give no definite indication of it.

February 1936.

XXXIV. *The Magnetic Susceptibilities of the Silver-Lead, Silver-Antimony, and the Silver-Bismuth Series of Alloys.* *By* G. O. Stephens, *Ph.D.*, *and* Prof. E. J. Evans, *D.Sc.*, *Physics Department, University College of Swansea* ‡.

THE variation in the physical properties of a system of alloys with composition is intimately connected with changes in the crystalline structure of the alloys. At phase boundaries or at compositions corresponding to intermetallic compounds, sudden changes occur in the magnitude of the particular physical property under investigation. It therefore follows that measurements of the variation of any physical property of a system of alloys with composition may yield valuable information concerning the equilibrium diagram of the system.

It was with this end in view that the present investigation of the magnetic susceptibilities of the silver-lead, silver-antimony, and the silver-bismuth systems was undertaken.

The alloys belonging to each system were prepared from the purest metals available, and the values obtained

* Haken, *loc. cit.*
† Dupuy, *loc. cit.*
‡ Communicated by the Authors.

for the mass susceptibilities of silver, lead, antimony, and bismuth are in reasonably good agreement with those determined by other observers.

In all cases the alloys were prepared by melting the constituent metals under a layer of powdered wood charcoal to prevent oxidation as far as possible. The molten alloys were thoroughly stirred to ensure uniformity of composition before being cast into small cylindrical rods.

The estimation of the silver in the silver-antimony and the silver-bismuth alloys was carried out by the thiocyanate method. Several of the silver-lead alloys were analysed by cupellation, and as the percentages of the metals in the alloys were in close approximation to those calculated from the weights of the metals used in their preparation, the percentages of lead and silver in the remaining alloys were calculated from the proportions weighed out.

All the alloys were carefully annealed *in vacuo* at temperatures deduced from the equilibrium diagrams. The alloys of higher melting-points were annealed in sealed evacuated quartz tubes, whilst those of lower melting-points were annealed in sealed evacuated Pyrex tubes. The silver-lead alloys were annealed in stages from 250° C. to room-temperature. Most of the silver-antimony alloys were annealed from 450° C. to room-temperature, but alloys near the silver end of the series were annealed initially at higher temperatures. The highest annealing temperature employed in the case of these alloys was 780° C. The silver-bismuth alloys were annealed from 250° C. down to room-temperature.

The measurements were carried out by means of the Curie-Chéneveau magnetic balance [1], and a comparison method was employed. It has been found [2] that, with suitable precautions, the balance will yield accurate relative measurements of magnetic susceptibility.

The cylindrical specimen of an alloy was placed in a glass tube attached to one end of the torsion arm, which was suspended by a fine phosphor bronze wire. The specimen tube was always hung in exactly the same position, which was practically mid-way between the poles of the permanent circular magnet of the balance. As the permanent magnet was rotated about a vertical axis the force exerted on the specimen varied, and the

deflexion of the torsion arm reached a maximum value in one direction, followed by a maximum in the other direction. These maximum deflexions were measured by a lamp, mirror, and scale, in the usual manner. Similar experiments were then carried out with the tube containing water of the same volume as the alloy. Finally, the maximum deflexions due to the empty tube were measured. From these measurements, knowing the mass susceptibility ($K = -0{\cdot}72 \times 10^{-6}$) of the pure water [3], which was the standard substance employed in these experiments, it is possible to determine the mass susceptibilities of all the alloys.

All the observations were carried out at room-temperature, which varied between 16° C. and 19° C. As all the metals and alloys examined in this investigation were diamagnetic, the exact value of the room-temperature was not recorded.

TABLE I.

The Silver-Lead Alloys.

Percentage of silver by weight.	Density in grams/c.c. at 18° C.	Mass susceptibility $\times 10^6$. Average temperature = 17° C.
0·00 (100 % Pb)	11·34	−0·118
6·30	11·26	−0·125
10·00	11·22	−0·128
17·40	11·16	−0·132
28·00	11·11	−0·140
36·25	11·00	−0·148
44·00	10·93	−0·153
49·00	10·91	−0·159
53·20	10·89	−0·160
70·19	10·77	−0·172
76·00	10·65	−0·178
90·00	10·56	−0·189
100·00	10·49	−0·197

Experimental Results.

The experimental results for the three systems of alloys are given in the accompanying tables. These tables give the densities of the alloys in addition to their mass susceptibilities. The densities of the Ag–Pb, Ag–Sb, and Ag–Bi alloys are plotted in graphs I., II., and III. respectively, and their mass susceptibilities in graphs IV., V., and VI.

TABLE II.

The Silver-Antimony Alloys.

Percentage of silver by weight.	Density in grams/c.c. at 18° C.	Mass susceptibility × 10^6. Average temperature = 18·0° C.	
		Before annealing.	After annealing.
0·00 (100 % Sb)	6·68	−0·950	−0·950
25·00	7·54	−0·722	−0·761
40·00	8·20	−0·599	−0·612
50·00	8·58	−0·519	−0·541
55·00	8·77	−0·491	−0·499
65·00	9·27	−0·404	−0·401
67·60	9·35	−0·376	−0·367
70·00	9·61	−0·310	−0·310
71·50	9·69	−0·305	−0·305
72·90	9·73	−0·279	−0·291
76·39	9·80	−0·253	−0·212
78·30	9·90	−0·246	−0·206
80·89	9·91	−0·251	−0·241
82·50	9·93	−0·266	−0·259
84·71	9·98	−0·250	−0·234
88·90	10·03	−0·229	−0·252
91·00	10·04	−0·216	−0·240
94·49	10·32	−0·153	−0·187
96·90	10·38	−0·184	−0·211
100·00	10·49	−0·197	−0·197

TABLE III.

The Silver-Bismuth Alloys.

Percentage of silver by weight.	Density in grams/c.c. at 18° C.	Mass susceptibility × 10^6. Average temperature = 18° C.	
		Before annealing.	After annealing.
0·00 (100 % Bi)	9·80	−1·400	−1·400
1·10	9·82	−1·440	−1·440
2·53	9·83	−1·460	−1·460
4·10	9·84	−1·441	−1·441
10·00	9·93	−1·333	−1·361
19·50	10·01	−1·202	−1·332
30·00	10·10	−0·981	−1·079
45·00	10·23	−0·783	−0·890
56·00	10·29	−0·601	−0·748
70·00	10·36	−0·503	−0·632
80·00	10·40	−0·430	−0·565
90·00	10·42	−0·289	−0·456
92·50	10·42	−0·274	−0·451
94·00	10·43	−0·256	−0·437
96·40	10·45	−0·247	−0·293
98·00	10·47	−0·206	−0·249
100·00	10·49	−0·197	−0·197

Graph I.

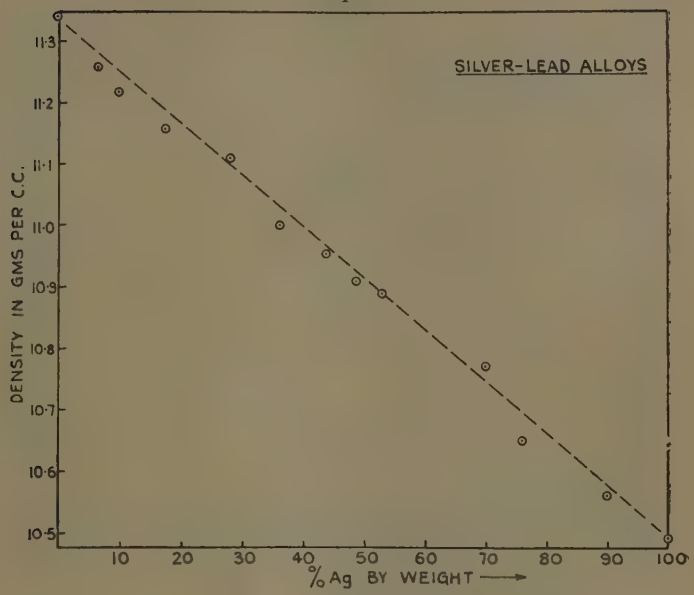

Graph II.

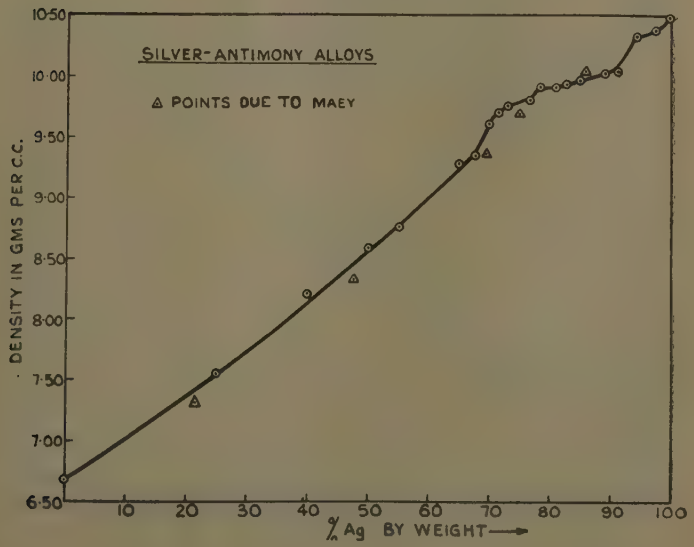

Graph III.

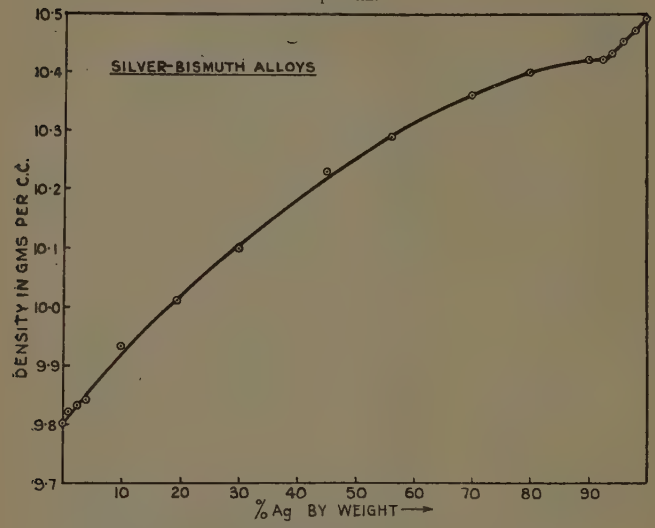

Graph IV.

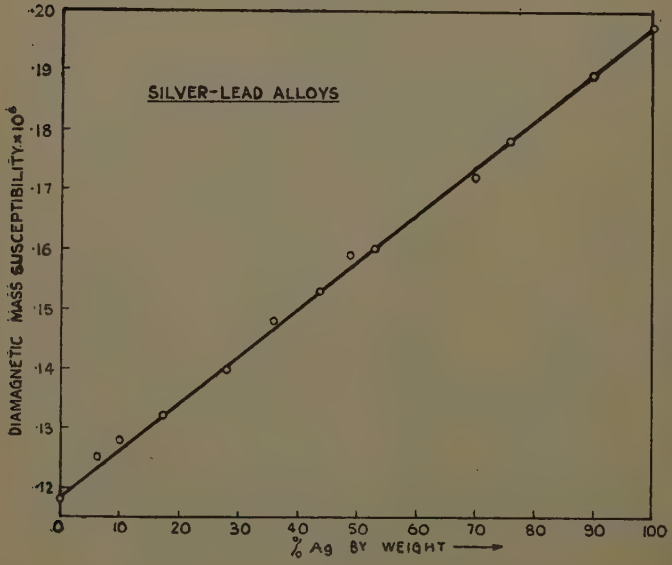

Graph V.

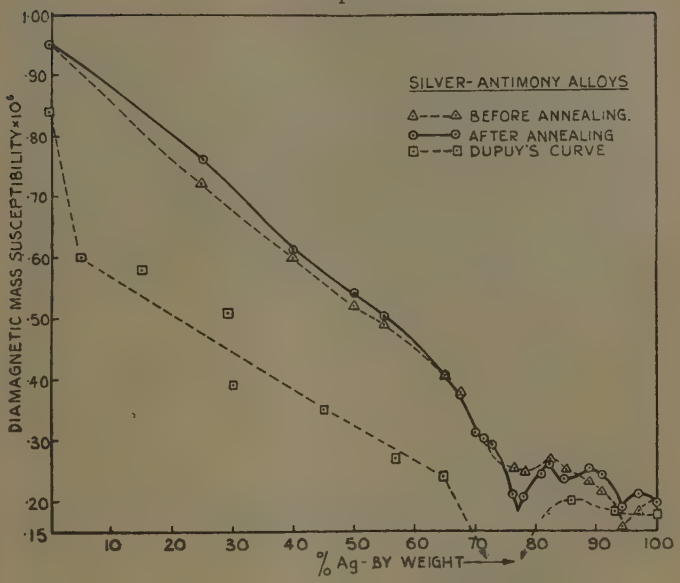

Graph VI.

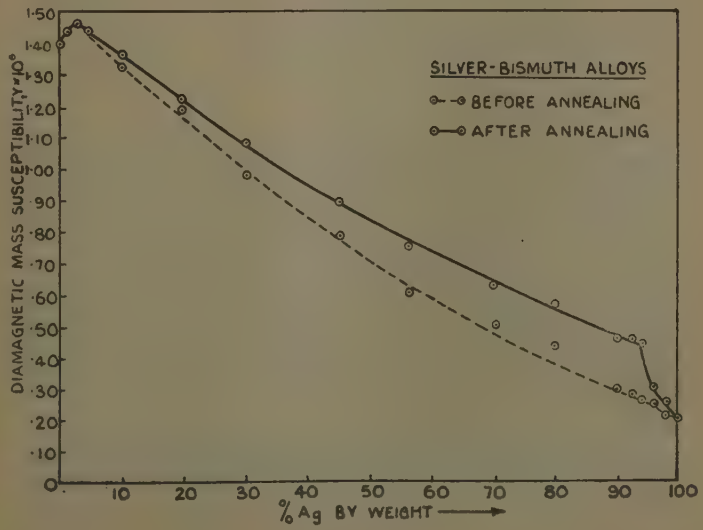

Discussion.

Silver-Lead Alloys.

Annealing had little effect on the mass susceptibilities of the alloys belonging to this system. The density-concentration and susceptibility-concentration curves, plotted in graphs I. and IV. respectively, are seen to be linear. These results are in agreement with Friedrich's [4] equilibrium diagram (fig. 1), according to which the system is a series of mechanical mixtures of the two constituent metals throughout the whole range of composition. No solid solutions or intermetallic compounds exist in the system.

Fig. 1.

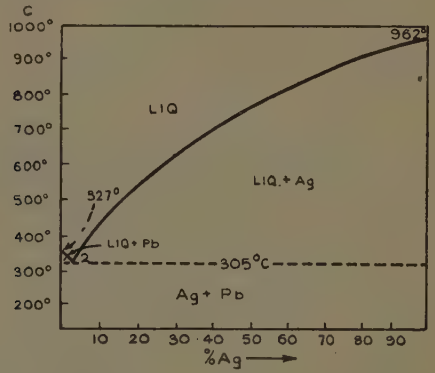

The alloys are all diamagnetic, in contradiction to the results of Spencer and John [5], who obtained strongly paramagnetic alloys in the neighbourhood of the composition corresponding to 29 per cent. by weight of lead.

After completing the work on this system, it was found that the susceptibilities had been recently measured by Montgomery and Ross [6], who obtained results in agreement with those given in this paper. The density measurements agree with those given by Maey [7], who found a linear relation between density and composition.

The Silver-Antimony Alloys.

Raeder [8], and Westgren, Hägg, and Eriksson [9] have given for the silver-antimony system phase boundaries which disagree with those given in the previously accepted

diagram due to Petrenko [10]. Raeder's phase boundaries, which agree with those given by Westgren, are shown in fig. 2, together with Petrenko's freezing-point curve. The density-concentration curve plotted in graph II. shows slight discontinuities in the region between 70 per cent. silver and the end of the series. These discontinuities, although not very definite, correspond to the positions of the phase boundaries as given by Raeder The relation between susceptibility and concentration is given in graph V., which also includes the curve due to Dupuy [11], who deduced the presence of a solid solution

Fig. 2.

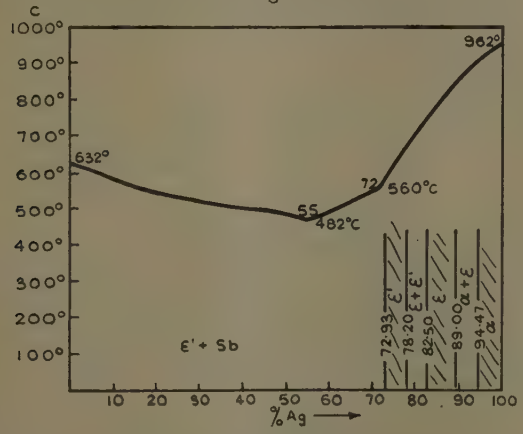

of silver in antimony extending to 5 per cent. silver. The present experiments give no indication of this solid solution at the antimony end of the series, and this conclusion is strongly supported by the recent electrical measurements of John and Evans [12]. The present investigation shows that all the alloys are diamagnetic, but Dupuy obtained an alloy which was practically non-magnetic at the composition corresponding to 75 per cent. silver. The annealed curve in graph V. gives evidence of the compound Ag_3Sb at nearly 73 per cent. silver, and also the phase boundaries at 78, 82·5, 89, and 94·5 per cent. silver. The effect of annealing on the mass susceptibilities of the alloys is irregular, and depends upon the composition of the alloys.

The Silver-Bismuth Alloys.

Petrenko's equilibrium diagram [13] (fig. 3) shows the existence of a solid solution of bismuth in silver extending to a concentration of 5·7 per cent. bismuth. The end of this solid solution is well marked in both the density-concentration and the susceptibility-concentration curves, which are plotted in graphs III. and VI. respectively. Maey [14] gives a linear relation between density and concentration for this system of alloys. An interesting feature of the

Fig. 3.

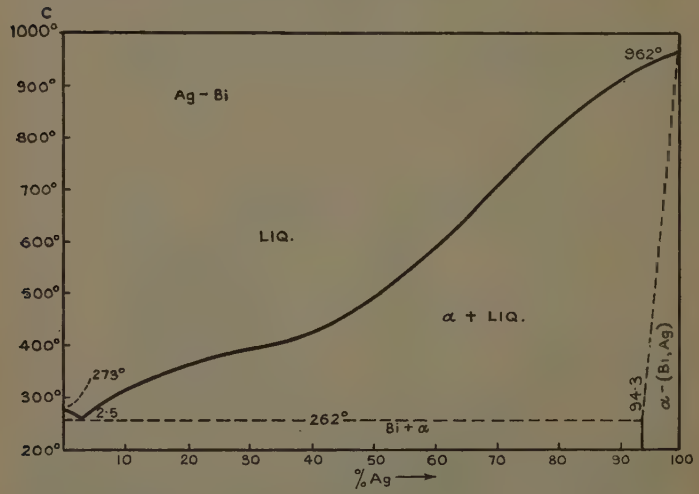

susceptibility curve is the presence, at the eutectic composition, of a maximum, which was unaffected by annealing. The addition of a small percentage of silver to bismuth has caused a small increase in the diamagnetic susceptibility, and the result is somewhat surprising, when it is remembered that the diamagnetism of silver is small compared with that of bismuth. Some observers have put forward the possibility of the existence of a compound of silver and bismuth, but no evidence of such a compound was obtained in the present investigation. The results of these experiments are in good agreement with the equilibrium diagram of Petrenko.

References.

(1) Curie and Chéneveau, *J. de Phys.* ii. p. 796 (1903) ; Chéneveau and Jolley, Phil. Mag. xx. p. 357 (1910).
(2) Spencer and John, Proc. Roy. Soc. A, cxvi. p. 61 (1927).
(3) de Haas and Drapier, Int. Crit. Tables, vi. p. 357.
(4) K. Friedrich, 'Metallurgie,' iii. p. 1 (1906).
(5) Spencer and John, *loc. cit.*
(6) Montgomery and Ross, Phys. Rev. xliii. (March 1, 1933).
(7) E. Maey, *Zeits. Phys. Chem.* l. p. 203 (1905).
(8) Raeder, *Zeits. f. phys. Chem.* vi. Abt. B l, pp. 40–42 (Nov. 1929).
(9) Westgren, Hägg, and Eriksson, *Zeits f. phys. Chem.* iv. Abt. 6. pp. 453–468 (Aug. 1929).
(10) Petrenko, *Zeits. Anorg. Chem.* l. p. 139 (1906).
(11) Dupuy, *Comptes Rendus*, clviii. p. 793 (1914).
(12) W. G. John and E. J. Evans, Phil. Mag. xxii. p. 417 (1936).
(13) Petrenko, *Zeits. f. Anorg. und Allgem. Chem.* l. p. 133 (1896).
(14) E. Maey, *Zeits. Phys. Chem.* xxxviii. p. 295 (1901).

XXXV. *The Power-loss and Electromagnetic Shielding due to the Flow of Eddy-currents in Thin Cylindrical Tubes.* *By* C. W. Oatley, *M.A.*, *M.Sc.* *

Abstract.

The induction of eddy-currents in thin cylindrical tubes, by the action of an alternating magnetic field parallel to the axis of the tube, is investigated mathematically. Formulæ are obtained for the power dissipated in such tubes and for the electromagnetic shielding due to them.

Introduction.

About two years ago J. B. Smith and the author carried out some measurements on the power-loss due to eddy-currents induced in thin cylindrical tubes by an alternating magnetic field parallel to the axis of the tube ; the results of these measurements are recorded in the preceding paper. In a preliminary attempt to explain the results, the following simple theory was used.

Let r be the internal radius of the tube, b its thickness, and ρ the resistivity of the material of which it is made. The tube is assumed to be infinitely long and to be situated in a magnetic field $H_0 \cos \omega t$, parallel to its axis.

* Communicated by Prof. E. V. Appleton, F.R.S.

The E.M.F. induced in the tube is $-\pi r^2\omega H_0 \sin \omega t$ and the resistance per unit length $2\pi r\rho/b$. If the tube is sufficiently thin, the field due to induced current will be negligible compared with the external field and the current density will be uniform over the cross-section of the tube. We may express this in another way by saying that the reactance of the tube is negligible in comparison with its resistance. If, under these circumstances, i is the current per unit length of tube,

$$i=-(br\omega H_0 \sin \omega t)/\rho. \quad . \quad . \quad . \quad . \quad . \quad (1)$$

If the reactance of the tube is small but not negligible compared with its resistance, the current density will still be very nearly uniform, and we may write for the inductance per unit length of tube

$$L=4\pi^2r^2.$$

We then have

$$i=-\frac{\pi r^2\omega H_0 \sin(\omega t+\psi)}{[(2\pi r\rho/b)^2+(4\pi^2r^2\omega)^2]^{1/2}}. \quad . \quad . \quad . \quad (2)$$

From (2) it is easy to calculate the power-loss per unit length of tube. On inserting numerical values and comparing with experimental results, it was found that equation (2) was reasonably consistent with these results in spite of the fact that, in all cases investigated, the resistance of the tube was *very small* compared with its reactance, so that the assumption of uniform current density could not have been even approximately true.

Under these conditions the current induced per unit length of tube is

$$i=-[H_0 \sin(\omega t+\psi)]/4\pi.$$

The mean power-loss per unit length of tube then becomes

$$P=H_0^2r\rho/16\pi b. \quad . \quad . \quad . \quad . \quad . \quad . \quad (3)$$

Shortly after this work had been completed a full theoretical investigation of the flow of eddy-currents in cylindrical tubes was published by McLachlan and Meyers [1], [2]. Since their analysis was rigorously true, the final equations were necessarily very cumbersome. They could be reduced to simple approximate forms, valid at sufficiently high and sufficiently low frequencies respectively, but neither of these forms was applicable

to the conditions under which the experimental measurements, previously recorded, were made. The following investigation of the theoretical validity of equation (3) was therefore undertaken.

The special feature of the present analysis is that the limitation to thin tubes is made at the outset. The appropriate differential equation is thereby greatly simplified, so that the final solution, which is valid for all frequencies, is not very cumbersome.

General Theory.

Let x be the radial distance of any annular element of the tube from the inside wall. We suppose the thickness of the tube to be small compared with its radius, so that the circumference of any annular ring does not differ appreciably from $2\pi r$. From considerations of symmetry we see that the eddy-currents will flow in circular paths coaxial with the tube. Let σ be the current density in that portion of the tube lying between cylindrical surfaces distant x and $x+dx$ from the inner wall. Then, if H be the magnetic field,

$$\sigma = -\frac{1}{4\pi} \cdot \frac{\partial H}{\partial x} \cdot \quad . \quad . \quad . \quad . \quad . \quad . \quad . \quad (4)$$

Also, considering the E.M.F. induced and the current flowing in any cylindrical element of thickness dx,

$$2\pi r \rho \sigma = E - 2\pi r \mu \int_0^x \frac{\partial H}{\partial t} \cdot dx, \quad . \quad . \quad . \quad . \quad (5)$$

where μ is the permeability of the material of the tube and E is the E.M.F. induced by the change of flux inside the inner wall of the tube. E is therefore a function of t but not of x. From (4) and (5) we get

$$-\frac{2\pi r \rho}{4\pi} \cdot \frac{\partial H}{\partial x} = E - 2\pi r \mu \int_0^x \frac{\partial H}{\partial t} \cdot dx.$$

Differentiating with respect to x,

$$\frac{\partial^2 H}{\partial x^2} = \frac{4\pi\mu}{\rho} \cdot \frac{\partial H}{\partial t} \cdot \quad . \quad . \quad . \quad . \quad . \quad (6)$$

Since, in the steady state, H will be periodic, we may write

$$H = H_1 \cos \omega t + H_2 \sin \omega t,$$

where H_1 and H_2 are functions of x but not of t. Substituting in (6) and equating coefficients,

$$\frac{d^2H_1}{dx^2} = m^2H_2, \qquad \frac{d^2H_2}{dx^2} = -m^2H_1, \quad . \quad . \quad . \quad (7)$$

where

$$m^2 = 4\pi\mu\omega/\rho.$$

Eliminating H_2, we get

$$\frac{d^4H_1}{dx^4} = -m^4H_1, \quad . \quad . \quad . \quad . \quad . \quad . \quad (8)$$

the solution of which is

$$H_1 = A_1\epsilon^{mx(1+i)/\sqrt{2}} + A_2\epsilon^{mx(1-i)/\sqrt{2}} + A_3\epsilon^{-mx(1+i)/\sqrt{2}} + A_4\epsilon^{-mx(1-i)/\sqrt{2}},$$

where A_1, A_2, A_3, and A_4 are arbitrary constants. If we take four other constants, B_1, B_2, B_3, and B_4, and put $m/\sqrt{2} = p$, this solution may be written in the slightly different form

$$H_1 = \epsilon^{px}(B_1 \cos px + B_2 \sin px) + \epsilon^{-px}(B_3 \cos px + B_4 \sin px)$$
$$= \cos px(B_1\epsilon^{px} + B_3\epsilon^{-px}) + \sin px(B_2\epsilon^{px} + B_4\epsilon^{-px}). \quad . \quad (9)$$

Differentiating twice with respect to x and substituting in (7), we obtain

$$H_2 = \cos px(B_2\epsilon^{px} - B_4\epsilon^{-px}) + \sin px(-B_1\epsilon^{px} + B_3\epsilon^{-px}). \quad (10)$$

To determine the arbitrary constants we insert the values of H and x corresponding to the inner and outer surfaces of the cylinder. At the outer surface $x = b$, $H_1 = H_0$, and $H_2 = 0$. Therefore

$$\cos pb(B_1\epsilon^{pb} + B_3\epsilon^{-pb}) + \sin pb(B_2\epsilon^{pb} + B_4\epsilon^{-pb}) = H_0, \quad (11)$$

$$\cos pb(B_2\epsilon^{pb} - B_4\epsilon^{-pb}) + \sin pb(-B_1\epsilon^{pb} + B_3\epsilon^{-pb}) = 0 \quad . \quad (12)$$

At the inner surface, where $x = 0$, we see from (6) and (7) that the field is

$$H' = (B_1 + B_3) \cos \omega t + (B_2 - B_4) \sin \omega t. \quad . \quad . \quad (13)$$

Since this field is uniform over the whole of the inside of the cylinder, the E.M.F. induced in a layer of thickness dx next to the inner surface is

$$-\pi r^2 \frac{dH'}{dt}.$$

If σ' is the corresponding current density,

$$2\pi r\rho\sigma' = -\pi r^2 \frac{dH'}{dt}.$$

Substituting the value of H′ from (13),

$$\sigma' = \frac{r\omega}{2\rho}[(B_1+B_3)\sin\omega t-(B_2-B_4)\cos\omega t]. \quad . \quad (14)$$

But

$$\sigma = -\frac{1}{4\pi}\cdot\frac{\partial H}{\partial x} = -\frac{1}{4\pi}\left(\frac{dH_1}{dx}\cos\omega t+\frac{dH_2}{dx}\sin\omega t\right).$$

After insertion of values corresponding to $x=0$, this gives

$$\sigma'_1 = -\frac{p}{4\pi}[(B_1+B_2-B_3+B_4)\cos\omega t + (-B_1+B_2+B_3+B_4)\sin\omega t]. \quad (15)$$

Equating coefficients in (14) and (15) and putting $p\rho/2\pi r\omega=\kappa$, we get

$$B_1(1-\kappa)+B_2\kappa+B_3(1+\kappa)+B_4\kappa=0, \quad . \quad . \quad (16)$$

$$B_1\kappa-B_2(1-\kappa)-B_3\kappa+B_4(1+\kappa)=0. \quad . \quad . \quad (17)$$

We now have to solve equations (11), (12), (16), and (17) for B_1, B_2, B_3, and B_4. The algebra is rather long, and it will be convenient to express the results in terms of the following symbols :—

$$\phi = pb, \quad . \quad . \quad . \quad . \quad . \quad . \quad . \quad (18)$$

$$\Delta = \epsilon^{2\phi}(2\kappa^2+2\kappa+1)+\epsilon^{-2\phi}(2\kappa^2-2\kappa+1) - 4\kappa\sin 2\phi-2(1-2\kappa^2)\cos 2\phi. \quad (19)$$

We then have

$$\left.\begin{aligned}
B_1 &= \frac{H_0}{\Delta}[(2\kappa^2+2\kappa+1)\epsilon^{\phi}\cos\phi-2\kappa\epsilon^{-\phi}\sin\phi \\
&\qquad -(1-2\kappa^2)\epsilon^{-\phi}\cos\phi], \\
B_2 &= \frac{H_0}{\Delta}[(2\kappa^2+2\kappa+1)\epsilon^{\phi}\sin\phi-2\kappa\epsilon^{-\phi}\cos\phi \\
&\qquad +(1-2\kappa^2)\epsilon^{-\phi}\sin\phi], \\
B_3 &= \frac{H_0}{\Delta}[(2\kappa^2-2\kappa+1)\epsilon^{-\phi}\cos\phi-2\kappa\epsilon^{\phi}\sin\phi \\
&\qquad -(1-2\kappa^2)\epsilon^{\phi}\cos\phi], \\
B_4 &= \frac{H_0}{\Delta}[(2\kappa^2-2\kappa+1)\epsilon^{-\phi}\sin\phi-2\kappa\epsilon^{\phi}\cos\phi \\
&\qquad +(1-2\kappa^2)\epsilon^{\phi}\sin\phi].
\end{aligned}\right\} \quad (20)$$

The Eddy-current Power-loss per Unit Length of Tube.

From equation (4) we have

$$\sigma = -\frac{1}{4\pi}\left[\left(\frac{dH_1}{dx}\right)\cos\omega t + \left(\frac{dH_2}{dx}\right)\sin\omega t\right].$$

Therefore the mean value of σ^2 is given by

$$\overline{\sigma^2} = \frac{1}{32\pi^2}\left[\left(\frac{dH_1}{dx}\right)^2 + \left(\frac{dH^2}{dx}\right)^2\right].$$

Substitution of the appropriate expressions for $\frac{dH_1}{dx}$ and $\frac{dH_2}{dx}$ gives

$$\overline{\sigma^2} = \frac{p^2}{16\pi^2}[(B_1^2+B_2^2)\epsilon^{2px}+(B_3^2+B_4^2)\epsilon^{-2px} + 2(B_2B_4-B_1B_3)\cos 2px - 2(B_1B_4+B_2B_3)\sin 2px].$$

The loss of power per unit length of tube due to eddy-currents is

$$P = 2\pi r\rho\int_0^b \overline{\sigma^2}\,dx.$$

Substituting for $\overline{\sigma^2}$ we now obtain

$$P = \frac{r\rho p}{16\pi}[B_1^2+B_2^2)(\epsilon^{2\phi}-1)-(B_3^2+B_4^2)(\epsilon^{-2\phi}-1) + 2(B_2B_4-B_1B_3)\sin 2\phi + 2(B_1B_4+B_2B_3)(\cos 2\phi - 1)]. \quad . \; . \; . \quad (21)$$

The substitution in (21) of the values of the constants from (20) is somewhat laborious; taking the terms one at a time, we find eventually,

$$\left.\begin{aligned} B_1^2+B_2^2 &= H_0^2(2\kappa^2+2\kappa+1)/\Delta, \\ B_3^2+B_4^2 &= H_0^2(2\kappa^2-2\kappa+1)/\Delta, \\ B_2B_4-B_1B_3 &= H_0^2(1-2\kappa^2)/\Delta, \\ H_1B_4+B_2B_3 &= H_0^2.2\kappa/\Delta. \end{aligned}\right\} \quad . \; . \quad (22)$$

Hence

$$P = \frac{H_0^2 r\rho p}{16\pi\Delta}[(2\kappa^2+2\kappa+1)(\epsilon^2{}_\phi-1)-(2\kappa^2-2\kappa+1)(\epsilon^{-2\phi}-1) + 2(1-2\kappa^2)\sin 2\phi - 4\kappa(\cos 2\phi - 1)]$$

$$= \frac{H_0^2 r\rho p}{16\pi} \left[\frac{(2\kappa^2+2\kappa+1)\epsilon^{2\phi} - (2\kappa^2-2\kappa+1)\epsilon^{-2\phi} + 2(1-2\kappa^2)\sin 2\phi - 4\kappa\cos 2\phi}{(2\kappa^2+2\kappa+1)\epsilon^{2\phi} + (2\kappa^2-2\kappa+1)\epsilon^{-2\phi} - 2(1-2\kappa^2)\cos 2\phi - 4\kappa\sin 2\phi} \right]$$

$$= \frac{H_0^2 r\rho p}{16\pi} \left[\frac{(\sinh 2\phi + \sin 2\phi) + 2\kappa^2(\sinh 2\phi - \sin 2\phi) + 2\kappa(\cosh 2\phi - \cos 2\phi)}{(\cosh 2\phi - \cos 2\phi) + 2\kappa^2(\cosh 2\phi + \cos 2\phi) + 2\kappa(\sinh 2\phi + \sin 2\phi)} \right]. \quad . \quad . \quad . \quad (23)$$

Special Cases.

Equation (23) can be considerably simplified under certain conditions, which we proceed to consider :—

(*a*) if $\phi > 1{\cdot}5$, $\cosh 2\phi$ will be very nearly equal to $\sinh 2\phi$, and both will be large in comparison with $\cos 2\phi$ and $\sin 2\phi$. We then have

$$P = H_0^2 r\rho p/16\pi, \quad . \quad . \quad . \quad . \quad . \quad . \quad (24)$$

which is also the formula for a solid rod. This case corresponds, therefore, to a tube so thick and a frequency so high that the magnetic field strength inside the tube is almost equal to zero.

(*b*) If $\phi < 0{\cdot}15$, we may write

$$\cosh 2\phi = \cos 2\phi = 1,$$
$$\sinh 2\phi = \sin 2\phi = 2\phi.$$

Then

$$P = H_0^2 r\rho p\phi/16\pi\kappa^2$$
$$= H_0^2 \pi r^3 b\omega^2/4\rho.$$

This corresponds to a tube thickness so small and a frequency so low that the reactance of the tube is negligible compared with its resistance, and, in consequence, the current distribution is uniform over the cross-section of the tube.

(*c*) If $0{\cdot}15 < \phi < 0{\cdot}4$, we may expand the circular and hyperbolic functions in powers of ϕ and neglect all terms higher than ϕ^3. Then

$$P = \frac{H_0^2 r\rho p}{16\pi} \left[\frac{\phi + 2\kappa\phi^2 + \frac{4}{3}\kappa^2\phi^3}{\kappa^2 + \phi^2 + \frac{4}{3}\kappa\phi^3} \right]. \quad . \quad . \quad 25)$$

(*d*) If $0{\cdot}15<\phi<0{\cdot}4$, and, in addition, κ is small compared with ϕ, equation (25) may be still further reduced to

$$P=H_0^2 r\rho p/16\pi\phi=H_0^2 r\rho/16\pi b, \quad . \quad . \quad . \quad (26)$$

which is identical with equation (3).

Although the range of values of the various parameters, over which equations (25) and (26) are applicable, is somewhat limited, this range does, in fact, cover a large proportion of the cases encountered in the practical eddy-current heating of thin metal electrodes. From equation (26) we see that the experimental results, recorded in the previous paper, are entirely in accordance with theory.

Electromagnetic Shielding due to Thin Cylindrical Tubes.

The subject of electromagnetic shielding has been treated in great detail by King [3], who obtains accurate formulæ for the shielding due to spherical shells, and cylindrical tubes of infinite length. These formulæ, are, however, very cumbersome and, for purposes of calculation, are reduced to a number of approximate forms, each of which is valid over a definite range of frequencies.

From the results already obtained in the present paper we may deduce a formula for an infinite cylindrical tube placed parallel to the direction of the field, which is limited to thin tubes, but which is valid for all frequencies. Thus, from (10), the amplitude of the field inside the cylinder is given by

$$|H'|=[(B_1+B_3)^2+(B_2-B_4)^2]^{\frac{1}{2}}.$$

Substituting from (19), we find for the shielding ratio

$$\frac{|H'|}{|H_0|}=\frac{2\sqrt{2}\,\kappa}{\sqrt{\Delta}}$$

$$=2\kappa/\left[(\cosh 2\phi-\cos 2\phi)+2\kappa^2(\cosh 2\phi+\cos 2\phi)\right.$$
$$\left.+2\kappa(\sinh 2\phi-\sin 2\phi)\right]^{\frac{1}{2}}. \quad (27)$$

At sufficiently high frequencies, κ becomes small compared with unity, and the terms in κ and κ^2 may be neglected in the denominator. Equation (27) then reduces to

$$\frac{|H'|}{|H_0|}=\frac{\sqrt{2}\,\kappa}{(\sinh^2\phi+\sin^2\phi)^{\frac{1}{2}}}. \quad . \quad . \quad . \quad (28)$$

Again, at low frequencies, ϕ will be less than unity, and the denominator of (27) can be expanded in powers of ϕ. If ϕ^4 and higher powers may be neglected, this gives

$$\frac{|H'|}{|H_0|} = \frac{\kappa}{[\kappa^2+\phi^2+\frac{4}{3}\kappa\phi^3]^{\frac{1}{2}}} \quad . \quad . \quad . \quad . \quad . \quad (29)$$

If the term in ϕ^3 is also negligible,

$$|H'|/|H_0| = (1+\phi^2/\kappa^2)^{-\frac{1}{2}} = [1+(2\pi r\omega b/\rho)^2]^{-\frac{1}{2}}. \quad (30)$$

Equations (28) and (30) are in agreement with equations (39), (63), and (66) of King's paper.

Acknowledgement.

Dr. N. W. McLachlan very kindly communicated to the author the results contained in the letter by McLachlan and Meyers [2], some time before these results appeared in print.

References.

(1) McLachlan, N.W., and Meyers, A. L., Phil. Mag. xviii. p. 610 (1934).
(2) McLachlan, N. W., and Meyers, A. L., Phil. Mag. xix. p. 846 (1935).
(3) King, L. V., Phil. Mag. xvi. p. 201 (1933).

Wheatstone Laboratory,
King's College, Strand, W.C. 2.

XXXVI. *The Design of Eddy-Current Heating Apparatus for Outgassing Electrodes in a Vacuum.* *By* C. W. Oatley, *M.A.*, *M.Sc.*, *and* J. B. Smith, *M.Sc.**

Abstract.

The conditions of operation of eddy-current heating apparatus are investigated experimentally, particular attention being paid to the heating of tubes and disks constructed of thin sheet metal. The design of the heating coil is considered in detail and a method of determining the optimum working frequency is described. Measurements of the efficiency of the heating coil are given for a number of cases corresponding to those encountered in practice.

* Communicated by Prof. E. V. Appleton, F.R.S.

Introduction.

ALTHOUGH the use of eddy-current heating for outgassing metal electrodes *in vacuo* has been fairly common for some years past, comparatively little has been published concerning the design of suitable apparatus for this purpose. The pioneer work of Northrup [1] and the more recent theoretical investigations of Burch and Davis [2] and of Strutt [3] are well known, but these authors deal chiefly with the general principles involved in the use of eddy-current heating for melting metals on a fairly large scale. A description of an experimental plant for the same purpose has been given by Bell [4]. The problems arising in the design of small-scale laboratory apparatus for use in vacuum work are rather different, and the object of the present paper is to show how the optimum conditions of working can be obtained in any given case.

The essential parts in apparatus of the kind which we are considering are a generator of radio-frequency power and a heating coil. The latter consists of a coil of wire surrounding, or adjacent to, the electrode to be heated, and radio-frequency current from the generator passes through this coil. In order to deal with the various contingencies which arise in vacuum work, it will generally be convenient to have a number of alternative heating coils of different shapes and sizes. Since the impedances of these coils under working conditions will vary over a fairly wide range of values it is advantageous to interpose, between the heating coil and the generator, a radio-frequency transformer of variable ratio, so that the impedances of the two parts of the apparatus may be correctly matched to each other.

The principles underlying the design of suitable radio-frequency generators and transformers are well known and need not be further considered here. Before such designs can be undertaken, however, the operating frequency and the effective impedance of the heating coil under working conditions must be known. Furthermore, the optimum number of turns and the best gauge of wire for the heating coil must also be determined.

The Design of the Heating Coil.

When a piece of metal is placed in an alternating magnetic field, eddy-currents will be set up in it and, as a

result, let W_1 units of energy be generated in the metal per second, in the form of heat. Then W_1 will depend only on the field-strength and the frequency of alternation. If the field is produced by an alternating current flowing in the heating coil, then heat will also be generated in the coil itself; let this rate of generation be W_2 units per second. Since, for our present purpose, W_1 is useful heat, while W_2 is useless, we define the efficiency of the coil to be

$$E = W_1/(W_1+W_2). \quad . \quad . \quad . \quad . \quad (1)$$

Both W_1 and W_2 will be proportonal to the square of the current passing through the heating coil, so that E will be independent of the magnitude of this current, but will, in general, depend upon its frequency. Since W_2, which is to be kept as small as possible, is proportional to the resistance of the heating coil, this latter should clearly be no larger than is necessary to produce the required magnetic field throughout the volume occupied by the metal to be heated. For vacuum work the metal will be enclosed in a glass envelope and the coils employed will usually be of solenoid or pancake form.

For the purpose of the present investigation, a solenoidal coil of length $2\frac{1}{2}''$, wound on a former $3''$ in diameter was taken as standard, and all calculations and experiments refer to this shape and size. There is no reason to suppose, however, that the general conclusions do not apply equally to coils of other shapes and sizes. It will be assumed throughout that the heating coil is wound with wire or tube of circular cross-section. In practice, coils are often made of strip, of rectangular cross-section, wound edgewise, but it is doubtful whether this plan has much to commend it.

We consider first the effect on the efficiency of varying the number of turns while keeping the frequency constant. Butterworth has shown [5] that, for a given frequency and given number of turns, there is an optimum diameter for the wire, which will make the coil resistance a minimum. Furthermore, if the coil is a single-layer solenoid with spaced turns, the value of this minimum resistance is given by

$$R = l\sqrt{fm}/c, \quad . \quad . \quad . \quad . \quad . \quad . \quad (2)$$

where l is the total length of wire, c the distance between

turns, f the frequency, and m a constant depending on the shape of the coil.

If n be the total number of turns, then, for a given frequency and given current flowing through the heating coil, W_1 will be proportional to n^2 and W_2 will be proportional to R. Therefore

$$\frac{1}{E}-1=\frac{W_1+W_2}{W_1}-1$$

$$=\frac{W_2}{W_1}$$

$$=kR/n^2, \quad . \quad . \quad . \quad . \quad . \quad . \quad . \quad . \quad (3)$$

where k is a constant. Hence the efficiency will be a maximum when R/n^2 is a minimum. From equation (2) we see that, when f is constant, R varies as l/c. Now l is directly proportional and c inversely proportional to n, so that R/n^2 is a constant. Thus the efficiency of the coil is independent of the number of turns. Equation (2) will not be true for closely-wound or multi-layer solenoids, but the variation of efficiency with number of turns will always be comparatively small, so that the latter will usually be decided by practical considerations. From this point of view, a coil wound with from ten to twenty turns of thick wire has much to recommend it. With such a coil sufficient rigidity can be obtained without too much support for the wire; furthermore, the turns are well-spaced and bare wire can be used, thus greatly facilitating the dissipation of heat. Sometimes coils are wound with copper tube which is water-cooled.

Determination of the Optimum Frequency.

A theoretical determination of the optimum frequency can only be carried out when the metal to be heated has a simple geometrical form, and even then it is a matter of considerable difficulty. An experimental method of approach, based on the following considerations, was therefore used.

As was first shown by Maxwell, if a primary circuit of inductance L and resistance R_1, be coupled to a closed secondary circuit of inductance L_2 and resistance R_2, so that their mutual inductance is M, then, owing to the presence of the secondary, the effective primary resistance

is increased by amount δR and its inductance is decreased by δL, where

$$\delta R = R_2 M^2 w^2/(R_2^2 + L_2^2 w^2) \quad . \quad . \quad . \quad (4)$$

$$\delta L = L_2 M^2 w^2/(R_2^2 + L_2^2 w^2) \quad . \quad . \quad . \quad (5)$$

and $w = 2\pi \times$ frequency.

If a current i be passed through the primary, the rate of doing work in the primary is $i^2 R_1$ and in the secondary $i^2 \delta R$. Suppose now that, instead of the simple secondary circuit, we have a piece of metal which is to be heated. Then the efficiency of the primary, considered as a heating coil, is

$$E = \delta R/(R_1 + \delta R)$$

Thus by making a series of measurements of R_1 and δR, using in each case a primary coil wound with wire of the most suitable gauge, the optimum working frequency could be found. The measurements would, however, be rather tedious, and the following method is more instructive.

Consider the constants M, L_2, R_2 when the secondary consists of a piece of metal. We can determine their ratios by measuring δR and δL, but equations (4) and (5) do not suffice to give their actual values. We cannot assume that they will be the same at all frequencies, and this point must be settled before we can usefully carry the theory any further. If there is a variation, it is very unlikely that R_2 and L_2 will change in the same proportion. Therefore the constancy or otherwise of the ratio $R_2/L_2 = \delta R/\delta L$ is a convenient test. We shall see later that, for the particular pieces of metal used and over the frequency range of the measurements, the ratio $\delta R/\delta L$ was, in fact, almost constant, so we assume that R_2 and L_2 are, for our present purpose, independent of frequency. Since we have already decided that a single-layer coil with well-spaced turns should be used, equation (2) will apply, so that, for a given number of turns, the resistance of the coil may be written $\phi f^{\frac{1}{2}}$, where ϕ is a constant. Then, substituting from equation (4) for δR, we may write

$$\frac{1}{E} - 1 = \frac{R_1}{\delta R}$$

$$= \phi f^{\frac{1}{2}}(L_2^2\omega^2 + R_2^2)/R_2 M^2 \omega^2$$

$$= \phi(L_2^2 \omega^{\frac{1}{2}} + R_2^2 \omega^{-\frac{3}{2}})/R_2 M^2 \sqrt{2\pi}.$$

Differentiating with respect to ω, we see that E is a maximum when

$$\tfrac{1}{2}L_2{}^2\omega^{-\frac{1}{2}} - \tfrac{3}{2}R_2{}^2\omega^{-\frac{5}{2}} = 0,$$

i. e.,

$$\omega^2 = 3R_2{}^2/L_2{}^2$$

or

$$f = \frac{\sqrt{3}}{2\pi}\frac{R_2}{L_2} = \frac{\sqrt{3}}{2\pi}\cdot\frac{\delta R}{\delta L} \quad . \quad . \quad . \quad . \quad . \quad (6)$$

Experimental Investigation.

For the purpose of an experimental investigation, a number of metal disks and hollow metal cylinders were

TABLE I.

Specimen.	Form.	Metal.	Thickness.	Diameter.	Length.
			cm.	cm.	cm.
A.....	Hollow cylinder.	Copper.	0·0087	4·13	6·35
B.....	„	Copper.	0·0070	4·13	6·35
C	„	Copper.	0·0054	4·13	6·35
D	„	Eureka.	0·0261	4·13	6·35
E	„	Eureka.	0·0124	4·13	6·35
F.....	„	Copper.	0·0087	1·27	6·35
G	„	Copper.	0·0054	1·27	6·35
H	„	Eureka.	0·0261	1·27	6·35
I.....	„	Eureka.	0·0124	1·27	6·35
J	Solid cylinder.	Copper.	—	1·27	6·35
K	Disk.	Copper.	0·0087	3·81	—
L.....	„	Copper.	0·0054	3·81	—
M	„	Eureka.	0·0261	3·81	—
N	„	Eureka.	0·0124	3·81	—

constructed to represent in size and form a variety of electrode structures which, in practice, one might wish to heat *in vacuo*. The details of these are given in Table I. The heating coils used were all solenoids of the same dimensions, viz., 3″ in diameter and 2½″ long. Since, as we have shown, the efficiency of a coil is independent of the number of turns, this number was chosen so that, at the frequency at which the coil was to be used, the parallel capacity required for resonance was about 300$\mu\mu f$.

A separate coil was used for each frequency and each was wound with the best gauge of wire for that frequency.

All resistance measurements were made by the Resistance Variation method, and are probably correct to about 1 per cent. The usual correction for the self-capacity of the coil was applied, and amounted to about 10 per cent. of the total resistance of the coil. Since this correction is of the same order as the expected change in resistance due to the introduction of a metal electrode, it was necessary to ascertain whether the introduction of the electrode had an appreciable effect on the self-capacity of the coil. To decide this, a cylinder of tinfoil, glued on cardboard, was constructed of the same size and shape as the largest electrode. When this cylinder was placed inside the coil, a change δR in the resistance of the coil was observed, and also a change δC in the capacity required to tune the coil to resonance. Clearly, δC might be due partly to a true alteration of the effective inductance of the coil and partly to a change in the self-capacity of the coil. To separate these two effects, three narrow longitudinal slots were cut in the tinfoil cylinder. This would greatly reduce the flow of eddy-currents while, presumably, leaving unchanged the effect of the cylinder on the self-capacity of the coil. It was then found that both δR and δC had fallen to less than 2 per cent. of their former values. Any effect which the test electrodes may have upon the self-capacity of the coil is therefore quite negligible.

The results of the measurements are summarized in Table II.

Discussion of Results.

As explained above, it was found convenient to use heating coils with different numbers of turns for different frequencies. The actual values of δR and δL obtained at the different frequencies are, therefore, not comparable, and the ratios $\delta R/\delta L$ and $\delta L/n^2$, where N is the total number of turns on the heating coil, are tabulated instead.

The results can best be interpreted with reference to equations (4) and (5). We see that, with the exception of those obtained for specimen J, the values of $\delta R/\delta L$, and therefore of R_2/L_2, are roughly constant for any one specimen over a wide range of frequencies. In extreme cases the variation is not more than about 30 per cent.

This may be taken as evidence that both R_2 and L_2 separately are constant to the same degree, and therefore that equation (6) may usefully be applied. The optimum frequencies given in the last column of Table II. are calculated from this equation.

TABLE II.

n = Number of turns on heating coil.
E = Percentage efficiency of heating coil.
f = Frequency in kilocycles per second.
δR = Resistance change in ohms.
δL = Inductance change in henries.

Specimen.	$f=10^3$ *kc/s.*			$f=5\times10^2$ *kc/s.*			$f=10^2$ *kc/s.*			Optimum frequency.
	$\delta L/n^2$. $\times10^8$.	$\delta R/\delta L$ $\times10^{-4}$.	E.	$\delta L/n^2$ $\times10^8$.	$\delta R/\delta L$ $\times10^{-4}$.	E.	$\delta L/n^2$ $\times10^8$.	$\delta R/\delta L$ $\times10^{-4}$.	E.	
A ...	1·35	1·37	13	1·33	1·58	26	1·31	1·62	39	4·2
B ...	1·35	1·76	16	1·33	1·91	23	1·31	2·14	46	5·3
C ...	1·35	2·24	19	1·33	2·53	29	1·31	2·80	54	7·0
D ...	1·35	18·4	66	1·33	17·8	74	1·31	19·1	87	51
E ...	1·35	35·8	79	1·33	35·3	85	1·31	—	—	98
F....	—	—	—	·114	7·0	9	·092	7·4	17	20
G ...	—	—	—	·105	7·6	9	·093	8·2	19	22
H ...	—	—	—	·112	44	38	·062	44	46	121
I....	—	—	—	·097	86	51	·024	104	44	262
J ...	—	—	—	·097	7·6	8	·092	2·0	5	—
K ...	—	—	—	·28	11·6	28	·26	9·7	43	30
L....	—	—	—	·27	11·9	28	·24	9·4	41	30
M ...	—	—	—	·25	59	64	·13	45	64	143
N ...	—	—	—	·18	128	74	·057	94	62	306

Further evidence for the constancy of L_2 may be obtained in the following way. From the value obtained for R_2/L_2, it appears that, at the frequencies used, $L_2\omega$ was generally large compared with R_2. Hence, from equation (5), we see that δL should be approximately equal to M^2/L_2. Now M will be proportional to n, the number of turns on the heating coil, so that if L_2 is constant, $\delta L/n^2$ should be independent of frequency and should also have the same value for all specimens of the same size and shape. This we see to be nearly true except in a few cases where the above approximation is not valid.

When the specimen is a thin-walled cylindrical tube and the frequency is low, we may calculate the values of

R_2 and L_2 on the assumption that the current density is uniform over the cross-section of the tube. We then find

$$R_2 = 2\pi r\sigma/bl, \qquad L_2 = 4\pi^2 r^2/l,$$

where l is the length of the tube, r its radius, b its thickness, and ρ the resistivity of the material of which it is made. Thus

$$R_2/L_2 = \delta R/\delta L = \rho/2\pi rb. \quad . \quad . \quad . \quad . \quad (7)$$

At higher frequencies the assumption of uniform current density is, of course, no longer true. A full theoretical analysis of the problem is given in a following article, and it is there shown that a non-uniform current density is not *necessarily* inconsistent with constant *effective* values of R_2 and L_2. It was found, in fact, that the values of $\delta R/\delta L$ recorded in Table II., for specimens A to I, agreed reasonably well with those calculated from equation (7). Exact agreement could not, in any case, be expected, since the magnetic field due to the heating coil was far from uniform.

Practical Conclusions.

Perhaps the most striking features of the above results are the high efficiencies which can be obtained when thin metal electrodes are being heated and the comparatively low values of the optimum frequencies. It must be remembered that these optimum frequencies refer only to the heating coil, and it is assumed that, in each case, a matching transformer of the correct ratio has been connected between the heating coil and the radio-frequency generator. If this is not done, the best results will usually be obtained at much higher frequencies because, although the heating coil itself is then less efficient, its impedance will be much higher and therefore more nearly matched to that of the generator.

The foregoing results also make clear the essential difference, from the point of view of eddy-current heating, between thin tubes and solid cylinders. As we have seen, the effective resistance in the case of the former remains approximately constant, so there is an optimum frequency, given by equation (6). The effective resistance of a solid rod, however, increases with frequency at about the same rate as does that of the heating coil, so the

efficiency is independent of the frequency so long as this is above a certain critical value.

So far as practical design is concerned, the efficiency of the coil is not the only factor which influences the choice of frequency. From a consideration of the results given in Table II., and also of the sizes of the components required to construct a radio-frequency generator, it appears that a frequency of about one hundred kilocycles per second would be a suitable compromise,

In designing the matching transformer, it must be remembered that the effective resistance of the heating coil under working conditions will usually be two or three times as great as the actual resistance of the coil itself, but that, under certain circumstances, it may become much higher than this. Thus, in one experiment, it was found that, when a cylinder of tinfoil was placed inside a certain heating coil, the resistance of the latter rose from about five ohms to ninety ohms. Such exceptional changes of resistance are not without importance, since, when the radio-frequency generator consists of a valve oscillator, the increase of load may cause it to cease oscillating and thus damage the valve.

Finally, it has been shown above that, if a frequency of about one hundred kilocycles per second is used, the efficiency of the heating coil, for an electrode of given size and shape, will in general increase as the thickness of the electrode material is reduced and as the resistivity of this material is increased. Since the output power of laboratory eddy-current heating apparatus is usually rather small, it is suggested that electrodes may often with advantage be constructed of thin sheet eureka. This nickel-copper alloy possesses several other properties to recommend it for the purpose, since it has a fairly high melting-point, is practically non-magnetic, and can easily be spot-welded.

References.

(1) Northrup, E. F., Trans. Am. Electrochem. Soc. xxxv. p. 69 (1919).
(2) Burch and Davis, Phil. Mag. i. p. 768 (1926).
(3) Strutt, M., *Ann. d. Phys.* lxxxii. p. 605 (1927); *Arch. f. Elektrotechnik*, xix. p. 424 (1928).
(4) Bell, G. E., Proc. Phys. Soc. xl. p. 193 (1928).
(5) Butterworth, S., 'Experimental Wireless,' iii. p. 316 (1926).

Wheatstone Laboratory,
King's College,
Strand, W.C. 2.

XXXVII. *The Air-Carbon Arc in High Vacuum.* *By* F. H. Newman, *D.Sc., F.Inst.P., Professor of Physics, University College, Exeter* *.

[Plate II.]

THE mechanism of the cold-cathode arc is still a subject of diverse opinion. According to the thermionic theory the electrons are thermionically emitted by the cathode hot spot, but this theory demands a high temperature of the spot, and measurements of the spot temperature in different arcs are very discordant. On the other hand the high electrical field theory, developed originally by Langmuir, attributes the electrons emanating from the cathode to an intense electric field in the immediate neighbourhood of the cathode. Electron currents, drawn from cold cathodes by extremely high electric fields of the order of 10^7 volts per cm., are greater in value than is to be expected on any theory, and it is assumed that this is due to the existence of submicroscopic sharp points on the cathode at which the field is greater than the average value in the vicinity.

It has been shown by the author in previous work † that the cold-cathode arc is difficult to strike if the electrodes are of very pure metal, or if they are covered with any film, such as an oxide. This is attributed to the fact that the submicroscopic points are then absent, or covered, but if a pure metal electrode, such as tungsten, is used, the arc can be started and maintained provided that the electrode surface is first roughened. This supports the theory that the presence of the sharp points is necessary to produce the abnormal electron current, sufficient to generate intense ionization within the cathode fall space. Impurities, if present on the electrode surface, increase the initial electron current for two reasons. In the first place they are, or form, the sharp points, and secondly, there is abnormal heating at these points, due to the fact that the electron current is localized thereat.

The present paper describes experiments with the cold-cathode arc between carbon electrodes at very low gas

* Communicated by the Author.

† Phil. Mag. xi. p. 796 (1926); vi. pp. 807 and 811 (1928); vii. p. 1085 (1929); xiv. pp. 712 and 718 (1932).

pressures. As in the previous investigations, three electrodes—all of carbon in this case—were utilized. Between two of these, the ends of which were about one centimetre apart, a steady potential difference was applied, and the arc was started by passing a momentary electrical discharge between one of these two electrodes—it was immaterial whether it was the positive or negative one—and the third electrode. The arc tube was of pyrex, and tungsten rods were sealed into the glass and fitted tightly into holes bored along the carbon rod electrodes. This arrangement eliminated wax seals, which are always unsatisfactory where a considerable current is passing. The carbons were not cored and the material was of no special purity, so that it contained the usual impurities—particularly sodium—associated with such carbon electrodes. Before striking the arc the gas pressure in the tube was reduced to the desired value and the pumping arrangement was then disconnected, the residual gases being the usual ones associated with air discharge-tubes, *i. e.*, nitrogen, oxygen, carbon monoxide, carbon dioxide, and hydrogen. The arc radiation was examined and photographed through a glass window at the end of the arc tube.

With this arrangement the arc could be struck with an applied potential difference as low as 70 volts—by passing a momentary electrical discharge—although the arc was not maintained at this voltage unless the current, controlled by an external resistance, exceeded 5 amperes. It would, however, continue to burn at 100 volts even when the current was as low as 1·5 amperes. The non-maintenance of the arc at the lower voltage is attributed to the fact that the electric field in the neighbourhood of the cathode is too small for the extraction of a sufficient supply of electrons from the cathode. As the applied voltage was further increased the arc started and was maintained more easily.

The gas pressure necessary for the successful operation covered a range from 1 to 0·01 mm. of mercury. The upper limit is higher than that associated with the other metallic arcs investigated. At the lower pressures the luminous column was wide and diffuse and wandered along the electrodes, but at the higher pressures it was localized between the ends of the two electrodes. Careful examination showed that the arc passed between very

bright spots on the electrodes, these spots being the sharp points, or traces of impurities previously mentioned.

When the arc is restarted after passing for a considerable time, it does not strike so readily, a fact which is attributed to a deposit of amorphous carbon on both electrodes. Removing this deposit the arc shows all the original characteristics. The film of amorphous carbon covers the sharp points and impurities and therefore, as explained previously, prevents the initial emission of electrons from the cathode.

Spectrographic observation of the arc radiation showed the presence of many lines corresponding to those in the spectrum of the uncondensed electrical discharge through the residual gases (Pl. II.). No detailed examination of the spectrograms was made since the carbons employed were not pure, but the photographs indicate that the arc current is carried mainly by the residual gases. This is especially the case during the initial stage of the arc before the positive electrode reaches a high temperature, and agrees with the results noted with metallic electrodes.

Preliminary experiments have shown that if a small quantity of a substance to be examined spectroscopically is placed on the end of the positive carbon electrode, and the arc struck as described above, the spectrum of the substance can be seen, and photographed, at the instant the arc is started. This method is of particular service when volatile metals are to be determined, and since there is little continuous spectrum, it should prove preferable to the more usual method of packing the substance in a hole bored in the positive carbon.

In conclusion, the experiments support the view previously advanced that thermionic emission cannot be solely responsible for the starting and maintenance of the electric arc ; the fact that it starts instantaneously with the application of the electrical discharge supports the high-field theory. In practice, if for any reason the arc does not strike when the high tension is applied, a continuance of the electrical discharge is seldom effective, even if the electrodes are raised to a high temperature by the ionic bombardment arising from the discharge.

XXXVIII. *On the Application of certain Heat Conduction Solutions for a Uniform Medium to the Temperature Distribution in the Gas surrounding a Metal Sphere.* *By* ROBERT S. SILVER, *B.Sc., M.A., Research Student, The University, Glasgow* *.

Introduction.

IN connexion with some recent experiments on the ignition of gaseous mixtures by heated spheres, the writer found it desirable to obtain an expression for the distribution of temperature in the gas surrounding a metal sphere of known initial temperature. The expression was required to allow numerical calculation of the temperature and temperature gradients at a point in the gas. A search through the literature of heat conduction problems failed to produce such an expression. So far as the writer is aware, no solution capable of arithmetical treatment has been given to the above general problem. Robertson [1] has given a solution using the wave-train method developed by Green [2], but it is not convenient for numerical evaluation. The direct methods of Fourier analysis are inapplicable, because the coexistence of the different media destroys the conditions which allow determination of coefficients. R. E. Langer [3] has explained a method of overcoming this difficulty in the case of a certain cylindrical problem. This may be capable of development for the case of a sphere immersed in a different medium, but it is again doubtful if it would lend itself to arithmetical treatment. The internal temperatures in a sphere with known surface conditions are discussed by J. H. Awbery [4], but an external medium is not considered. Carslaw [5], by conventional analysis, and Bromwich [6], by the Heaviside "operational method," treat of the temperatures in a sphere with a surrounding thin shell of different material. Their solutions admit of numerical calculation, as do those of Awbery, but the condition that the outer medium is a thin shell renders them inapplicable to the present problem.

Thus, since no exact solution was found for the general problem, we sought for a good approximation that might be taken to serve for our special circumstances. The

* Communicated by Prof. E. Taylor Jones, D.Sc.

argument proceeded as follows. There are several known solutions of the Fourier equation for temperature distribution in a uniform conducting medium. It seemed reasonable therefore to consider what conditions prevailing in a uniform medium would approach most closely to those produced in the gas by the presence of the sphere. It is then possible that some of the known solutions might fulfil such conditions. Then, by identifying the gas with the uniform medium and considering only temperatures outside a radius equal to the radius of the metal sphere, it was thought that a serviceable approximation to the actual temperature distribution would be found. Such solutions have been investigated and may be used, in the manner indicated by the present paper, to give arithmetical values required in connexion with experimental work on ignition. Apart, however, from this application, the form of the combination of solutions for a uniform medium may be of theoretical interest in showing how the source and sink method due to Kelvin may be applied to satisfy arbitrary additional conditions. It must be remarked, however, that the solutions discussed are considered only with regard to certain very limited intervals of time, such as those which are alone concerned in explosion work.

The Condition assumed in the Uniform Medium.

The first step is to enquire what conditions may be assumed to exist in the metal sphere and gas problem. They are :—

(*a*) That the gas in contact with the surface of the metal has the temperature of the surface.

(*b*) That this temperature at the sphere surface may be assumed to be constant at its initial value for a short but finite time.

We are neglecting entirely convection and radiation, so that these assumptions are justified by the following considerations :—

(1) The thermal capacity of the gas per unit volume is very much less than that of the metal, and its conductivity is also much smaller. The gas in contact with the sphere must thus be raised almost immediately to the surface temperature.

(2) Again, because of the large difference in capacity, the heat lost by the sphere will have comparatively little effect on its temperature, although it causes considerable rise in the adjacent gas.

We are, in fact, treating the thermal capacity of the sphere as infinite in comparison with that of an equal volume of gas, and are regarding the surface temperature of the sphere as practically constant during a short interval of time. Thus, since our object is to find the temperature state in the space *outside* the sphere, we may change to a uniform medium problem simply by regarding the sphere as an apparatus for maintaining a spherical surface at constant temperature for a short but finite time. We now enquire whether the above conditions can be satisfied by superposing the known effects of certain sources in a *uniform* medium.

The Maintenance of Constant Temperature at a Spherical Surface in a Uniform Medium.

The Fourier equation for a spherically symmetrical distribution of temperature in a uniform medium is

$$\frac{\partial^2\theta}{\partial r^2}+\frac{2}{r}\frac{\partial\theta}{\partial r}=\frac{1}{k}\frac{\partial\theta}{\partial t}, \quad \ldots\ldots \quad (1)$$

where k is the thermometric conductivity of the medium, *i. e.*, its thermal conductivity K divided by its specific heat per unit volume c. The following solutions of equation (1) are known for the different types of source indicated :—

(1) Instantaneous point source, generating amount of heat q :

$$\theta=\frac{qe^{-\frac{r^2}{4kt}}}{8c(\pi kt)^{3/2}}. \quad \ldots\ldots \quad (2)$$

(Fourier, ' Theorie de la Chaleur,' § 385.)

(2) Continued point source, supplying q units of heat per second:

$$\theta=\frac{q}{2kc\pi^{3/2}r}\int_{\frac{r}{2\sqrt{kt}}}^{\infty}e^{-x^2}\,dx. \quad \ldots\ldots \quad (3)$$

(Taylor-Jones, Morgan, and Wheeler, Phil. Mag. xliii. p. 364 (Feb. 1922.))

(3) Instantaneous spherical surface source, supplying Q units of heat distributed uniformly over the whole surface, radius b :

$$\theta = Q\frac{e^{-\frac{(r-b)^2}{4kt}} - e^{-\frac{(r+b)^2}{4kt}}}{8cbr\pi^{3/2}(kt)^{1/2}}. \quad . \quad . \quad . \quad . \quad (4)$$

(Lord Kelvin, Enc. Brit. 9th ed. Art. "Heat," Appendix.) The expression there should be divided by π.

(4) Instantaneous spherical volume source radius b, total heat supply Q :

$$\theta = \frac{3Q}{4cb^3\pi^{3/2}}\left\{\int_0^{\frac{r+b}{2\sqrt{kt}}} e^{-x^2}\,dx - \int_0^{\frac{r-b}{2\sqrt{kt}}} e^{-x^2}\,dx\right\}$$

$$- \frac{3Q}{4cb^3\pi^{3/2}}\frac{(kt)^{1/2}}{r}\left\{e^{-\frac{(r-b)^2}{4kt}} - e^{-\frac{(r+b)^2}{4kt}}\right\}. \quad (5)$$

(Taylor-Jones, Morgan, and Wheeler, *loc. cit.* p. 367.)

To those we may add :

(5) A continued spherical surface source supplying heat Q per second. The distribution due to this source can be derived by integrating equation (4), thus :

$$\theta = Q\int_0^t \frac{e^{-\frac{(r-b)^2}{4kt}} - e^{-\frac{(r+b)^2}{4kt}}}{8cbr\pi^{3/2}(kt)^{1/2}}dt. \quad . \quad . \quad . \quad (6)$$

Where $r<b$, the substitution $x = \dfrac{b-r}{2\sqrt{kt}}$ leads to the expression

$$\theta = \frac{Q}{4\pi^{3/2}bc}\left[\left(\frac{t}{k}\right)^{1/2} e^{-\frac{(r-b)^2}{4kt}} - e^{-\frac{(r+b)^2}{4kt}}}{r}\right]$$

$$- \frac{Q}{4\pi^{3/2}bc}\left[\frac{b-r}{kr}\int_{\frac{b-r}{2\sqrt{kt}}}^{\infty} e^{-x^2}\,dx - \frac{b+r}{kr}\int_{\frac{b+r}{2\sqrt{kt}}}^{\infty} e^{-x^2}\,dx\right].$$

$$. \quad . \quad . \quad (7)$$

When $r>b$ the required substitution is $x=\frac{r-b}{2\sqrt{kt}}$, and gives

$$\theta=\frac{Q}{4\pi^{3/2}bc}\left[\left(\frac{t}{k}\right)^{1/2}\frac{e^{-\frac{(r-b)^2}{4kt}}-e^{-\frac{(r+b)^2}{4kt}}}{r}\right]$$

$$-\frac{Q}{4\pi^{3/2}bc}\left[\frac{r-b}{kr}\int_{\frac{r-b}{2\sqrt{kt}}}^{\infty}e^{-x^2}dx-\frac{r+b}{kr}\int_{\frac{r+b}{2\sqrt{kt}}}^{\infty}e^{-x^2}dx\right]. \quad . \quad . \quad . \quad (8)$$

Now let a be the radius of the surface whose temperature it is desired to maintain constant. We may begin by determining the effect of source (4) in the uniform medium. Let T_0 be written for $\frac{3Q}{4\pi a^3 c}$, the initial temperature of the source. If the resulting distribution is denoted by θ_1, we have

$$\theta_1=\frac{T_0}{\sqrt{\pi}}\left\{\int_0^{\frac{r+b}{2\sqrt{kt}}}e^{-x^2}dx-\int_0^{\frac{r-b}{2\sqrt{kt}}}e^{-x^2}dx\right\}$$

$$-\frac{T_0}{\sqrt{\pi}}\frac{(kt)^{1/2}}{r}\left\{e^{-\frac{(r-b)^2}{4kt}}-e^{-\frac{(r+b)^2}{4kt}}\right\}. \quad (9)$$

Then at the surface $r=a$,

$$\left(\frac{\partial\theta_1}{\partial t}\right)_{r=a}=\frac{T_0}{\sqrt{\pi}}\left\{\frac{a-b}{4\sqrt{k}\,t^{3/2}}e^{-\frac{(a-b)^2}{4kt}}-\frac{a+b}{4\sqrt{k}\,t^{3/2}}e^{-\frac{(a+b)^2}{4kt}}\right\}$$

$$-\frac{T_0}{\sqrt{\pi}}\frac{k^{1/2}}{2at^{1/2}}\left\{e^{-\frac{(a-b)^2}{4kt}}-e^{-\frac{(a+b)^2}{4kt}}\right\}$$

$$+\frac{T_0}{\sqrt{\pi}}\frac{(kt)^{1/2}}{a}\left\{e^{-\frac{(a+b)^2}{4kt}}\frac{(a+b)^2}{4kt^2}-e^{-\frac{(a-b)^2}{4kt}}\frac{(a-b)^2}{4kt^2}\right\}$$

$$. \quad . \quad . \quad (10)$$

Let $b=a$, i. e., let the instantaneous volume source have the required surface as its boundary. Then

$$\left(\frac{\partial\theta_1}{\partial t}\right)_{r=a}=\frac{T_0a}{2\sqrt{\pi k}}\cdot\frac{e^{-\frac{a^2}{kt}}}{t^{3/2}}-\frac{T_0k^{1/2}}{2\sqrt{\pi}\,at^{1/2}}\left\{1-e^{-\frac{a^2}{kt}}\right\}. \quad (11)$$

Since for small values of t, $e^{-\frac{a^2}{kt}}$ is very small, the negative term in (11) is much larger than the positive. θ_1 thus gives a rapid fall in temperature at $r=a$. It is clear that no choice of constants can make $\left(\frac{\partial\theta_1}{\partial t}\right)_{r=a}$ zero at all times. We can, however, superimpose another source upon that already present so as to obtain a resulting time derivative whose modulus is much less than that of $\left(\frac{\partial\theta_1}{\partial t}\right)_{r=a}$. For we see from equation (4) that the distribution due to an instantaneous surface source has $t^{-\frac{1}{2}}$ as a factor, as does the negative term in equation (11). This expression is, however, the time derivative of the distribution due to a continuous spherical surface source, as given in equations (7) and (8). Thus we may denote the distribution due to the continuous surface source by θ_2 and add it to θ_1. Since

$$\left(\frac{\partial\theta_2}{\partial t}\right)_{r=a} = \mathrm{Q}\frac{e^{-\frac{(a-b)^2}{4kt}} - e^{-\frac{(a+b)^2}{4kt}}}{8cba\pi^{3/2}(kt)^{1/2}}, \quad . \quad . \quad (12)$$

if we let the radius b of this source also equal a, then

$$\left(\frac{\partial\theta_2}{\partial t}\right)_{r=a} = \frac{\mathrm{Q}}{8ca^2\pi^{3/2}(kt)^{1/2}}\left\{1-e^{-\frac{a^2}{kt}}\right\}. \quad . \quad (13)$$

Adding this to $\frac{\partial\theta_1}{\partial t}$ and putting $\theta=\theta_1+\theta_2$, we get

$$\left(\frac{\partial\theta}{\partial t}\right)_{r=a} = \frac{\mathrm{T}_0 a}{2\sqrt{\pi k}}\cdot\frac{e^{-\frac{a^2}{kt}}}{t^{3/2}} + \frac{1-e^{-\frac{a^2}{kt}}}{t^{1/2}}\left\{\frac{\mathrm{Q}}{8ca^2\pi^{3/2}k^{1/2}} - \frac{\mathrm{T}_0 k^{1/2}}{2\sqrt{\pi}a}\right\}. \quad (14)$$

Clearly $\mathrm{Q}=4\pi ack\mathrm{T}_0$ makes the second term vanish for all values of t. This gives the value of the rate of heat supply which must be supposed in the superimposed surface source. We are left with

$$\left(\frac{\partial\theta}{\partial t}\right)_{r=a} = \frac{\mathrm{T}_0 a}{2\sqrt{\pi k}}\cdot\frac{e^{-\frac{a^2}{kt}}}{t^{3/2}}. \quad . \quad . \quad . \quad . \quad (15)$$

This positive residual quantity cannot in itself be considered negligible, but it will be shown by calculating arithmetical values of the expression for θ given by the superposition of the two above solutions that its effect during small intervals of time is negligible for at least a satisfactory length of time.

The expression for θ admits of convenient simplification, for, putting $Q = 4\pi ack T_0$ in the superimposed part, we get, for $r < a$,

$$\theta = \frac{T_0}{\sqrt{\pi}}\left\{\int_0^{\frac{a+r}{2\sqrt{kt}}} e^{-x^2}dx + \int_0^{\frac{a-r}{2\sqrt{kt}}} e^{-x^2}dx\right\}$$
$$- \frac{T_0}{\sqrt{\pi}}\frac{(kt)^{1/2}}{r}\left\{e^{-\frac{(r-a)^2}{4kt}} - e^{-\frac{(r+a)^2}{4kt}}\right\}$$
$$+ \frac{kT_0}{\sqrt{\pi}}\left[\left(\frac{t}{k}\right)^{1/2}\frac{e^{-\frac{(r-a)^2}{4kt}} - e^{-\frac{(r+a)^2}{4kt}}}{r}\right.$$
$$\left. - \frac{a-r}{kr}\int_{\frac{a-r}{2\sqrt{kt}}}^{\infty} e^{-x^2}dx + \frac{a+r}{kr}\int_{\frac{a+r}{2\sqrt{kt}}}^{\infty} e^{-x^2}dx\right], \quad (16)$$

$$= \frac{T_0}{\sqrt{\pi}}\left\{\int_0^{\frac{a+r}{2\sqrt{kt}}} e^{-x^2}dx + \int_0^{\frac{a-r}{2\sqrt{kt}}} e^{-x^2}dx\right\}$$
$$- \frac{T_0}{\sqrt{\pi}}\left(\frac{a-r}{r}\right)\int_{\frac{a-r}{2\sqrt{kt}}}^{\infty} e^{-x^2}dx$$
$$+ \frac{T_0}{\sqrt{\pi}}\left(\frac{a+r}{r}\right)\int_{\frac{a+r}{2\sqrt{kt}}}^{\infty} e^{-x^2}dx. \quad . \quad . \quad . \quad . \quad . \quad (17)$$

Some of the definite integrals combine to give

$$\int_0^{\infty} e^{-x^2}dx = \frac{\sqrt{\pi}}{2}$$

and θ becomes

$$= T_0 - \frac{T_0}{\sqrt{\pi}}\frac{a}{r}\int_{\frac{a-r}{2\sqrt{kt}}}^{\infty} e^{-x^2}dx + \frac{T_0}{\sqrt{\pi}}\frac{a}{r}\int_{\frac{a+r}{2\sqrt{kt}}}^{\infty} e^{-x^2}dx, \quad r < a.$$
$$. \quad . \quad . \quad (18)$$

Similar simplification of the corresponding expression for $r>a$ gives, since the signs of some of the definite integrals are changed,

$$\theta = \frac{T_0}{\sqrt{\pi}} \frac{a}{r} \int_{\frac{r-a}{2\sqrt{kt}}}^{\infty} e^{-x^2} dx + \frac{T_0}{\sqrt{\pi}} \frac{a}{r} \int_{\frac{r+a}{2\sqrt{kt}}}^{\infty} e^{-x^2} dx, \quad r>a. \quad (19)$$

This is zero when $t=0$, as is required. Moreover, the expressions (18) and (19) agree when $r=a$, and we have, when $t \neq 0$,

$$\theta_{r=a} = \frac{T_0}{2} + \frac{T_0}{\sqrt{\pi}} \int_{\frac{a}{\sqrt{kt}}}^{\infty} e^{-x^2} dx. \quad . \quad . \quad . \quad (20)$$

Now because of the instantaneous volume source, the initial temperature of the surface $r=a$ is T_0. But a characteristic of the distribution due to that source is that the surface temperature, as soon as t is not zero, drops to $T_0/2$ (*vide* Taylor-Jones, Morgan and Wheeler, *loc. cit.* p. 367). The same happens in our case, but then the growth of temperature due to the coincident continued spherical surface source compensates for any further fall. The temperature at $r=a$ is then appreciably constant at $T_0/2$, until the term $\frac{T_0}{\sqrt{\pi}} \int_{\frac{a}{\sqrt{kt}}}^{\infty} e^{-x^2} dx$ becomes significant. This is clearly seen from equation (20). The smaller the radius a, the sooner will the rise in temperature be appreciable.

Tables I. and II. show the distribution given by θ at various times for values of a respectively 0·25 cm. and 0·1 cm. They show that this combination of sources, which we shall call Solution I., does serve to keep the surface $r=a$ at constant temperature for an appreciable time after $t=0$. They also indicate the time at which the temperature at the surface begins to rise perceptibly. The temperatures are shown as fractions of T_0, and are calculated for air, taking $k=0{\cdot}5$.

The plotting of these values in figs. 1 and 2 shows clearly how the distribution curves rotate round the point $r=a$, $\theta=T_0/2$, as t increases, for small times.

The Application to the Metal and Gas Problem.

This has been made directly by taking $T_0/2$ as the original temperature of the metal sphere and a as its radius. The values given above, for $r>a$, can then be

TABLE I.

Solution I. $a=0{\cdot}25$ cm.

t, seconds.	Temperature / T_0 at r cm.							
	0	0·22	0·25	0·26	0·30	0·35	0·45	0·60
0·0001	1·0000	0·9984	0·5000	0·1527	0	0	0	0
0·001	0·9999	0·8053	0·5000	0·3613	0·0475	0·0006	0	0
0·01	0·9123	0·5657	0·5000	0·4423	0·257	0·1135	0·0125	0
0·02	0·7044	0·5278	0·5002	0·4536	0·3016	0·1713	0·0437	0·0027

TABLE II.

Solution I. $a=0{\cdot}1$ cm.

t, seconds.	Temperature / T_0 at r cm.							
	0	0·07	0·1	0·11	0·13	0·20	0·25	0·35
0·0001	1	0·9980	0·5000	0·1444	0·0011	0	0	0
0·001	0·9653	0·7552	0·5000	0·3416	0·1318	0·0004	0	0
0·02	0·5160	0·5194	0·5227	0·4345	0·3022	0·0801	0·0268	0·0017

used as approximations to the temperature distribution in the gas, so long as the time in question is one for which the rise in temperature at $r=a$ is negligible. Tables I. and II. thus give us an idea of the limit of time up to which Solution I. may be applied to the metal sphere and gas problem. This time may be called the *Limit of Application* of Solution I. For $a=0{\cdot}25$ cm. it is somewhat greater than 0·02 second, and for $a=0{\cdot}1$ cm. it is about

0·01 second. We are, of course, here concerned only with temperatures in the gas outside the radius $r=a$, and the portions of the curves in figs. 1 and 2 for $r>0{\cdot}25$ cm. and $>0{\cdot}1$ cm. respectively are thus assumed to give the required values.

Fig. 1.

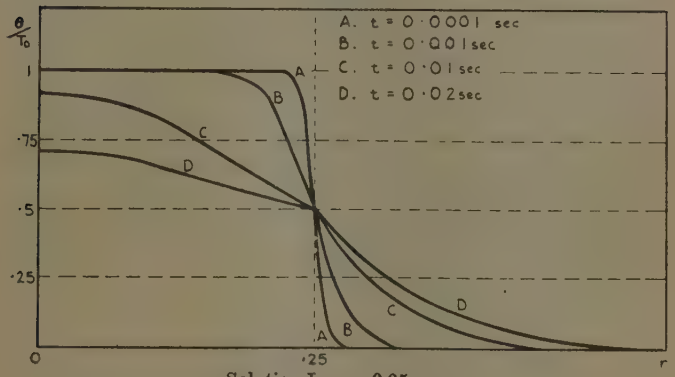

Solution I. $a=0{\cdot}25$ cm.

Fig. 2.

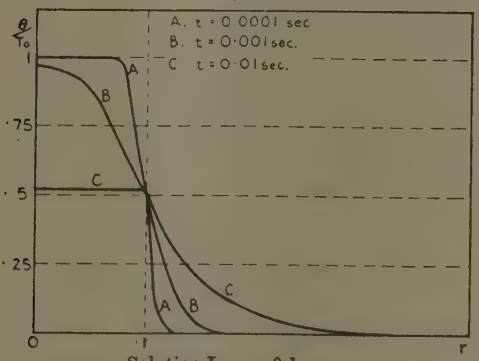

Solution I. $a=0{\cdot}1$ cm.

It may be pointed out that, in making this application, the instantaneous temperature T_0 of the surface of the instantaneous volume source in the uniform medium is entirely ignored. This is justifiable, considering the suddenness of the drop to $T_0/2$.

An Alternative Solution.

We have seen that Solution I. causes a rise in temperature at $r=a$ when the initial period of constancy is past. This is a distinct difference from the conditions prevailing in the sphere and gas problem, where the temperature must begin to fall. It is possible, however, to add another of the spherical solutions given on pp. 468–470 to Solution I. so as to obtain a distribution which indicates falling temperature at $r=a$, after a preliminary period of approximate constancy. (The instantaneous volume source alone would, of course, provide such a fall of temperature, but this would be much too rapid for the conditions of our problem, since it would make no allowance for the capacity of the sphere relative to that of the gas.)

This second solution, which we shall call Solution II., may be obtained as follows :—Let the distribution given by Solution I. be denoted by ϕ. Then

$$\left(\frac{\partial\phi}{\partial t}\right)_{r=a} = \frac{T_0 a}{2\sqrt{\pi k}} \frac{e^{-\frac{a^2}{kt}}}{t^{3/2}} \quad . \quad . \quad . \quad . \quad . \quad (21)$$

Examining the list of known solutions, we find that equation (2), which represents the distribution due to an instantaneous point source, consists of a term in $t^{-\frac{3}{2}}$, *i. e.*, the derivative of a continuous point source solution consists of a term in $t^{-\frac{3}{2}}$, which is the power of t in equation (21). So let us imagine that we have, in addition to the sources of Solution I., a continuous point *sink* at the centre, which absorbs heat q per second, If the resulting distribution is now θ, we have

$$\left(\frac{\partial\theta}{\partial t}\right)_{r=a} = \frac{T_0 a}{2\sqrt{\pi k}} \frac{e^{-\frac{a^2}{kt}}}{t^{3/2}} - q \frac{e^{-\frac{a^2}{4kt}}}{8c(\pi kt)^{3/2}} \quad . \quad . \quad (22)$$

Defining q as $4\pi ack T_0$, this becomes

$$\left(\frac{\partial\theta}{\partial t}\right)_{r=a} = \frac{T_0 a}{2\sqrt{\pi k}} \cdot \frac{e^{-\frac{a^2}{kt}} - e^{-\frac{a^2}{4kt}}}{t^{3/2}} \quad . \quad . \quad (23)$$

Now $e^{-\frac{a^2}{4kt}} > e^{-\frac{a^2}{kt}}$, so that $\left(\frac{\partial\theta}{\partial t}\right)_{r=a}$ is negative at $r=a$.

The expression for the temperature distribution due to all three sources superimposed now becomes :

(a) $r > a$,

$$\theta = \frac{T_0}{\sqrt{\pi}} \frac{a}{r} \int_{\frac{r-a}{2\sqrt{kt}}}^{\infty} e^{-x^2} dx + \frac{T_0}{\sqrt{\pi}} \frac{a}{r} \int_{\frac{r+a}{2\sqrt{kt}}}^{\infty} e^{-x^2} dx - \frac{2T_0}{\sqrt{\pi}} \cdot \frac{a}{r} \int_{\frac{r}{2\sqrt{kt}}}^{\infty} e^{-x^2} dx ; \quad . \quad (24)$$

(b) $r < a$,

$$\theta = T_0 - \frac{T_0}{\sqrt{\pi}} \frac{a}{r} \int_{\frac{a-r}{2\sqrt{kt}}}^{\infty} e^{-x^2} dx + \frac{T_0}{\sqrt{\pi}} \frac{a}{r} \int_{\frac{a+r}{2\sqrt{kt}}}^{\infty} e^{-x^2} dx - \frac{2T_0}{\sqrt{\pi}} \int_{\frac{r}{2\sqrt{kt}}}^{\infty} e^{-x^2} dx. \quad (25)$$

The temperature at $r = a$ according to (24) and (25) is

$$\theta_{r=a} = \frac{T_0}{2} + \frac{T_0}{\sqrt{\pi}} \int_{\frac{a}{\sqrt{kt}}}^{\infty} e^{-x^2} dx - \frac{2T_0}{\sqrt{\pi}} \int_{\frac{r}{2\sqrt{kt}}}^{\infty} e^{-x^2} dx. \quad (26)$$

We see that this is approximately constant at $T_0/2$, until the term $-\frac{2T_0}{\sqrt{\pi}} \int_{\frac{a}{2\sqrt{kt}}}^{\infty} e^{-x^2} dx$ becomes significant. It then begins to fall. This occurs much sooner than the rise in Solution I., as is shown by the numerical values given (also for $a = 0{\cdot}25$ cm. and $a = 0{\cdot}1$ cm.) in Tables III. and IV. The corresponding curves for Solution II. are given in figs. 3 and 4.

Now if we are to confine the use of Solutions I. and II. in the metal sphere and gas problem only to values of t for which the surface temperature may be assumed constant, Solution II. will cease to apply sooner than the first, since $2\int_{\frac{a}{2\sqrt{kt}}}^{\infty} e^{-x^2} dx$ becomes significant before $\int_{\frac{a}{\sqrt{kt}}}^{\infty} e^{-x^2} dx$. We see from equations (19) and (25) that the

two solutions give identical distributions for $r > a$, up to the time when the second begins to fall at $r = a$. After that, II. has a smaller gradient than I. For $r < a$ they do not coincide, because the presence of the sink requires $-\infty$ for the temperature at the centre.

TABLE III.

Solution II. $a = 0{\cdot}25$ cm.

t, seconds.	Temperature / T_0 at r cm.							
	0	0·22	0·25	0·26	0·30	0·35	0·45	0·60
0·0001	$-\infty$	0·9984	0·5000	0·1527	0	0	0	0
0·001	$-\infty$	1·0000	0·5000	0·3613	0·0475	0·0006	0	0
0·01	$-\infty$	0·5340	0·4875	0·4334	0·2548	0·1135	0·0125	0
0·02	$-\infty$	0·3917	0·4232	0·3911	0·2734	0·1618	0·0873	0·0027

TABLE IV.

Solution II. $a = 0{\cdot}1$ cm.

t, seconds.	Temperature / T_0 at r cm.							
	0	0·07	0·10	0·11	0·13	0·20	0·25	0·35
0·0001	$-\infty$	0·9980	0·5000	0·1444	0·0011	0	0	0
0·001	$-\infty$	0·7011	0·4984	0·3412	0·1318	0·0004	0	0
0·01	$-\infty$	0·2969	0·2150	0·1878	0·1530	0·0576	0·0218	0·0017

Since the distributions are at first equal for $r > a$, the question as to which of the two solutions is more suitable in the application is simply the question of how long we are entitled to assume constancy of temperature at the surface of the metal sphere. It depends, therefore, on the capacity of the metal sphere relative to that of the gas. The larger this is, the longer we can assume constancy to continue, so that for a very large capacity

we may use Solution I. up to its limit of constancy. With a sphere of smaller capacity constancy can only be assumed to last for a shorter time, so that it may be un-

Fig. 3.

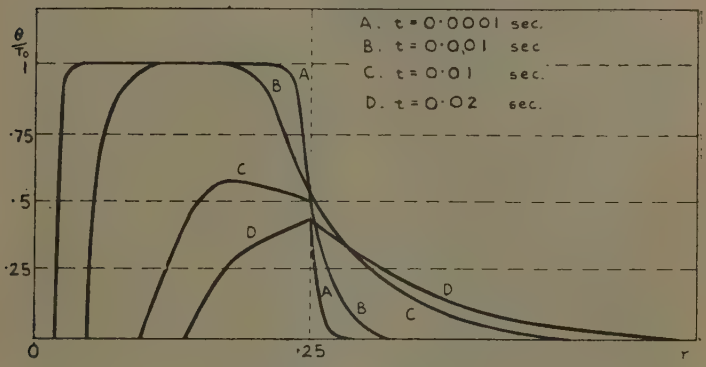

Solution II. $a = 0{\cdot}25$ cm.

Fig. 4.

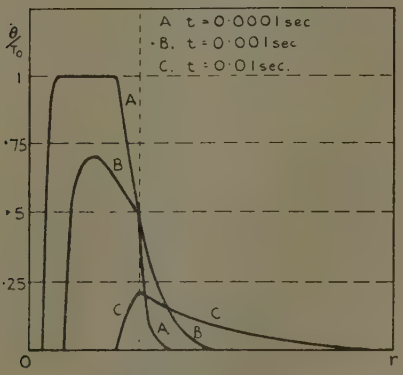

Solution II. $a = 0{\cdot}1$ cm.

suitable to use the solutions for times after the beginning of the fall of temperature at $r = a$ in Solution II.

It is possible that a still closer approximation to the conditions of the sphere and gas problem, applicable to still later times, could be arrived at by superposing the

effects of a fourth or a fifth hypothetical source in a uniform medium, but it is thought that for the purposes of the experimental work in connection with which these calculations were undertaken, Solutions I. and II. give a sufficiently close approximation, provided they are not used beyond their time limitations.

It is tempting to suppose that Solution II. will continue to hold as an approximation to the distribution in the gas even after it shows appreciable fall in the surface temperature, since this actually occurs with the metal sphere. The same, however, might be said for an instantaneous volume source alone, except for the difference in degree. Solution II. only represents an improvement upon the instantaneous volume solution in so far as, its fall of temperature at $r=a$ being more gradual, it allows for the capacity of the sphere. This allowance may be inadequate if it is used beyond the point we have discussed. Hence it is advisable meantime to confine the application of these solutions in the problem of the temperature distribution in the gas round a metal sphere rigidly to the supposition of constant temperature maintained at the surface of the sphere.

I should like to acknowledge the valuable help and encouragement I have received from Professor E. Taylor-Jones, both in the matter of this paper and in the experimental work to which it refers. I am indebted to Imperial Chemical Industries, Ltd., at whose suggestion the experimental work was undertaken, for permission to publish, and for a personal grant ; also to Dr. G. Green for his interest and for a number of references.

The experimental work is being carried out in the Research Laboratories of the Natural Philosophy Department of Glasgow University. It is hoped to publish an account of that work in the future.

References.

(1) J. Robertson, Phil. Mag. xviii. p. 165 (1934).
(2) G. Green, Phil. Mag. ix. p. 241 (1930) (and previous).
(3) R. E. Langer, Tohoku Math. Journ. xxxv. p. 260 (1932).
(4) J. H. Awbery, Phil. Mag. iv. p. 629 (1927).
(5) H. S. Carslaw, Proc. Camb. Phil. Soc. xx. p. 401 (1920–21).
(6) T. J. Bromwich, Proc. Camb. Phil. Soc. xx. p. 411 (1920–21).

XXXIX. *Reproduction of Transients by a Television Amplifier.* By N. W. McLachlan, *D.Sc., M.I.E.E.* *

1. *Introduction.*

THE approach of television has been heralded by thermionic valve amplifiers designed to cover a very wide frequency range. Using screened-grid valves and suitable circuit arrangements, the response

Fig. 1 *a*.

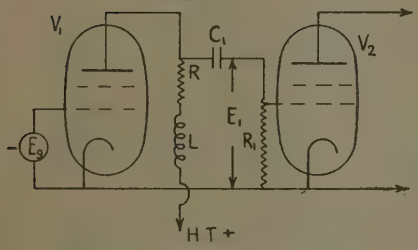

Fig. 1 *b*.

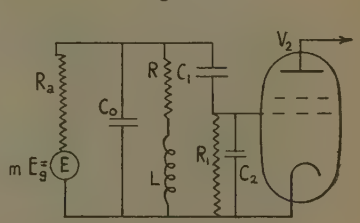

Fig. 1 *a*. Illustrating coupling circuit between two screened-grid valves.
Fig. 2 *b*. Equivalent circuit of fig. 1 *a*. C_0=anode to cathode capacitance+leads; C_2=grid to cathode capacitance+leads.

Fig. 2 *a*.

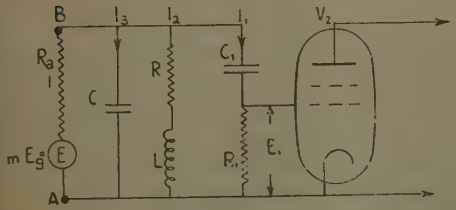

Fig. 2 *b*.

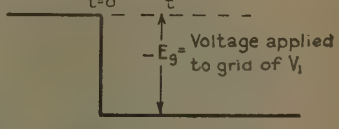

Fig. 2 *a*. Circuit equivalent to figs. 1 *a* and 1 *b*, when $C_1 >> C_2$ and $R_1 >> 1/\omega C_1$; $C = C_0 + C_2$; E_1=output voltage from V_1=input voltage to V_2.
Fig. 2 *b*. Illustrating form of voltage applied to input of V_1 in fig. 1 *a*.

characteristic of an amplifier can be made sensibly flat over a range of about a megacycle. A circuit described by C. H. Smith † is illustrated in figs. 1 *a* and 1 *b*. If $C_1 >> C_2$ and the impedance of $R_1 >>$ that of C_1 over the frequency

* Communicated by the Author.
† 'World Radio,' June 8th, 1934, p. 834.

range, C_2 can be considered to be in parallel with C_0. Under these conditions fig. 1 *b* degenerates to fig. 2 *a*, where $C=C_0+C_2$, this being the sum of the following capacitances: (*a*) anode to cathode of the valve V_1, (*b*) grid to cathode of valve V_2, (*c*) leads and wiring associated with (*a*) and (*b*). The inductance L, whose self-capacitance and capacitance to earth are assumed to be negligible, offsets the shunting effect of C at the upper or radio-frequency end of the range. Each transient is accompanied by a highly damped oscillation whose frequency is given approximately by $n=\frac{1}{2\pi}\sqrt{\frac{1}{LC}-\frac{R^2}{4L^2}}$, provided $\frac{1}{LC}>\frac{R^2}{4L^2}$ and ωC, ωL, and R are small enough compared with R_a and R_1. The oscillation can be suppressed either by increasing R or by connecting a damping resistance in parallel with L, but this modifies the performance of the amplifier.

We shall consider the response of the circuit of fig. 2 *a* to a transient whose form is that of Heaviside's unit function, as shown in fig. 2 *b* *. The mathematical solution of the problem is obtained first in terms of the operator $\sigma=d/dt$, and it is then interpreted in terms of the running variable *t*.

2. *Analysis of Circuit of Fig.* 2 *a*.

This circuit is equivalent to the valve circuit of fig. 1 *a*. R_a represents the internal A.C. resistance of V_1, whilst $mE_g=E$ is the product of the amplification factor and the voltage applied to the grid. The voltage across AB, namely, $E-IR_a$, is applied to the three branches C, RL, and C_1R_1 in parallel. Thus we have the following relationships:

$$E-R_aI=\frac{I_3}{\sigma C}=(R+\sigma L)I_2=\left(R_1+\frac{1}{\sigma C_1}\right)I_1. \quad . \quad (1)$$

The alternating current in the valve is equal to the sum of the three branch currents, so

$$I=I_1+I_2+I_3. \quad , \quad . \quad . \quad . \quad . \quad . \quad (2)$$

* The voltage applied to the grid of the valve is $-E_g$, since the phase of the voltage in the equivalent circuit of fig. 2 *a* is opposite to this.

From (1) we obtain

$$I = \frac{E}{R_a} - \left(\frac{1+\sigma C_1 R_1}{\sigma C_1 R_a}\right) I_1; \quad . \quad . \quad . \quad . \quad (3)$$

$$I_2 = \frac{(1+\sigma C_1 R_1) I_1}{\sigma C_1 (R+\sigma L)}; \quad . \quad . \quad . \quad . \quad . \quad . \quad . \quad (4)$$

and

$$I_3 = (1+\sigma C_1 R_1) \frac{C}{C_1} I_1. \quad . \quad . \quad . \quad . \quad . \quad . \quad . \quad (5)$$

Substituting from (3), (4), and (5) in (2), we get

$$I_1 \left\{ 1+(1+\sigma C_1 R_1)\left[\frac{1}{\sigma C_1 R_a} + \frac{1}{\sigma C_1 (R\sigma+L)} + \frac{C}{C_1}\right]\right\} = E/R_a,$$

. . . (6)

which, after simplification, gives

$$I_1 = \frac{E}{LCR_1 R_a} \cdot \left[\frac{\sigma(R+\sigma L)}{\sigma^3+\alpha\sigma^2+\beta\sigma+\gamma}\right], \quad . \quad . \quad . \quad (7)$$

where

$$\alpha = \frac{R}{L} + \frac{1}{R_1}\left(\frac{1}{C} + \frac{1}{C_1}\right) + \frac{1}{CR_a},$$

$$\beta = \frac{1}{LC}\left(1 + \frac{R}{R_a} + \frac{R}{R_1}\right) + \frac{1}{C_1 R_1}\left(\frac{R}{L} + \frac{1}{CR_a}\right),$$

and

$$\gamma = (R+R_a)/LCC_1 R_1 R_a.$$

The following values are based on data in C. H. Smith's paper :—

$R_a = 5\times10^5$ ohms ; $R_1 = 10^6$ ohms ; $R = 5\times10^3$ ohms ; $L = 5\times10^{-4}$ henry ; $C_1 = 10^{-1}$ mfd. ; $C = 30$ mmfd.; m of valve 3000. Using these values we find, with adequate approximation, that $\alpha = R/L = 10^7$; $\beta = 1/LC = 6{\cdot}667\times10^{13}$; and $\gamma = 1/LCC_1R_1 = 6{\cdot}667\times10^{14}$. To interpret the operational solution (7) in terms of t, we must first solve the cubic equation

$$\sigma^3+\alpha\sigma^2+\beta\sigma+\gamma = (\sigma+a)(\sigma+b)(\sigma+c) = 0. \quad . \quad . \quad . \quad (8)$$

From above we see that $\alpha<<<\beta<<\gamma$, and the first root of (8) is obtained with adequate accuracy by putting $\beta\sigma+\gamma=0$, which gives

$$a = \gamma/\beta = 1/C_1R_1 = 10^{-1} \ldots \quad . \quad . \quad . \quad . \quad . \quad (9)$$

The remaining roots of (8) are found on dividing by $(\sigma+a)$, which yields

$$b=\frac{1}{2}\frac{R}{L}+i\sqrt{\frac{1}{LC}-\frac{R^2}{4L^2}}$$

and

$$c=\frac{1}{2}\frac{R}{L}-i\sqrt{\frac{1}{LC}-\frac{R^2}{4L^2}},$$

where $i=\sqrt{-1}$.

3. *Interpretation of* (7) *in terms of* t.

By the Bromwich rule * we have

$$E_1=I_1R_1=\frac{E}{LCR_a}\left[\frac{1}{2\pi i}\int_L\frac{e^{zt}(R+zL)\,dz}{(z+a)(z+b)(z+c)}\right]. \quad (10)$$

Fig. 3.

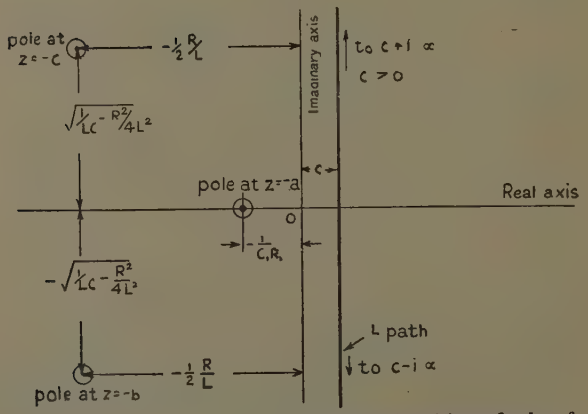

Showing z-plane, L-path of integration, and positions of poles of integrand in (10).

The integrand in (10) has three simple poles at $z=-a$, $-b$, and $-c$, as shown in fig. 3. The integral along the L-path † is then equal to that round a circle which encloses all the poles, and the value of that part of (10) within the brackets is equal to the sum of the residues at the

* Jeffreys, ' Operational Methods in Mathematical Physics,' Chapter 2.

† The symbol L for the L-path of integration must not be confused with the symbol L for inductance.

poles. The residue at $z=-a$ is $(R-aL)e^{-at}/(b-a)(c-a)$; at $z=-b$ it is $(R-bL)e^{-bt}/(a-b)(c-b)$; and at $z=-c$ it is $(R-cL)e^{-ct}/(a-c)(b-c)$. Hence the voltage output from one stage of amplification is*

$$E_1 \doteqdot \frac{E}{LCR_a}\left[\frac{Re^{-t/C_1R_1}}{bc} + \frac{(R-bL)e^{-(R/2L+iq)t}}{b(b-c)} - \frac{(R-cL)e^{-(R/2L-iq)t}}{c(b-c)}\right], \quad . \quad . \quad . \quad (11)$$

where $q=\sqrt{\frac{1}{LC}-\frac{R^2}{4L^2}}$, and certain terms containing a are omitted as being negligible. When the numerical values of b, c, and q are used, it is found that (11) can be written

$$E_1 \doteqdot \frac{ER}{R_a}\left[e^{-t/C_1R_1} - \frac{e^{-Rt/2L}}{CRq}\sin(qt+\theta)\right], \quad . \quad (12)$$

where $\theta=\tan^{-1} CRq\left(\frac{CR^2}{2L}-1\right)$, and $\sin\theta=CRq$. From (12) we see that the quantity in brackets vanishes at $t=0$, as it should. The voltage output consists of two parts: (1) an exponential decay component, (2) a highly damped sine wave of frequency about one megacycle per second. The beginning of the reproduced transient is illustrated in curve 1 of fig. 4. Owing mainly to the charge to capacitance C in fig. 2 *a*, the voltage does not attain the value ER/R_a until after a lapse of time of $2{\cdot}04\times10^{-7}$ second. Having reached this value, it overshoots by 15 per cent., owing to the oscillation arising from the LCR circuit. This oscillation is superposed upon the main voltage, which would be of square form in the absence of distortion due to the inter-valve coupling circuit.

The time to reach the voltage $E_1=ER/R_a$ is easily found from (12). When $\sin(qt+\theta)$ has its first zero, t is extremely small and $e^{-t/C_1R_1}\doteqdot1$. We have, therefore, $qt+\theta=\pi$, or $6{\cdot}46\times10^6t+1{\cdot}824=\pi$, which gives $t\doteqdot2{\cdot}04\times10^{-7}$ or about $\frac{1}{5}$th microsecond.

4. *Approximation to* (10) *when t is very small.*

When t is of the order of a few hundredths of a microsecond, the main contribution to the value of (10) occurs

* $\doteqdot$ means "approximately equal to."

when z is very large. Consequently a, b, c, and R are negligible, and we may write

$$E_1 \doteqdot \frac{E}{CR_a} \cdot \frac{1}{2\pi i}\int_L \frac{e^{zt}}{z^2}dz = Et/CR_a. \quad . \quad . \quad (13)$$

From (13) it follows that the initial portion of the reproduced voltage curve 1 of fig. 4 is linear.

By differentiating (12) and equating to zero we can determine the time which elapses between the application of the voltage $-E_g$ to the grid of the valve and the occurrence of the first maximum of the voltage across the output resistance R_1 (fig. 2 *a*).

Fig. 4.

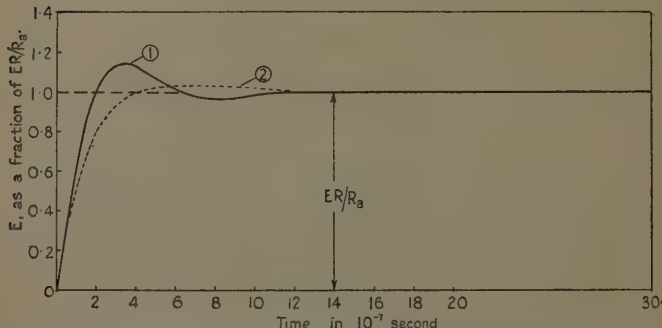

Curve 1.—Reproduced transient using the circuit of fig. 1 *a* ≡ fig. 2 *a*.
Curve 2.—Reproduced transient using the circuit of fig. 1 *a* and a damping resistance R_3 across L to make the LCR circuit aperiodic. In each case, the voltage across R_1 is plotted.

Thus

$$\frac{dE_1}{dt} = \frac{ER}{R_a}\left\{ -\frac{e^{-t/C_1R_1}}{C_1R_1} + \frac{e^{-R/2L}}{CR\sqrt{1-CR^2/4L}}[\sin(qt+\theta-\phi)]\right\}, \quad . \quad . \quad (14)$$

where $$\phi = \tan^{-1} 2Lq/R.$$

Inserting in (14) the numerical data given above, and equating to zero, we obtain

$$\sin(0{\cdot}646\tau + 0{\cdot}913) \doteqdot 1{\cdot}185 \times 10^{-6} e^{\frac{1}{2}\tau}. \quad . \quad . \quad (15)$$

As an approximation assume the right-hand side of (15) to be zero, then

$$\sin(0{\cdot}646\tau+0{\cdot}913)=0, \text{ or } 0{\cdot}646\tau+0{\cdot}913=\pi,$$

which gives $\tau=3{\cdot}45$ and, therefore,

$$t=3{\cdot}45\times10^{-7}\doteqdot\tfrac{1}{3} \text{ microsecond.} \quad . \quad . \quad . \quad (16)$$

If we put $\tau=3{\cdot}45$ in the right hand-side of (15) its value is of order 7×10^{-6}, so the preceding approximation is justifiable.

If the source $-E_0$ in fig. 1 *a* is short-circuited after a time t_1 when $E_1\doteqdot ER/R_a$, there is a transient oscillation as discussed above, and condenser C_1 discharges through the remainder of the circuit. The voltage across R_1 is therefore reduced to zero and ultimately becomes very slightly negative [according to the value of $(e^{-t_1/C_1R_1}-1)$].

5. *Transient of the Form* $E=E_0e^{-\alpha t}\sin\omega t$.

The solution in this case is obtained in operational form if E in (7) is replaced by the operational expression for $E_0e^{-\alpha t}\sin\omega t$. This is

$$E_0\omega\sigma/[\sigma+\alpha)^2+\omega^2],$$

so we have

$$E_1=\frac{E_0\omega}{LCR_a}\cdot\frac{1}{2\pi i}\int_L\frac{e^{zt}z(R+zL)dz}{(z+a)(z+b)(z+c)\{(z+\alpha)^2+\omega^2\}}. \quad (17)$$

The integrand of (17) has five simple poles at $z=-a$, $-b$, $-c$, and $-\alpha\pm i\omega$. To evaluate (17) it is necessary to find the residue at each pole in the usual way. The residue at the pole $z=-a$ on the real axis introduces an exponential term Ae^{-t/C_1R_1}, the residues at the poles $-b$, $-c$ introduce a term $Be^{-\frac{1}{2}Rt}\sin(qt+\psi)$, whilst those at $-\alpha\pm i\omega$ give a damped oscillation of the type $e^{-\alpha t}\sin(\omega t+\chi)$. The solution of (17), therefore, takes the form

$$E_1=Ae^{-t/C_1R_1}+Be^{-\frac{1}{2}Rt}\sin(qt+\psi)+Ce^{-\alpha t}\sin(\omega t+\chi), \quad . \quad (18)$$

where A, B, C, ψ, and χ are constants. The solution for any other type of transient is obtained in like manner.

The distortion of the impressed transient is represented by the first two terms of (18) plus the phase shift χ. The first term is associated with the charging of condenser

C_1 of fig. 2 *a*, and the second with the transient oscillation discussed heretofore.

By making z very large and neglecting the quantities R, a, b, c, α, and ω, we can determine the form of E_1 when t is extremely small. Thus (17) becomes

$$E_1 \doteqdot \frac{E_0\omega}{CR} \cdot \frac{1}{2\pi i}\int_L \frac{e^{zt}}{z^3}dz = E_0\omega t^2/2CR_a. \quad . \quad (19)$$

The slope of $E_0e^{-\alpha t}\sin\omega t$ at $t=0$ is ωE_0, whereas from (19) the slope of the reproduced transient is zero. The influence of the circuit is—as in the previous case—to cause a time lag in the initiation of the impulse, this lag being due chiefly to the time taken to charge C in fig. 2 *a*.

6. *n Identical Stages of Amplification*: *Transient of Fig. 2 b.*

If the short-lived transient oscillation, which occurs after switching on, is neglected, then from (17)

$$E_1 = \frac{ER}{R_a}e^{-t/C_1R_1}, \quad . \quad . \quad . \quad . \quad . \quad . \quad (20)$$

this being the voltage across R_1.

The operational form of (20) is

$$E_1 = \frac{ER}{R_a} \cdot \sigma \Big/ \left(\sigma + \frac{1}{C_1R_1}\right),$$

so that E_2, the voltage output from the second valve, is obtained by substituting E_1 in this formula for E, and multiplying by the m-factor of the valve.

Thus

$$E_2 = mE_1\frac{R}{R_a} \cdot \sigma \Big/ \left(\sigma + \frac{1}{C_1R_1}\right) = E\left(\frac{R}{R_a}\right)^2 \frac{m\sigma^2}{\left(\sigma + \frac{1}{C_1R_1}\right)^2}; \quad (21)$$

and obviously

$$E_n = E\left(\frac{R}{R_a}\right)^n \frac{m^{n-1}\sigma^n}{(\sigma + 1/C_1R_1)^n} \quad . \quad . \quad . \quad (22)$$

$$= E_g\left[\frac{R}{R} \cdot \frac{m\sigma}{\sigma + 1/C_1R_1}\right]^n \quad . \quad . \quad . \quad . \quad (23)$$

$(n \geqslant 1)$, since $E = mE_g$.

The interpretation of (22) is

$$E_n = E\left(\frac{R}{R_a}\right)^n m^{n-1} \cdot \frac{1}{2\pi i}\int_L \frac{e^{zt}z^{n-1}}{(z+a)^n}\,dz\,; \quad . \quad (24)$$

where $a = 1/C_1R_1$.

The only singularity of the integrand in (24) is a pole of order n at $z=-a$. To evaluate (24) we find the residue at the pole, this being the coefficient of $1/(z+a)$ in the integrand. The procedure is to multiply the integrand by $(z+a)^n$, thereby removing the pole—in effect—differentiate the remainder $(n-1)$ times, divide by $(n-1)!$ and put $z=-a$. Thus we obtain

$$E_n = E\left(\frac{R}{R_a}\right)^n \frac{m^{n-1}}{(n-1)!} \cdot \frac{d^{n-1}}{dz^{n-1}}\left[e^{zt}z^{n-1}\right]_{z=-a}, \quad . \quad (25)$$

which is a convenient form for the solution, since the differentiation is simple. In deducing (25), the time delay in reaching the ultimate voltage (corresponding to ER/R_a in fig. 4) was neglected. For one stage of amplification the delay was computed in § 3 to be about $\frac{1}{5}$ microsecond, so to a first approximation the lag for three stages will be $\frac{3}{5}$ microsecond.

When the value of E_n is found for n identical stages, without neglecting the transient oscillation, we have from (7), operationally,

$$E_n = \frac{E_g}{(LCR_a)^n}\left[\frac{m\sigma(R+\sigma L)}{(\sigma+a)(\sigma+b)(\sigma+c)}\right]^n, \quad . \quad . \quad (26)$$

and interpretationally

$$E_n = \frac{E_g m^n}{(LCR_a)^n}\,\frac{1}{2\pi i}\int_L \frac{e^{zt}z^{n-1}(R+zL)^n dz}{[(z+a)(z+b)(z+c)]^n}. \quad . \quad (27)$$

Using the same procedure as at (25), the contribution arising from the residue at the pole $z=-a$ is

$$\frac{E_g}{(LCR_a)^n}\,\frac{m^n}{(n-1)!}\,\frac{d^{n-1}}{dz^{n-1}}\left[\frac{e^{zt}z^{n-1}(R+zL)^n}{\{(z+b)(z+c)\}^n}\right]_{z=-a}. \quad . \quad . \quad (28)$$

The contributions arising from the poles $z=-b$, $-c$ are obtained in like manner, the sum of the three being the value of E_n.

By making z very large in (27) and neglecting a, b, c,

and R, we find the voltage, when t is extremely small, to be

$$E_n \doteqdot \frac{Em^{-1}}{(CR_a)^n} \cdot \frac{1}{2\pi i} \int \frac{e^{zt}}{z^{n+1}} dz = Em^{n-1}t^n/(CR_a)^n n ! \quad . \quad . \quad (29)$$

It follows from (29) that the initial rate of rise of voltage is decreased by increasing the number of stages of amplification, as one would anticipate from practical considerations. To find the time at which the maximum value of E_n occurs, we differentiate (27) with respect to t and equate to zero, which gives

$$\frac{dE_n}{dt} = \frac{Em^{n-1}}{(LCR_a)^n} \cdot \frac{1}{2\pi i} \int_L e^{zt} \left[\frac{z(R+zL)}{(z+a)(z+b)(z+c)} \right]^n dz = 0. \quad . \quad . \quad . \quad (30)$$

To determine t the contour integral must first be evaluated, as shown above, and the result equated to zero.

7. *Circuit of Fig.* 2 *a with Damping Resistance across* L.

We have seen that each transient is accompanied by a highly damped oscillation whose frequency is approximately one megacycle per second, and that the voltage shoots beyond its proper value (fig. 4, curve 1). To curb the oscillation, a damping resistance R_3 may be connected in parallel with L in fig. 2 *a*. The operational form of the solution is obtained when σL in (6) is replaced by $\sigma LR_3/(R_3+\sigma L)$, the latter being the impedance operator for L and R_3 in parallel. If R_3 is of the same order of magnitude or less than R, then, using the same data as before, the output voltage of the valve V_1 is given by

$$E_1 = E\sigma(kR+\sigma L)/LCR_a(\sigma^3+\alpha_1\sigma^2+\beta_1\sigma+\gamma_1), \quad (31)$$

where $\alpha_1 \doteqdot \frac{kR}{L} + \frac{1}{CR_4}$; $\beta_1 \doteqdot \frac{k}{LC}$; $\gamma_1 \doteqdot \frac{k}{LCC_1R_1}$; $k = R_3/R_4$;

and $R_4 = R+R_3$. The cubic equation in the denominator of (31) can be written

$$\left(\sigma + \frac{1}{C_1R_1}\right)\left(\sigma^2 + \frac{kR}{L}\sigma + \frac{k}{LC}\right).$$

The initial part of the transient can be modified by altering the value of k, i. e., of R_3. The condition for aperiodicity is

$$k/LC \leqslant \frac{1}{4}\left(\frac{kR}{L} + \frac{1}{CR_4}\right)^2$$

Using the above numerical data we obtain

$$R_3 \leqslant 1890 \text{ ohms.}$$

If $R_3 = 1890$ ohms the third degree equation in σ gives

$$\left(\sigma + \frac{1}{C_1 R_1}\right)\left(\sigma + \sqrt{\frac{k}{LC}}\right)^2 = 0. \quad . \quad . \quad . \quad (32)$$

Interpreting (31) in terms of t, we have

$$E_1 = \frac{E}{LCR_a} \cdot \frac{1}{2\pi i}\int_L \frac{e^{zt}(kR + zL)}{(z + 1/C_1R_1)(z+d)^2}dz\,;$$

$$\doteqdot \frac{ER}{R^{a}}\left[e^{-t/C_1R_1} + e^{-dt}\left\{t\left(\frac{1}{CR} - d\right) - 1\right\}\right] . \quad (33)$$

where $d = \sqrt{\frac{k}{LC}} = 4{\cdot}27 \times 10^6$ and $kR = 1370$ ohms.

When t is a fraction of a microsecond, the first exponential term in (33) is substantially unity. Thus the time taken for E_1 to reach the value ER/R_a occurs when the second exponential term is zero, namely, when

$$t = 1/(1/CR_1 - d) = 4{\cdot}16 \times 10^{-7} \text{ second.}$$

The maximum value of E_1 corresponds to that of the second exponential term in (33), and it occurs when

$$t = 1/d + 1/(1/C_1R_1 - d) = 6{\cdot}51 \times 10^{-7} \text{ second.} \quad . \quad (34)$$

The value of E_1 is then $1{\cdot}035\, ER/R_a$, so the aperiodic condition reduces the overshooting of the voltage appreciably. The relationship between E_1 and t is illustrated in curve 2 of fig. 4. The initial rate of rise is equal to E/CR_a, this being identical with the rate of rise without the damping resistance R_3. As time progresses, however, the voltage rises more slowly than that in curve 1, and the time taken to reach the value ER/R_a is twice as long as with R_3 absent. The influence of R_3 is also to retard the occurrence of the maximum value (although this is of little consequence since the top of the curve is so flat) and to reduce the amplification in the upper part of the frequency range. Whether the reduction in definition of the televiewed image is of importance can, of course, be decided by experiment only.

XL. *Diffusion in Zeolitic Solids.* *By* MAX H. HEY, *M.A., B.Sc., Assistant-Keeper in the Mineral Department of the British Museum (Natural History)* *.

DIFFUSION in crystalline solids may be divided into four types: diffusion along microscopic or submicroscopic cracks and fissures or along intercrystalline boundaries; diffusion by direct interchange of adjacent atoms or groups; electrolytic diffusion; and zeolitic diffusion.

Zeolitic substances are those crystalline substances which are capable of undergoing partial or complete dissociation and loss of a volatile or soluble component without their crystal structure collapsing. A new solid phase does not appear during their dissociation, and the partially dissociated compound, instead of being a heterogeneous mixture, is (in the equilibrium state) a homogeneous mixed crystal of the dissociated and undissociated compounds. Zeolitic compounds include not only the zeolites but such substances as ferrous sulphide, selenide and oxide, calcium sulphate hemihydrate, the palladium-hydrogen alloys, the compounds of potassium benzene sulphonate with various vapours, and many others.

In a partially dissociated zeolitic compound a part of the lattice positions which in the undissociated substance are occupied by the volatile (or soluble) component have become vacant, a process which is often accompanied by a measurable shrinkage of the lattice †. The diffusion of the volatile or soluble component in the crystal in the process of dissociation or recombination takes place by migration of the diffusing molecules from one position to an adjacent vacant position, and it is this process which is understood by the term zeolitic diffusion. It is in general a much more rapid process than diffusion by direct interchange. The theory of this mode of diffusion has been treated by the author ‡ on a basis of simple kinetic theory, but the equations derived could not at that time be properly tested because the only available diffusion

* Communicated by the Author.

† As evidenced, for instance, by the density measurements of G. Friedel (Bull. Soc. franç. Min. 1896, xix. p. 94), and more directly by the X-ray measurements of F. A. Bannister (M. H. Hey, "Studies on the Zeolites, Parts II.–VI.," Min. Mag. 1930–34).

‡ M. H. Hey, Min. Mag. xxiv. p. 124 (1935).

data referred to the very complex case of heulandite. Additional data is now available for analcime-ammonia * and palladium-hydrogen †.

For analcime - ammonia A. Tiselius finds at 302° C. a diffusion constant normal to (100), $K_{100}=1{\cdot}2\times10^{-8}$ cm.²/sec., and normal to (110), $K_{110}=1{\cdot}3\times10^{-8}$ cm.²/sec.; he also determined the ratio of the mean diffusion constant for all crystallographic directions at various temperatures to the constant at 302° C. Some evidence was obtained ‡ that the diffusion constant does not vary with the ammonia constant, but this was not conclusively proved. But since the activation energy of migration and the activation energy for removal of the ammonia from the lattice are of the same order it is probable that if the latter does not vary with the ammonia concentration neither will the former; attention was therefore first directed to the equilibrium ammonia pressures.

For the equilibrium dissociation pressure of a zeolitic compound the author § found, on a basis of simple kinetic theory, equating the rate of condensation and dissociation, the equation ‖

$$\log p = C_0 + \tfrac{1}{2}\log T - \log x/(1-x) - 2\log\{1+\phi(x)\} + \tfrac{1}{2}\log\{1+f(x)\} - E_0\{1+f(x)\}(\log e)/RT,$$

where p is the vapour pressure in mm. Hg, T the absolute temperature, x the vacant fraction of the lattice positions available for the volatile component, E_0 the net activation energy in cals. for removal of one gram-mol. of the volatile component from an indefinitely large quantity of the undissociated substance, $f(x)$ and $\phi(x)$ unknown functions of x, generally found in practice to be approximately linear, and C_0 a constant. The functions $f(x)$ and $\phi(x)$, one or both of which are often negligible, represent the effects of the lattice shrinkage, the former taking account of the effect of the shrinkage on the heat of reaction and the latter its effect on the dimensions of the channels

* A. Tiselius, *Zeits. physikal. Chem.* Abt. A, clxxiv. p. 401 (1935).

† W. Jost and A. Widmann, *Zeits. physikal. Chem.* Abt. B, xxix. p. 247 (1935).

‡ *Loc. cit.* p. 418.

§ *Loc. cit.*

‖ If the volatile component occupies several sets of crystallographically distinct positions a modified treatment becomes necessary; this does not arise in the present instance, as the water or ammonia positions in the analcime structure are all nearly if not quite equivalent.

along which the volatile component migrates in the crystal. If the effective radius of these channels in the undissociated substance (in Å.) is r_0, and of the molecules or atoms of the volatile component is ρ, and if the distance (in Å.) between adjacent lattice positions for the volatile component, measured along the channels, is D, then C_0 can be expanded thus: $C_0 = 5{\cdot}22 + \log \sqrt{E_0/\pi(r_0-\rho)^2 D}$ (neglecting an unknown and numerically small correction factor).

From A. Tiselius's data for the equilibrium ammonia pressures dissociation constants for analcime-ammonia (the unit cell formula of which is near $Na_{16}Al_{16}Si_{32}O_{96}\cdot 16NH_3$) were calculated to be: $E_0 = 1{\cdot}58\times10^4$ cals., $C_0 = 7{\cdot}940$, $\phi(x) = -0{\cdot}06\,x$, $f(x) = 0$. The lattice shrinkage, first demonstrated by G. Friedel *, is thus found to affect only the dimensions of the migration channels, the activation energy difference being invariable. This value of E_0 gives a better representation of the data than the value of $1{\cdot}664\times10^4$ cal. computed by A. Tiselius; with two exceptions the difference between the calculated and observed values of $\log p$ does not exceed 0·012.

It may be noted in passing that the above value of C_0 leads to a figure of 0·12 Å. for the difference, $r_0-\rho$, between the effective radii of the ammonia molecule and the channels of the analcime structure. Taking the channel radius as 1·71 Å. † the radius of the ammonia molecule appears to be about 1·59 Å.; the value of 1·80 Å. previously accepted for comparison with some other gases is certainly much too high; according to P. Lueg and K. Hedfeld ‡ the radius of the circle through the three hydrogen nuclei is 1·00 Å., to which must be added the effective radius of a hydrogen atom, making a total of not more than 1·5–1·6 Å. It may therefore be accepted as highly probable that the activation energy of migration does not vary appreciably with the ammonia content.

Kinetic treatment of the diffusion process gave the author the following expression for the diffusion constant along the channels, the lattice positions for the volatile component being all equivalent (a condition which was not fulfilled in the case of heulandite):—

$$K = [D\sqrt{2N\mu_0\{1+\psi(x)\}/\pi\chi\sqrt{M}}\,.\,[1+x(1-x)\psi'(x) \times N\mu_0/RT]\,.\,e^{-N\mu_0\{1+\psi(x)/RT\}},$$

* *Loc. cit.*

† M. H. Hey, *loc. cit.* p. 121.

‡ P. Lueg and K. Hedfeld, *Zeits. Physik*, lxxv. p. 999 (1932).

where M is the molecular weight of the volatile component, D is measured in cm., μ_0 is the activation energy of migration in the undissociated substance in ergs per molecule of volatile component, and $\psi(x)$ an unknown function representing the variation of the activation energy with the degree of dissociation x; χ is a correction factor introduced to correct for assumptions made as to the equations of motion of the migrating molecules, and as it is probably numerically small it will be neglected. Where, as in analcime, the activation energy of migration does not vary appreciably ($\psi(x)=0$) this equation reduces to

$$K_0=[D\sqrt{2N\mu_0}/\pi\chi\sqrt{M}] \, . \, e^{-N\mu_0/RT}.$$

The best value of $N\mu_0$, computed from Tiselius's data for the temperature coefficient of diffusion by a method of trial and error, is $N\mu_0 = (1{\cdot}35\pm0{\cdot}05)\times10^4$ cal. The distance D between ammonia lattice positions along the channels * is 5·93 Å. Substituting these values, and neglecting the unknown correction constant,

$$K_c^{\rightarrow}=(3{\cdot}5\pm2)\times10^{-8}\text{cm.}^2/\text{sec.}$$

along the channels at 302° C. But as the channels are not all parallel this is not the constant for the crystal as a whole.

Now if in a cubic crystal the channels along which diffusion may take place are divided into n independent sets (where n must be one of the numbers 3, 4, 6, 12, or 24), then the diffusion constant normal to any face F is $K_F=[K_c/n] \, . \, \Sigma \cos^2 FP$, where K_c is the diffusion constant along the channels, FP is the angle between the normal to F and one of the sets of channels, and the summation is taken over the n sets. This equation the author has solved for $n=3$, 4, and 6, finding in each case that $\Sigma \cos^2 FP = n/3$, so that $K_F=\frac{1}{3}K_c$, independent of the direction of the face F, and this probably holds also for $n=12$ and 24. Thus it appears that in general, at least if the sets of diffusion channels are independent, the diffusion constant for a cubic crystal is independent of direction (a conclusion which is by no means evident

* The channels are inclined at 54° 44′ to (100), not at 45° as supposed by A. Tiselius. This error does not, however, affect Tiselius's calculation of the vibration frequency, cancelling out.

a priori) * and is $\frac{1}{3}$ the value for diffusion along any one set of channels.

Thus the calculated diffusion constant for analcime-ammonia from the known structure and Tiselius's data for the temperature effect is $(1{\cdot}2\pm0{\cdot}7)\times10^{-8}$ cm.^{2}/sec.. comparing unexpectedly well with Tiselius's experimental results.

For palladium-hydrogen the data are much less satisfactory. W. Jost and A. Widmann found a value $K=5{\cdot}95\times10^{-3}.e^{-5720/RT}$ cm.^{2}/sec., but give no evidence as to whether or no the activation energy $N\mu$ is constant. Since the heat of combination of palladium and hydrogen has been shown to vary markedly with the hydrogen concentration † it appears probable that $N\mu$ also will vary, decreasing with increase of hydrogen content. Then the apparent constant derived by use of the equation $\partial x/\partial t=K\partial^2x/\partial z^2$ will be higher than the true value derived from $\partial x/\partial t=\partial(K\partial x/\partial z)\partial z$, $\partial K/\partial x$ being positive. Moreover, the equation for K now involves a factor $[1+x(1-x)\psi'(x)N\mu_0/RT]$ which is larger than unity, while the temperature coefficient will not give $N\mu$ directly, but the smaller quantity :

$$N\mu[1-x(1-x)\psi'(x)/\{1+\psi(x)\}\{1+x(1-x)\psi'(x)N\mu_0/RT\}].$$

Fourthly, there is the question how far the observed rate of diffusion was due to diffusion along intercrystalline boundaries in the metal ‡ ; it appears to the author that the polycrystalline nature of the material will always be a serious difficulty in obtaining accurate diffusion data for palladium-hydrogen. All four factors tend to make the observed value of K, based on the assumption of a constant activation energy, higher than the value calculated from the observed temperature coefficient and the structure of PdH on the same assumption, so that the calculated value of $5{\cdot}24\times10^{-3}.e^{-5720/RT}$ agrees unexpectedly with the observations.

Jost and Widmann also found that the diffusion constant for deuterium was about 0·74 of that for hydrogen. If it is assumed (as they do) that the activation energies

* A. Tiselius (*loc. cit.* p. 420) states that the diffusion must be isotropic in view of the cubic symmetry, but gives no proof. W. Jost and A. Widmann (*loc. cit.*) assume that it will be anisotropic.

† M. H. Hey, Journ. Chem. Soc. p. 1254 (1935).

‡ Compare D. P. Smith and G. J. Derge, Trans. Electrochem. Soc. lxvi. p. 25 (1934).

of migration are nearly the same, this is in agreement with the appearance of $1/\sqrt{M}$ in the expression for K, which would lead to a ratio of 0·707.

The activation energy of migration of hydrogen in palladium, about $5{\cdot}7 \times 10^3$ cal. per gram-atom, is actually higher than the net heat of combination of palladium and molecular hydrogen, per gram-atom, which does not exceed 5×10^3 cal.*. This is probably largely responsible for the difficulty with which hydrogen absorption in any one metal grain is initiated †, for a hydrogen atom in the surface layer must actually require more energy to migrate further into the lattice than to combine with another hydrogen atom and escape. And if, as seems probable, the value of $5{\cdot}7 \times 10^3$ cal. is merely an average, the activation energy of migration decreasing rapidly with increase of hydrogen content, the reason for the auto-catalytic nature of the absorption in any one metal grain, and the persistence of a false equilibrium in which two phases appear to be present, becomes clear.

Both A. Tiselius and W. Jost and A. Widmann dealt with the problem of diffusion in zeolitic solids theoretically. They treated the matter in a totally different manner from that of the author, and it may be taken as an indication of the general correctness of all three treatments that they lead to fairly close agreement in the results.

XLI. *The Widths of certain* L-*Absorption Edges.*

By Arne Eld Sandström ‡.

VERY few determinations of the widths of X-ray absorption edges have hitherto been made. Largely this may be due to the fact that it is difficult to give a good definition of the width of an absorption edge. Richtmyer, Barnes, and Ramberg § have pointed out that it is also difficult to interpret its true significance. Although it is impossible to find such an adequate measure

* L. Mond, W. Ramsay, and J. Shields, Proc. Roy. Soc. lxii. p. 290 (1893); M. H. Hey, *loc. cit.*

† A. R. Ubbelohde, Trans. Faraday Soc. xxviii. p. 275 (1932).

‡ Communicated by Prof. Manne Siegbahn, D.Sc.

§ F. K. Richtmyer, S. W. Barnes, and E. Ramberg, Phys. Rev. xlvi. p. 843 (1934).

of the widths as the well-defined half-width of spectral lines in the case of emission spectra, it will be shown below that it is possible to obtain the magnitudes of the widths of absorption edges with an accuracy high enough to allow a study of the dependence of the width on the atomic number of the absorbing material. Before that, however, it is necessary to discuss some factors that may be of influence on the measurements.

Influence of the Thickness of the Absorbing Screen.

In a short note * Richtmyer has drawn attention to the fact that the thickness of the absorbing screen may influence the shape, the position, and the width of an absorption edge. The first point is obvious. Besides, the influence may be studied in the following way :—

The coefficient of absorption is a function of the wave-length λ. Thus, if I_0 is the initial intensity and a the thickness of the absorbing screen, the variation of the intensity I is given by the equation

$$I = I_0 . e^{-F(\lambda) . a} . \quad . \quad . \quad . \quad . \quad . \quad . \quad (1)$$

The first and the second derivatives are

$$\frac{dI}{d\lambda} = -I_0 . a . [F'(\lambda)] . e^{-F(\lambda) . a}, \quad . \quad . \quad . \quad . \quad . \quad . \quad (2)$$

$$\frac{d^2I}{d\lambda^2} = I_0 . a^2 . [F'(\lambda)]^2 . e^{-F(\lambda) . a} - I_0 . a . [F''(\lambda)] . e^{-F(\lambda) . a}. \quad (3)$$

The inflexion point is given by eq. (3), when

$$a . [F'(\lambda)]^2 - [F''(\lambda)] = 0. \quad . \quad . \quad . \quad . \quad (4)$$

From eq. (2) we find that the points of minimum and maximum intensity are independent of the screen-thickness. In this respect the distance between these two points—that is, the full width of the edge—may be determined without a systematic error arising from the thickness of the absorbing screen ; but, as is easily seen from fig. 1, it is very difficult to determine the maximum point (the long wave-length end of the edge) with any accuracy, mainly because of the smooth decline of the curve. Therefore it is scarcely correct to use this point for the determination of the wave-length of the edge, as this

* F. K. Richtmyer, S. W. Barnes, Phys. Rev. xlv. p. 754 (1934).

may be done with far higher accuracy by measuring on the middle of the edge (the inflexion point) or really the middle of the straight part of the edge, since all absorption edges are more or less asymmetrical. Eq. (3) shows us, however, that the wave-length of this point depends on the screen thickness. Owing to the difficulty in determining the function * F (λ) it is impossible to estimate the influence of the thickness of the absorbing screen mathematically. Experimentally such an effect has hitherto never been observed. Unfortunately the range is very narrow inside which the thickness of the absorbing screen can be varied without causing too long exposures. However, in a recently published investigation † the author obtained nine values of the wave-

TABLE I

Thickness (in μ) of absorb. screen.	The difference (in X.U.) between the separate values and the average.		
0·6	+1·1	+0·6	
0·8	+0·1		
1·0	−0·3		
1·5	−0·7	+1·5	−1·5
2·1	+1·0		
3·7	−1·4		

length of the L_{III} -edge of selenium with absorbing screens of five different thicknesses. Table I. gives the screen-thicknesses and the corresponding differences between the separate values and the average of all the nine determinations. From the table it is easily seen that there is no systematic variation of the wave-length of the edge for varying screen thicknesses. It is interesting to

* Richtmyer, Barnes, and Ramberg have tried to calculate the absorption coefficient in the region of an absorption edge as a function of the frequency. They obtained a very complicated function, the derivatives of which are quite impossible to handle. For the wave-length of the edge they use the wave-length for which the curve of the absorption coefficient has an inflexion point (Phys. Rev. xlvi. p. 843 (1934)).

† Arne Sandström, *Nova Acta Reg. Soc. Scient. Upsaliensis*, ser. iv 9, no. 11. When this was published the author was unaware of the papers of Richtmyer and his co-workers.

compare the values for the 0·6 μ and 3·7 μ screens with those of the 1·5 μ screen. Those of the former lie between the lowest and the highest of the latter, thus indicating that the accidental distribution of the values exceeds the effect of the screen thickness. It is to be noted that the largest deviation from the average corresponds to 0·018 per cent. of the wave-length. Thus, an alteration in the thickness of the absorbing screen from 0·6 μ to 3·7 μ * cannot cause a displacement of the middle of the edge exceeding 0·018 per cent. In this connexion it must be remembered that a much larger uncertainty arises from the fact that our present knowledge does not allow us to decide upon which part of the edge really represents the transition to the first level allowed by the selection rules. The same thing is true when the measurements are carried out on the curve of the absorption coefficient. However, in this latter case Richtmyer, Barnes, and Ramberg, from not very convincing assumptions, conclude that the true wave-length is given by the inflexion point. Thus, it may be of interest to find the condition allowing the intensity curve (curve of blackening provided that the blackening is moderate) to have an inflexion point at the same wave-length as the curve of the absorption coefficient. The inflexion point of the latter is given by $F''(\lambda)=0$ and that of the former by eq. (4). Thus we find that the two inflexion points have the same wave-length value if $a \to 0$—that is, if the thickness of the absorbing screen can be considered very small. Now we find from fig. 1 (p. 505) that this is certainly true at the thicknesses usually used in spectroscopic work. Then we may really suppose that the wave-length measured on intensity and blackening curves coincides with the wave-length of the inflexion point of the curve of the absorption coefficient within the errors of measurement.

According to eq. (4) the influence of the screen thickness will diminish when the edges become broader and the jump in the absorption coefficient lower. With regard to the considerable width of most edges we may suppose that when very thick absorbing screens are not used the effect predicted by Richtmyer and Barnes will appear only at the K-edges of the higher elements.

* These are the boundaries inside which the thickness of the absorbing screen conveniently may be varied in the case of selenium.

For the determination of the widths of absorption edges it is especially important to note that the screen thickness has no influence at all on the position of the points of minimum and maximum intensity. Thus, in most cases it ought to be possible to measure the full width of an edge.

A method for the determination of the relative widths of edges was given by Ross *, who defined the width of an edge as the wave-length distance between the intersection points between the tangent through the inflexion point and two horizontal lines through the points of minimum and maximum intensity. The angular coefficient of the tangent is given by eq. (2). From what has been said above we may assume the wave-length λ_m of the inflexion point to be constant. It is then possible to calculate the wave-length difference $\Delta\lambda$ between the two intersection points. If λ_1 is the wave-length of the minimum point and λ_2 that of the maximum point, we get

$$\Delta\lambda = \frac{e^{a[F(\lambda_m)-F(\lambda_2)]} - e^{a[F(\lambda_m)-F(\lambda_1)]}}{a.[F'(\lambda_m)]}. \quad . \quad . \quad (5)$$

In this case the measured quantity evidently depends on the thickness of the absorbing screen. $\Delta\lambda$ has its minimum value for $a=0$. Thus, this measure of the widths of these edges is less adequate than the total width. However, provided that the material is homogeneous and only a relative comparison is required of the widths of the same edge at elements which are not too widely separated in the periodic table, this measure may be used even for photographically obtained spectra. In the latter case we will call it the width of the "idealized" edge. As in this case the time of exposure will also be of influence, the discussion will be continued in the next section. The above measure is also convenient for the comparison of edges in the same series of the same element † in cases when it is especially difficult to determine the maximum points of the intensity (blackening) curve.

Indirectly the screen-thickness may influence the appearance of the edge when there is a structure in the edge itself ‡. This is illustrated in fig. 3 (p. 506). It is evident that, if the structure is very close and if the

* P. A. Ross, Phys. Rev. xliv. p. 977 (1933).

† Arne Sandström, *Ark. f. Mat., Astr. o. Fysik*, xxv. B. no. 8 (1935).

‡ Arne Sandström, *Nov. Act. Reg. Soc. Scient. Ups.* iv. 9. no. 11, p. 57 (1935).

resolving power of the spectrograph does not allow the edges to be separated well enough, the "structure" edges may disturb one another, and thus cause a variation in their widths.

Influence of the Time of Exposure.

As in the X-ray region the rectilinear part of the blackening curve, is very long, it is not probable that there will be a variation in the wave-length of the edge due to the time of exposure. Really, for the L_{III}-edge of selenium an exposure of 560 mA hours gave $\lambda=8627{\cdot}5$ X.U., and another of 1010 mA hours gave $\lambda=8626{\cdot}7$ X.U., the

TABLE II.

Selenium.			Palladium.		
Time of exp. (mA hours) (μ).	Thickness of absorb. screen (μ).	Width of L_{III}-edge (X.U.).	Time of exp. (mA hours).	Thickness of absorb. screen (μ).	Width of L_{III}-edge (X.U.).
450	1·5	8·5	150	1·0	2·9
550	2·1	7·4	180	2·0	2·8
560	1·5	9·0	250	1·0	2·6
560	3·7	5·6	300	1·0	2·9
1010	0·8	10·0	490	2·0	3·2
1010	1·5	7·1	560	1·0	2·5
1075	1·0	7·2	590	2·6	3·1

difference being absolutely inside the errors of measurement. In both cases the thickness of the absorbing screen was $1{\cdot}5\mu$. The position of the points of minimum and maximum blackening can never be influenced by the time of exposure, although they may be less pronounced when the exposures are too short or too long. On the contrary, in the width of the "idealized" edge there may be variations due to the time of exposure. Experimentally we may obtain a survey over the conditions from Table II., where the widths of the "idealized" L_{III}-edges of Se and Pd are to be found for different times of exposure and for different thicknesses of the absorbing screens. In the case of Pd the variations are comparatively small

and no systematic influence is indicated. On the contrary, in the case of Se we have a very small value for the thickest absorbing screen and a very large value for the thinnest one. This is, however, contrary to what we would expect from eq. (5), and hence these two deviating values must be ascribed to accidentally large errors of measurement. Thus we may assume that the variations due to the time of exposure are small compared with those due to accidental errors.

The Broadening Effects of the Apparatus.

The spectroscopic apparatus has already been described by the author * in connexion with the measurement of the wave-lengths of the edges. The spectrograph was built after the concave crystal principle, and, accordingly, there is a broadening effect determined by the radius of the spectrograph and the optical opening of the crystal. As regards the points of maximal and minimal intensity no displacement is caused by this broadening effect. The same obtains for the reflexion range of the crystal †. As the latter is one-sided it also does not affect the width of the "idealized" edges. Likewise the broadening effect of the spectrograph will not cause this measure to be enlarged, as the straight part of the edge usually is wide enough for its slope not to be influenced by this effect ‡.

The Full Widths of the Main Edges.

As has been stated above the full widths of edges can be measured without any disturbing influences inside the rather large errors of measurement by taking the wave-length distance between the minimum and maximum points of the photometrical curves of the spectrograms. The measured quantities are further illustrated in fig. 1. In Table III. the full widths of the edges are given in X-units, frequency-units, and volts. The last three columns give the range of the energy distribution in per cent. of the energy of the edge.

Naturally the measurements had to be made on spectrograms with the point of maximal blackening distinctly appearing, and, accordingly, the author was compelled

* Arne Sandström, *Nova Acta Reg. Soc. Scient. Ups.* iv. 9, no. 11 (1935).

† P. P. Ewald, *Zeits. f. Phys.* ii. p. 332 (1920).

‡ Arne Sandström, *Zeits. f. Phys.* xcii. p. 622 (1934).

Table III.

	$\Delta\lambda$ (X.U.).			$\Delta\nu$/R (frequency U.).			ΔV (volts).			Width in per cent. of energy of edge.		
	L_I.	L_{II}.	L_{III}.	L_I.	L_{II}.	L_{III}.	L_I.	L_{II}.	L_{III}.	L_I.	L_{II}.	L_{III}.
52 Te	6·2	7·0	9·6	0·90	0·89	1·08	12·2	12·1	14·6	0·25	0·26	0·34
51 Sb	8·6	5·6	7·9	1·13	0·64	0·80	15·3	8·7	10·8	0·33	0·20	0·26
50 Sn	8·8	....	11·2	1·04	....	1·03	14·1	....	14·0	0·32	....	0·36
49 In	12·4	....	....	1·33	....	....	18·0	....	....	0·43		
48 Cd	12·2	8·5	10·5	1·17	0·70	0·78	15·8	9·5	10·6	0·39	0·26	0·30
46 Pd.....	12·5	9·3	11·7	0·97	0·61	0·70	13·1	8·3	9·5	0·37	0·25	0·30
45 Rh	....	12·0	13·1	....	0·71	0·70	....	9·6	9·5	....	0·31	0·32
44 Ru	....	11·3	13·7	....	0·60	0·66	....	8·1	8·9	....	0·28	0·32
42 Mo	....	14·3	14·7	....	0·59	0·56	....	8·0	7·6	....	0·30	0·30
39 Y	....	....	25·6	....	....	0·66	....	....	8·9	....	....	0·43
38 Sr	....	....	30·1	....	....	0·68	....	....	9·2	....	....	0·48
34 Se	....	....	27·5	....	....	0·34	....	....	4·6	....	....	0·32
33 As	....	....	38·1	....	....	0·40	....	....	5·4	....	....	0·41
30 Zn	....	60·0	59·2	....	0·39	0·37	....	5·3	5·0	....	0·51	0·49

to refrain from measuring the full width of some edges. As examples as to how distinctly the points to be measured appear in the primary material some photometrical

Fig. 1.

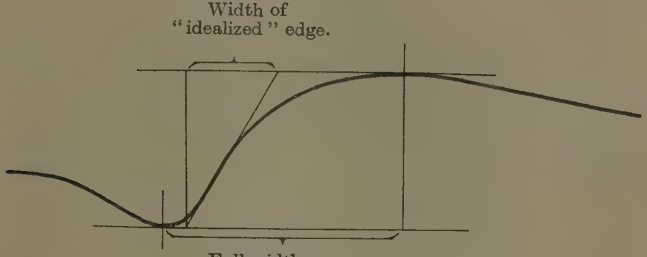

Definition of the width of an absorption edge.

Fig. 2.

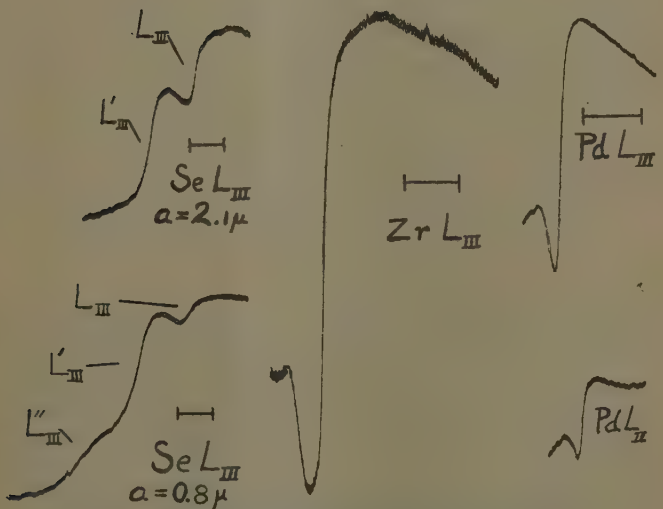

Photometrical curves of some of the absorption edges.
34 Se and 46 Pd: Abziss-enlargement 3X.
40 Zr: Abziss-enlargement 5X. ⊢ equals 25 X.U.

curves are reproduced in fig. 2. The maximum point was, naturally, the most difficult to determine. The

measurements were made on curves giving 0·16–0·27 X.U. per mm. in the case of the elements 42 Mo–52 Te and 0·7–2·0 X.U. per mm. in the case of the lower elements. In cases where many determinations could be made the distribution of the separate values shows that large accidental errors appear. In the author's opinion the error should be assumed to be 10–15 per cent.

In fig. 3 the widths of the edges (in X.U.) are plotted against the atomic number. The absorbing screens of yttrium and strontium were made of chemical compounds ($Y_2 O_3$, and Sr 0), and, as this may be of influence on the widths of the edges, the points for these elements are marked with crosses. There is nothing indicating different

Fig. 3.

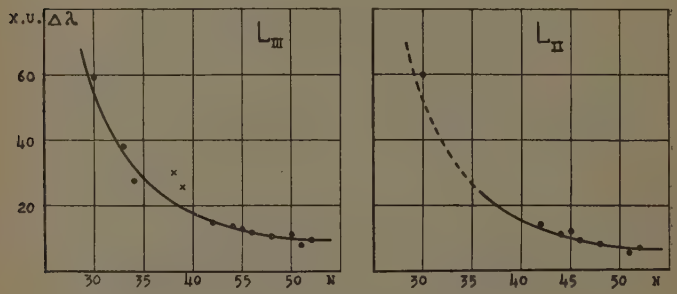

Variation of the full width, in X.U., of the L_{II}- and L_{III}-edges with the atomic number.

shapes of the curves in the case of the L_{III}- and L_{II}-edges, but the few points for L_I seem to demand another curvature. This is still more apparent in the curves representing the widths in frequency-units and volts (fig. 4). It is especially interesting that the energy widths of the edges in per cent. of the energy of the edge is practically constant (fig. 4). For the lower of the elements, however, there is a slight rise. That this rise is not accidental is indicated by the fact that it is practically the same for the L_{II}- and L_{III}-edges of zinc.

The Asymmetry of the Edges.

As has been stated above most edges show a pronounced asymmetry. As inside wide boundaries the

wave-length of the " middle " of the edge (the inflexion point) can be considered as uninfluenced by the thickness of the absorbing screen, we may easily determine this asymmetry. The results are to be found in Table IV.,

Fig. 4.

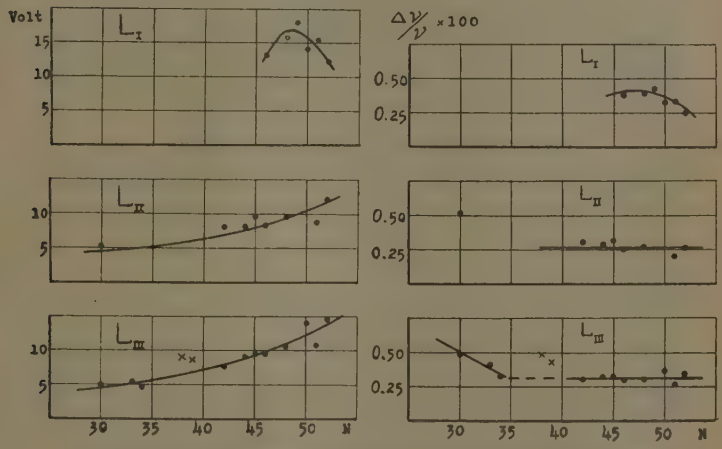

Variation with the atomic number of the full width of the L-edges in volts and in per cent. of the energy of the edge.

TABLE IV.

	L_I.	L_{II}.	L_{III}.
52 Te	2·4	4·0	4·6
51 Sb	3·3	2·0	3·0
50 Sn	1·8	..	3·9
49 In	2·0		
48 Cd	1·6	2·1	3·6
46 Pd	2·4	3·7	4·6
45 Rh.....	..	3·3	3·0
44 Ru.....	..	3·0	3·0
42 Mo.....	..	4·1	4·4
39 Y	..	..	3·6
38 Sr	..	..	3·8
34 Se	..	..	4·4
33 As	..	..	2·6
30 Zn	..	1·5	1·3

where the values give the ratio between the part of the edge on the long wave-length side of the inflexion point and that on the short wave-length side. It is reasonable to suppose that in this case the errors of measurement are about twice those of the values of the full widths. Accordingly the variations may be due entirely to accidental errors with the exception of the astonishingly small values at 30 Zn. The average asymmetry is then 3·5 for the L_{III}-edge, 3 for the L_{II}-edge, and 2 for the L_I-edge.

The Widths of the "Idealized" Edges.

For comparison purposes the widths of the "idealized" edges were also measured. In this way it was possible to

Fig. 5.

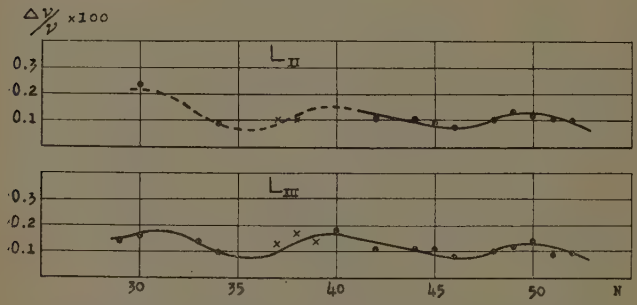

Variation with the atomic number of the Ross measure of the width of the L_{II}- and L_{III}-edges in per cent. of the energy of the edge.

measure certain additional edges. The results are to be found in Table V. The errors of measurement are in this case certainly smaller than at the full widths. Concerning the L_{III}-edge they certainly are not larger than 10 per cent.

In fig. 5 the widths of the L_{II}- and L_{III}-edges in per cent. of the energy of the edge are plotted against the atomic number. In this case the curve does not run smoothly, but shows a periodic variation following the building up of the outer electronic shells. The conformity between the curves for L_{II} and L_{III} shows that the periodical variation is real. It must be remarked that in this

Table V.

	$\Delta\lambda$ (X.U.).			$\Delta\nu$/R (frequency U.).			ΔV (volts).			Width in per cent. of energy of edge.		
	L_I.	L_{II}.	L_{III}.	L_I.	L_{II}.	L_{III}.	L_I.	L_{II}.	L_{III}.	L_I.	L_{II}.	L_{III}.
52 Te	2·5	2·6	3·1	0·36	0·34	0·35	4·9	4·6	4·7	0·099	0·100	0·109
51 Sb	2·9	3·0	3·0	0·41	0·35	0·30	5·6	4·7	4·1	0·118	0·108	0·099
50 Sn	4·0	3·6	4·6	0·47	0·37	0·42	6·4	5·0	5·7	0·14	0·12	0·14
49 In	4·8	4·1	4·1	0·51	0·38	0·34	6·9	5·1	4·6	0·16	0·13	0·12
48 Cd	6·8	3·5	3·7	0·65	0·29	0·27	8·8	3·9	3·7	0·22	0·106	0·103
46 Pd.....	4·1	3·0	3·3	0·32	0·19	0·19	4·3	2·6	2·6	0·12	0·077	0·082
45 Rh	....	3·7	4·7	....	0·21	0·25	....	2·8	3·4	....	0·091	0·11
44 Ru	....	4·4	4·7	....	0·23	0·23	....	3·1	3·1	....	0·105	0·11
42 Mo	....	5·1	5·5	....	0·21	0·21	....	2·8	2·8	....	0·108	0·11
40 Zr	....	....	9·5	....	....	0·29	....	....	3·9	....	....	0·18
39 Y	....	....	9·0	....	....	0·23	....	....	3·1	....	....	0·15
38 Sr	....	7·0	10·8	....	0·19	0·24	....	2·6	3·3	....	0·13	0·17
37 Rb	....	6·9	9·3	....	0·14	0·18	....	1·9	2·4	....	0·102	0·13
34 Se	19·5	7·6	8·1	0·32	0·098	0·103	4·3	1·3	1·4	0·26	0·090	0·098
33 As	....	....	12·5	....	....	0·14	....	....	1·9	....	....	0·14
30 Zn	....	28·8	20·4	....	0·19	0·12	....	....	1·6	....	0·24	0·16
29 Cu	....	....	19·0	....	....	0·098	....	....	1·3	....	....	0·14

case the points obtained with chemical compounds lie on the curve inside the errors of measurement.

For some elements there is an indication of a lower width of the L_{II}-edge than of the L_{III}-edge. Taken over the whole range of elements investigated here this difference seems to be accidental, as in several cases the value of the width of an L_{II}-edge is higher than that of the corresponding L_{III}-edge. In the case of Rb, however, the seemingly slight difference is especially interesting. The values were here obtained with three different compounds, RbCl, RbI, and Rb_2SO_4*, and in all cases the width of L_{III} was larger than that of L_{II}, the values being respectively 9·4 and 7·3, 9·7 and 6·8, 8·6 and 5·9 X.U. This difference is too consistent to be accidental.

The Widths of the "Structure" Edges.

Barnes † found that the K-edges of the elements 26 Fe–29 Cu had a fine structure in the edge itself. Recently the author found an analogous structure in the L_{III}- and L_{II}-edges of the elements 30 Zn, 33 As, 34 Se, and 48 Cd–52 Te, and was at the same time able to give an explanation for this phenomenon ‡.

In many cases the boundaries between these structure edges are only faintly recognizable, but in others, as at selenium and zinc, there are well developed minimum and maximum points between them. In those cases where there are no such points one may suspect that the edges overlap. This would then explain why in the curves for the L_{II}- and L_{III}-edges in figs. 3 and 4 the points of the elements 48 Cd–52 Te show a wider spreading than the points of the elements. However, with very few exceptions a determination of the full widths of the structure edges will be doubtful. Consequently we will measure their "idealized" widths. The values are, as usual, given in X.U., frequency-units, and volts (Table VI.). Some of them are to be regarded as extremely uncertain. For comparison purposes the values of the L_{II}- and L_{III}-main edges are included in the tables. It is interesting to see that the widths of the L'_{II}-, L''_{II}-, L'_{III}-, and L''_{III}-

* Arne Eld Sandström, *Ark. f. Mat. Astr. o. Fysik*, xxv. B, no. 8 (1935).

† S. W. Barnes, Phys. Rev. xliv. p. 141 (1933).

‡ Arne Sandström, *Nova Reg. Soc. Scient. Ups.* iv. 9, no. 11 (1935).

Table VI.

	$\Delta\lambda$ (X U.).				$\Delta\nu/R$ (frequency U.).				ΔV (volts).			
	L_{II}.	L_{II}'.	L_{II}''.	L_{II}'''.	L_{II}.	L_{II}'.	L_{II}''.	L_{II}'''.	L_{II}.	L_{II}'.	L_{II}''.	L_{II}'''.
52 Te	2·6	3·6	1·3	....	0·34	0·41	0·17	....	4·6	5·6	2·3	
51 Sb	3·0	3·5	1·5	....	0·35	0·40	0·18	....	4·7	5·4	2·5	
50 Sn	3·6	4·9	4·3	....	0·37	0·50	0·44	....	5·0	6·8	6·0	
48 Cd	3·5	4·3	2·2	4·3	0·29	0·36	0·18	0·36	3·9	4·9	2·5	4·9
34 Se	7·6	16·0	22·8	....	0·10	0·20	0·30	....	1·3	2·7	4·1	

Table VII.

	$\Delta\lambda$ (X.U.).				$\Delta\nu/R$ (frequency U.).				ΔV (volts).			
	L_{III}.	L_{III}'.	L_{III}''.	L_{III}'''.	L_{III}.	L_{III}'.	L_{III}''.	L_{III}'''.	L_{III}.	L_{III}'.	L_{III}''.	L_{III}'''.
52 Te	3·1	3·5	0·9	....	0·35	0·39	0·10	....	4·7	5·3	1·4	
51 Sb	3·0	5·0	1·4	....	0·30	0·51	0·14	....	4·1	6·9	1·9	
50 Sn	4·6	5·6	5·9	....	0·42	0·51	0·54	....	5·7	6·9	7·3	
48 Cd	3·7	3·8	2·6	4·3	0·27	0·27	0·19	0·32	3·7	3·7	2·6	4·3
34 Se	8·1	15·6	28·5	....	0·10	0·19	0·35	....	1·4	2·6	4·7	
30 Zn	20·4	13·7	35·6	....	0·12	0·09	0·21	....	1·6	1·2	2·8	

edges on the whole follow analogous curves to the L_{II}- and L_{III}-edges.

In the same way for elements belonging to the same group in the periodic system we would expect corresponding " structure " edges to have the same width in per cent. of the energy of the edge. However, the conditions at selenium are not in agreement with those at tellurium. In the case of zinc and cadmium the agreement is somewhat better. The values may also be influenced by the fact that the details of the edges of the elements 50 Sn–52 Te were badly resolved compared with those of the L_{III}-edges of selenium and zinc.

Unfortunately very few measurements of the widths of edges have hitherto been made, and in cases where measurements exist a comparison of the different results is often impossible because the width of the edge has been defined in different ways. However, a comparison between the values in Table V. and Ross's measurements in the K-series of the elements 40 Zr–53 J shows that the general tendency in both cases is the same for the variation of the width with atomic number, but the values obtained by Ross do not show the small variations with the position of the elements in the periodic system.

Summary.

1. The widths of certain L-edges have been measured in photographically registered spectra. The influence of the thickness of the absorbing screen, the properties of the plate, etc. are discussed.

2. Experimental evidence is given that the position of the middle of the straight part of the photometrical curve of the edge (the inflexion point) is uninfluenced by the thickness of the absorbing screen.

3. The full width of an absorption edge is defined as the distance (in X.U., frequency units, or volts) between the points of maximum intensity and minimum intensity. The distance between the intersection points between the two horizontal lines through the points of maximum and minimum intensity and the tangent to the inflexion point is called the width of the " idealized " edge. As the position of the points of maximum and minimum blackening is uninfluenced by screen thickness, sensitivity of plate, etc., it is possible to measure the *full* width of

edges in photographically obtained spectra. The width of the " idealized " edge, on the contrary, may easily be influenced, but from some experimental material is concluded that in the case of a homogeneous material this measure may be used for comparison purposes.

4. The full width of most of the L_{II}- and L_{III}-edges and some L_I-edges in the region 30 Zn–52 Te were measured. Curves are given which illustrate the variation of the width with atomic number. Further, the asymmetry of the edges was measured. The width of the " idealized " edge was measured also in some cases where from certain causes it was impossible to measure the full width.

In conclusion, I should like to thank Prof. Manne Siegbahn, D.Sc., for all the different ways in which he has facilitated my work in his institute.

Uppsala, Physics Laboratory of the University.
January 1936.

XLII. *Latent Energy in Explosions.*

By W. T. David, *Sc.D.*, *and* A. Smeeton Leah, *Ph.D.**

HIGH density inflammable gaseous mixtures contained in a large spherical explosion vessel yield on explosion maximum pressures which are in general only a little short of those calculated upon the basis of optical specific heat data †, due allowance being made for the heat lost during explosion. Under such conditions therefore the amount of incomplete combustion is relatively small. The experiments described in this paper show that the amount of incomplete combustion increases as the initial density of the inflammable mixtures decreases and

* Communicated by the Authors.

† The specific heat values used in this paper are those calculated by Johnston and Davies (J. A. C. S. lvi. pp. 271 and 1045 (1934)); Johnston and Walker (J. A. C. S. lvii. p. 682 (1935)); Kassel (J. A. C. S. lvi. p. 1841 (1934)); and Gordon (J. Chem. Phys. ii. pp. 65 and 549 (1934)). These values are just a little greater than those calculated by Nernst and Wohl and Johnston and Walker, which we proved by means of high density large vessel explosion experiments to be " substantially accurate " (Phil. Mag. xviii. p. 307 (1934)) with the possible exception of the values for H_2O above about 2000° C. These, however, are not required for the present paper.

becomes substantial in amount at subatmospheric densities.

An examination of our heat loss and pressure records does not indicate that there is any evolution of heat in the early stages of cooling, and we infer that the incomplete combustion at maximum pressure is not due to incomplete combination, but that it results from a long-lived latent energy left in the exploded gases. This is qualitatively in keeping with the deductions made from platinum thermometry investigations in flame gases *.

It is further shown that the amount of incomplete combustion or long-lived latent energy is dependent upon the nature of the combustible gas and also upon the nature of the diluent gases contained in the inflammable mixtures.

Experimental.

The explosion experiments described in this paper were carried out in a spherical vessel, 17·45 inches in internal diameter, fitted with central ignition. Full details of the experimental arrangements will be found in a previous paper †. The experiments were made with various inflammable mixtures at initial pressures of $\frac{1}{4}$, $\frac{1}{2}$, and 1 atmosphere, involving the use of diaphragms of different thicknesses for the pressure indicators. Special care had to be taken in the calibration of the thinnest diaphragms, for the variation of the calibration with the pressure applied and also with the temperature of the vessel was found to be appreciable. This was reduced to a minimum by using a modified diaphragm having a small corrugation round the perimeter.

The lower heats of combustion at constant volume and a temperature of 20° C. for the various combustible gases used have been taken to be as follows ‡ :—

CO to CO_2	67,370 calories per gram molecule.
H_2 to H_2O	57,500 calories per gram molecule.

* Phil. Mag. xvii. p. 172 (1934); xviii. p. 228; xxi. p. 280 (1936); 'The Engineer' June 1st, 1934, and Proc. South Wales Inst. Engineers, p. 375 (1936).

† Phil. Mag. xiv. p. 764 (1932).

‡ Rossini, Bur. of Stand. J. Res. vi. p. 1 (1931), and ii. p. 21 (1934). We are indebted to Mr. F. D. Rossini for kindly advising us in this connexion.

C_2H_2 to CO_2 & H_2O	300,300 calories per gram molecule.
C_2H_4 to CO_2 & H_2O	316,070 calories per gram molecule.
C_5H_{12} to CO_2 & H_2O ...	783,400 calories per gram molecule.

Effect of Initial Density upon the Latent Energy left in Exploded Gases.

The inflammable gaseous mixtures exploded were composed of one of the gases CO, H_2, C_5H_{12} (vapour), C_2H_2, C_2H_4, together with either O_2 or atmospheric air at initial pressures of $\frac{1}{4}$, $\frac{1}{2}$, and 1 atmosphere. In every case records both of heat loss and of pressure have been taken. We believe that a high degree of accuracy has been attained in our measurements.

From a large number of explosions we have selected those given in Table I. as representative. In the first column of the table is given the composition of the initial mixture, allowance being made for the small impurities present (chiefly N_2 and O_2, which are included in the air). Atmospheric air was used in the mixtures containing air, and this has been taken to contain 21·0 per cent. O_2 by volume in the succeeding calculations.

Column 2 shows the initial pressure at which the explosions were made. The initial temperature was in all cases about 20° C. Any small deviation from this temperature was corrected for in the determination of the ratios of the maximum pressure to the initial pressure given in the third column.

In the remaining columns are shown :—

The measured heat loss up to the moment of maximum pressure (h_m per cent.) expressed as a percentage of the heat of combustion (Q) in calories per gram-mol. of initial mixture.

The rise of temperature on explosion ($T_m - T_i$) °C.

The internal energy of the products of combustion at maximum pressure (E) expressed in calories per gram-mol. of initial mixture.

The energy accounted for expressed as a percentage of the heat of combustion (E per cent.).

TABLE I.

Percentage composition of inflammable mixture.	P_i atmos.	$\left[\frac{P_m}{P_i}\right]$ 20°.	h_m per cent.	$T_m - T_i$ ° C.	Q.	E.	E per cent.	U.E. per cent.
90·44 CO* + 9·56 O_2	0·25	6·63	2·3	1855	12780	11850	95·0	5·0
91·00 CO* + 9·00 O_2	0·5	6·45	2·0	1785	12020	11310	96·1	3·9
90·00 CO* + 10·00 O_2	1·0	6·80	1·5	1910	12820	12220	96·8	3·2
57·85 CO* + air	0·5	6·43	2·6	1780	12050	11210	95·6	4·4
54·85 CO* + air	1·0	6·74	1·7	1885	12630	11980	96·5	3·5
8·44 CO + 9·92 H_2 + air	0·25	6·18	3·3	1700	11390	10290	93·7	6·3
9·80 CO + 10·00 H_2 + air	1·0	6·75	1·8	1900	12350	11710	96·6	3·4
4·00 C_2H_2 + air	0·25	6·81	2·4	1745	12030	11070	94·6	5·4
3·99 C_2H_2 + air	0·5	6·86	1·9	1765	12000	11200	95·3	4·7
4·20 C_2H_2 + air	1·0	7·18	2·2	1855	12640	11880	96·2	3·8
4·35 C_2H_4 + 95·65 O_2	0·25	7·03	2·7	1770	13740	12320	92·4	7·6
4·21 C_2H_4 + 95·79 O_2	0·5	6·95	4·1	1745	13310	12030	94·5	5·5
4·57 C_2H_4 + 95·43 O_2	1·0	7·55	2·6	1920	14450	13480	95·9	4·1
2·21 C_5H_{12} + air	0·28	8·19	5·6	2005	17320	14770	90·9	9·1
2·18 C_5H_{12} + air	0·5	8·23	6·0	2010	17050	14630	91·8	8·2
2·20 C_5H_{12} + air	1·0	8·50	5·8	2090	17220	15420	95·2	4·8

* 1 per cent. H_2 included in the CO.

The energy unaccounted for, or latent energy, at maximum pressure expressed as a percentage of the heat of combustion (U.E. per cent.).

In deducing the energy accounted for and the energy unaccounted for at maximum pressure the measured heat loss has been taken into account. Dissociation is negligible in the case of all mixtures except the pentane mixtures, and in the case of these dissociation, calculated upon the basis of the equilibrium constants given by Kassel * and Gordon †, has been allowed for in the values given for E. E per cent., and U.E. per cent.

An examination of our pressure and heat loss records subsequent to maximum pressure make it clear that there is no evolution of heat in the early stages of cooling ‡. The unaccounted energy therefore would not appear to be due to incomplete *combination* at the moment of maximum pressure. We believe it results from a long-lived latent energy held within the exploded gases, as was deduced independently from platinum thermometry experiments during constant pressure burning.

The unaccounted or latent energies for the various mixtures are shown plotted against the initial pressure in fig. 1. It will be seen that they vary both with the nature of the combustible gas § and with the initial pressure. In the case of the pentane, the ethylene, and the $CO-H_2$ mixtures the latent energy is practically doubled as the initial pressure of the explosion is reduced from 1 atmosphere to ½ atmosphere. In the acetylene and CO mixtures the increase of the latent energy as the initial pressure is decreased over the same range amounts to about 50 per cent.

Explosion experiments with inflammable mixtures at higher initial pressures than 1 atmosphere have up to the present only been made with CO mixtures, and in these mixtures the latent energy decreases considerably with increase of initial pressure. Thus the mixture 89·59 per cent. CO + 10·41 per cent. O_2 when exploded at 3 atmospheres initial density leaves at maximum pressure

* J. A. C. S. lvi. p. 1841 (1934).
† J. Chem. Phys. ii. p. 65 (1934).
‡ See also "Hopkinson's Explosion Experiments," 'The Engineer,' 3rd April, 1936.
§ Maxwell and Wheeler, J. C. S. p. 2069 (1927), and p. 245 (1929).
‖ 1 per cent. H_2 included in the CO.

a latent energy amounting only to 1·1 per cent. of the heat of combustion. This compares with a latent energy of 3·2 per cent. in a mixture of the same composition exploded at an initial pressure of 1 atmosphere.

Fig. 1.

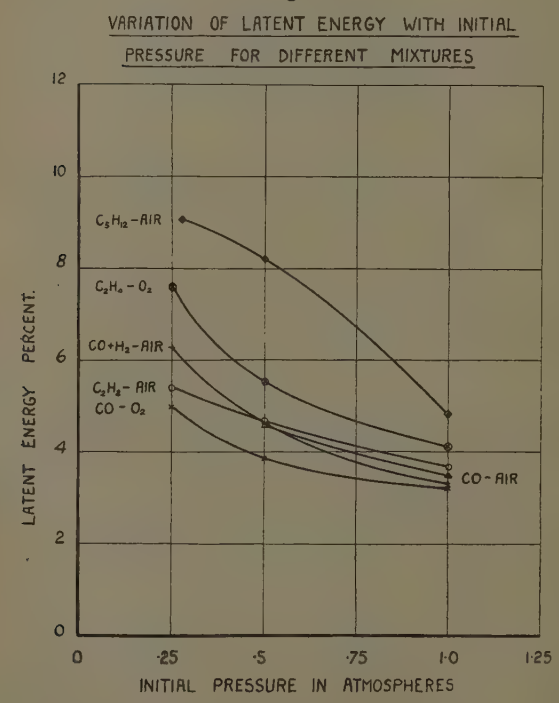

Influence of Diluent Gases upon Latent Energy.

A number of high density explosions which we made, using $2CO+O_2$ mixtures having argon as the main diluent, were found to give a greater amount of latent energy than similar mixtures containing diatomic gases only as diluents. We commented on this in a previous paper *,

* Phil. Mag. xviii. p. 307 (1934).

and we have since investigated the influence of various diluent gases upon the latent energy.

A combining proportion mixture consisting of 40 per cent. $CO+26{\cdot}67$ per cent. $H_2+33{\cdot}33$ per cent. O_2 was used, and was diluted with A, N_2, CO_2, CO, and O_2 in successive explosions. In the case of the first three diluents 2 per cent. of excess oxygen was added for reasons which will be discussed later, and the mixtures proportioned to give a temperature rise on explosion not greater than about 1900° C. The initial pressure was $\frac{1}{2}$ atmosphere in all the experiments.

The results of these experiments are tabulated in Table II. In estimating the energy accounted for and the unaccounted energy dissociation has been taken into account. It will be noticed that in the mixture containing argon as the main diluent a much greater latent energy was found than in the case of the mixtures diluted with the diatomic gases and CO_2. Even among the diatomic diluent mixtures there appears to be a small variation which cannot be due entirely to experimental error. The results bear out our previous statement, and quite definitely show that the nature of the diluent has a marked effect upon the amount of incomplete combustion or latent energy.

In the above experiments an excess of oxygen of fixed amount, viz.: 2 per cent., was included in the inflammable mixtures used, for it was found that the latent energy varied considerably with small variations in the excess oxygen content. That this is so will be seen from Tables III. and IV., which relate to experiments with mixtures containing nitrogen and argon respectively as the main diluents. As in the previous tables measured heat loss and dissociation have been allowed for in calculating the E, E per cent., and U.E. per cent. values. In all cases the U.E. per cent. values must, we think, be regarded as measures of long-lived latent energy, for our records of pressure and heat loss show no signs of evolution of heat in the early stages of cooling except a small amount which is wholly attributable to decreasing dissociation.

The latent energy values are shown plotted against excess O_2 in fig. 2. Curve A relates to the argon and curve N to the nitrogen diluted mixtures. It will be seen that the latent energy is greatest in those mixtures containing no excess oxygen. As excess oxygen is added the latent

TABLE II.

Inflammable mixture percentages.	Diluent gases percentages.	$\left[\frac{P_m}{P_i}\right]_{20°}$	h_m per cent.	$T_m - T_i$ °C.	Q.	E.	E per cent.	U.E. per cent.
8·15 CO+5·35 H_2+6·75 O_2 ...	77·18 A+0·57 N_2+2·00 O_2 ...	7·02	6·1	1910	8550	7410	92·8	7·2
11·95 CO+7·93 H_2+9·94 O_2 ...	68·18 N_2+2·00 O_2	6·66	3·4	1870	12610	11670	96·0	4·0
11·86 CO+7·75 H_2+9·80 O_2 ...	70·25 O_2+0·34 N_2	6·44	2·6	1800	12440	11530	95·4	4·6
17·00 CO+1·00 H_2+9·00 O_2 ...	73·00 CO	6·45	2·0	1785	12020	11300	96·0	4·0
18·03 CO+11·78 H_2+14·90 O_2...	53·00 CO_2+0·23 N_2+2·06 O_2..	6·31	2·9	1880	18940	17510	95·3	4·7

TABLE III.

Inflammable mixture percentages.	Diluent gases percentages.	$\left[\frac{P_m}{P_i}\right]_{20°}$	h_m per cent.	$T_m - T_i$ °C.	Q.	E.	E per cent.	U.E. per cent.
12·35 CO+8·21 H_2+10·28 O_2	69·16 N_2	6·62	2·5	1865	13040	11840	93·3	6·7
11·93 CO+7·91 H_2+9·92 O_2	69·76 N_2+0·48 O_2	6·55	3·8	1830	12600	11480	94·9	5·1
11·97 CO+7·95 H_2+9·96 O_2	68·99 N_2+1·13 O_2	6·61	3·7	1855	12620	11600	95·6	4·4
11·95 CO+7·93 H_2+9·94 O_2	68·68 N_2+1·50 O_2	6·66	3·3	1870	12610	11700	96·1	3·9
11·95 CO+7·93 H_2+9·94 O_2	68·18 N_2+2·00 O_2	6·66	3·4	1870	12610	11670	96·0	4·0
12·00 CO+8·00 H_2+10·00 O_2	67·00 N_2+3·00 O_2	6·66	3·7	1870	12680	11700	95·9	4·1

TABLE IV.

Inflammable mixture percentages.	Diluent gases percentages.	$\left[\frac{P_m}{P_i}\right]$ 20°.	h_m per cent.	$T_m°C. - T_i$	Q.	E.	E per cent.	U.E. per cent.
8·29 CO+5·43 H_2+6·86 O_2	78·90 A+0·49 N_2+0·03 O_2 ...	6·98	6·4	1875	8710	7416	91·5	8·5
8·18 CO+5·36 H_2+6·77 O_2	78·50 A+0·49 N_2+0·70 O_2 ...	7·02	6·2	1915	8590	7370	92·0	8·0
8·16 CO+5·36 H_2+6·76 O_2	78·05 A+0·57 N_2+1·10 O_2 ...	7·06	6·0	1925	8560	7442	92·9	7·1
8·15 CO+5·35 H_2+6·75 O_2	77·18 A+0·57 N_2+2·00 O_2 ...	7·02	6·1	1910	8550	7410	92·8	7·2
8·03 CO+5·27 H_2+6·65 O_2	76·50 A+0·53 N_2+3·02 O_2 ...	6·95	6·4	1885	8435	7289	92·8	7·2
8·00 CO+5·24 H_2+6·62 O_2	74·55 A+0·56 N_2+5·03 O_2 ..	6·90	6·0	1870	8410	7327	93·1	6·9
8·40 CO+5·50 H_2+6·95 O_2	71·05 A+0·57 N_2+7·53 O_2 ...	7·03	5·2	1915	8820	7740	93·0	7·0
8·41 CO+5·51 H_2+6·96 O_2	68·70 A+0·43 N_2+9·99 O_2 ...	6·96	5·0	1900	8825	7830	93·7	6·3

energy decreases and appears to reach sensibly steady values for excess oxygen contents greater than about 1·5 per cent.

We have in a previous paper referred to the interesting discovery of Wohl and Von Elbe of the effect of water vapour in hydrogen explosions, and suggested, in view of our heat loss measurements in wet and dry hydrogen

Fig. 2.

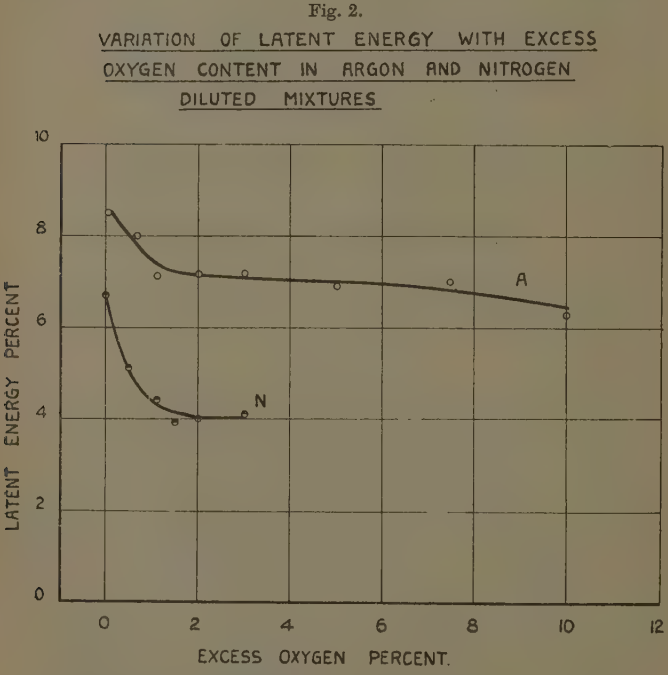

explosions, that the effect of the water vapour is to decrease the latent energy *. With this and the results shown in Tables III. and IV. in mind we hope to extend our experiments in the near future.

Conclusions.

Large vessel explosion experiments have been described in which the long-lived latent energy left in the exploded

* Phil. Mag. xviii. p. 311.

gases has varied between the limits 1·1 per cent. of the heat of combustion and 8·5 to 9·1 per cent. of the heat of combustion. The smaller value was obtained in an over-rich $CO–O_2$ mixture exploded at 3 atmospheres initial pressure, and the larger values in an argon diluted CO mixture at $\frac{1}{2}$ atmosphere pressure, and in a pentane air mixture at $\frac{1}{4}$ atmosphere initial pressure. Doubtless the smaller value would be decreased still further in explosions at higher initial pressures and the higher values increased in explosions at lower initial pressures.

The amount of latent energy obtaining in exploded gaseous mixtures varies with

(i.) the nature of the combustible gas,
(ii.) the nature of the diluent gas, and
(iii.) the initial pressure of the mixture before the explosion.

This is entirely in line with the deductions made in regard to latent energy in constant pressure combustion as deduced from platinum thermometry measurements *. In the case of constant pressure combustion there is, however, a much greater latent energy than in our large vessel explosions. We think that the reason for this is that combustion becomes more efficient, or, in other words, latent energy becomes less with distance of travel of the flame front †, for it is known that latent energy decreases with increase in the pressure at which combustion takes place and the instantaneous pressure in the flame front increases with distance of travel from the igniting source.

XLIII. *Lebesgue Complex Integration and Generalized Differentiation.* *By* W. Fabian, *M.A.*, *Ph.D.*‡

1. *Introduction.*

In the present paper we extend the theory of Riemann integration of functions of a complex variable. The principle of this extension is based on Lebesgue's theory of integration § of functions of a real

* Phil. Mag. xxi. p. 280 (1936).
† 'The Engineer,' 3rd April, 1936.
‡ Communicated by the Author.
† Lebesgue, *Annali di Mat.* (III *a*) vii. p. 258 (1902).

variable, and depends, like the latter, on the idea of the measure of a set of points. We begin therefore with a discussion of sets of points, which lie on curves in the complex plane. The theory of sets of points on the real axis, which has been developed by Borel *, Lebesgue †, and W. H. Young ‡, is used as a basis in this discussion.

In the fourth section we deal with the inverse operation of Lebesgue integration over sets of points, of which no theory whatever has as yet been given. We then employ the processes of generalized integration and differentiation for expanding functions in a series of terms containing the generalized differential coefficients studied in this paper.

2. *Sets of Points in the Complex Plane.*

(*a*) The curves which we shall use in this section will be bounded simple curves l, defined by

$$z=x+iy=x(t)+iy(t),$$

where $x(t)$ and $y(t)$ are continuous monotonic one-valued functions of a real parameter t for all values of t such that $t_0 \leqslant t \leqslant \mathrm{T}$, where t_0 and T are finite; and $x(t)+iy(t)$ does not assume the same value for any two different values of t in the range $t_0 \leqslant t \leqslant \mathrm{T}$.

The following notation will be used:—$\mathrm{E}(l)$ denotes a set of points on l; E_x and E_y are the sets of points corresponding to $\mathrm{E}(l)$ in the intervals $\{x(t_0),\ x(\mathrm{T})\}$, and $\{y(t_0),\ y(\mathrm{T})\}$ respectively; s denotes the length of that arc of l which corresponds to the interval $(t_0,\ t)$; and $s=\mathrm{S}$ when $t=\mathrm{T}$. E_s is the set of points corresponding to $\mathrm{E}(l)$ on the s-segment (O, S).

$\mathrm{E}(l)$ will be said to be measurable if E_x and E_y are measurable, and its measure $m[\mathrm{E}(l)]$ will be defined as §

$$m[\mathrm{E}(l)]=m(\mathrm{E}_x)+im(\mathrm{E}_y).$$

Theorem 1.—*If* $m[\mathrm{E}(l)]=0$, *then* $m(\mathrm{E}_s)=0$, *and conversely.*

This follows immediately from the fact that, in either case, the points composing $\mathrm{E}(l)$ or E_s are finite in number

* Borel, 'Leçons sur la théorie des fonctions' (1898).

† Lebesgue, *Annali di Mat.* (III.) vii. p. 231 (1902); 'Leçons sur l'intégration' (1904).

‡ W. H. Young, Proc. Lond. Math. Soc. (2) ii. p. 25 (1905).

§ $m(\mathrm{E}_x)$ and $m(\mathrm{E}_y)$ denote the measures of E_x and E_y respectively. Similarly, $m(\mathrm{E}_s)$ will be used to denote the measure of E_s when E_s is measurable.

or enumerably infinite, and hence form a set of measure zero on l and the s-segment under either hypothesis.

Hence :

Theorem 2.—*If* $\mathrm{E}(l)$ *is measurable, then* E_s *is measurable, and conversely.*

(*b*) A function $f(z)$ will be said to be measurable in $\mathrm{E}(l)$ if the real functions P and Q, where $\mathrm{P}+i\mathrm{Q}=f(z)$, are measurable in E_x and in E_y.

Theorem 3.—*If* $f(z)$ *is measurable in* $\mathrm{E}(l)$, *then* $f(z)$ *is measurable in* E_s, *and conversely.*

Proof.—I. Under the first hypothesis P and Q are measurable in E_x and E_y. Hence the sets of points in E_x and E_y, for which $\mathrm{P}>\mathrm{A}$, are measurable for every constant A. By theorem 2 the set of points in E_s, for which $\mathrm{P}>\mathrm{A}$, is measurable for every constant A. P is therefore measurable in E_s. Similarly Q, and hence $f(z)$, is measurable in E_s.

II. Under the second hypothesis the set of points in E_s, for which $\mathrm{P}>\mathrm{A}$, is measurable for every constant A. By theorem 2 the sets of points in E_x and E_y, for which $\mathrm{P}>\mathrm{A}$, are measurable for every constant A. Hence P is measurable in E_x and E_y. Similarly Q is measurable in E_x and E_y.

The theorem is proved.

3. *Lebesgue Complex Integration.*

(*a*) Let $\mathrm{E}(\mathrm{L})$ be a set of points on a simple curve L, which is defined by *

$$z=x(t)+iy(t),$$

and let E_t be the set of points corresponding to $\mathrm{E}(\mathrm{L})$ on the t-segment. We define the integral $\int_{\mathrm{E}(\mathrm{L})} f(z)\,dz$, taken over the set $\mathrm{E}(\mathrm{L})$, by

$$\int_{\mathrm{E}(\mathrm{L})} f(z)\,dz = \int_{\mathrm{E}_t} \mathrm{P}\,dx(t) - \int_{\mathrm{E}_t} \mathrm{Q}\,dy(t) + i\int_{\mathrm{E}_t} \mathrm{Q}\,dx(t) + i\int_{\mathrm{E}_t} \mathrm{P}\,dy(t),$$

* $x(t)$ and $y(t)$ need not be monotonic in this definition.

if each of these Lebesgue-Stieltjes integrals *, taken over E_r', exists.

The curves L, which we shall use here, will be such that they can be broken up into a finite number of bounded simple curves l, as defined in section 2, for each of which $x(t)$ and $y(t)$ are monotonic functions of t. If L be divided up into N such arcs l_r, and $E(l_r)$ be the set consisting of all points of E(L), which lie on l_r, then E(L) will be said to be measurable if each of the components $E(l_r)$ is measurable, and its measure $m[E(L)]$ will be defined as

$$m[E(L)] = \sum_{r=1}^{N} m[E(l_r)].$$

$f(z)$ will be said to be measurable in E(L) if $f(z)$ is measurable in each of the components $E(l_r)$.

From the known properties † of Lebesgue-Stieltjes integrals it follows that, if $f(z)$ is integrable over the measurable set E(L), then $f(z)$ is integrable over each of the components $E(l_r)$, and

$$\int_{E(L)} f(z)\,dz = \sum_{r=1}^{N} \int_{E(l_r)} f(z)\,dz.$$

Conversely, if each of the integrals $\int_{E(l_r)} f(z)\,dz$ exists, then $\int_{E(L)} f(z)\,dz$ exists in accordance with our definition.

We shall therefore continue to use the curve l in this section, as the theorems we shall establish here can be immediately extended to the general case for the curve L.

To prove the fundamental theorem of the calculus for the complex Lebesgue integral the following theorem will be required :—

Theorem 4.—*If* $f(z)$ *is integrable over a measurable set of points* $E(l)$, *then*

$$\int_{E(l)} f(z)\,dz = \int_{E_s} f(z)\frac{dz}{ds}\,ds.$$

* Hildebrandt, Bull. Amer. Math. Soc. (2) xxiv. p. 191 (1918). Also Hobson, 'Theory of Functions of a Real Variable,' vol. i. (1927) ch. vii. The properties of the Lebesgue integral for a real variable, in terms of which the Lebesgue-Stieltjes integral is defined, are fully discussed here.

† *Loc. cit.*

Proof.—Let $f_1(z)=P_1+iQ_1$, where P_1 and Q_1 are real, be a function which is equal to $f(z)$ at all points of $E(l)$ and zero at all other points of l. Then

$$\int_{E(l)} f(z)\,dz = \int_l f_1(z)\,dz$$

$$= \int_{t_0}^{T} P_1\,dx(t) - \int_{t_0}^{T} Q_1\,dy(t) + i\int_{t_0}^{T} Q_1\,dx(t) + i\int_{t_0}^{T} P_1\,dy(t),$$

where each of these integrals exists. By theorem 1 there corresponds to every set of points on the s-segment (O, S), of measure zero, a set of points on the x-segment $\{x(t_0), x(T)\}$, of measure zero. Hence

$$x = x(t_0) + \int_0^s \frac{dx}{ds}\,ds$$

in $(0 \leqslant s \leqslant S)$. We have therefore

$$\int_{t_0}^{T} P_1\,dx(t) = \int_0^S P_1 \frac{dx}{ds}\,ds\,;$$

consequently

$$\int_{E_t} P\,dx(t) = \int_{E_s} P\frac{dx}{ds}\,ds,$$

where E_t corresponds to $E(l)$.

Similarly,

$$\int_{E_t} Q\,dx(t) = \int_{E_s} Q\frac{dx}{ds}\,ds,$$

$$\int_{E_t} P\,dy(t) = \int_{E_s} P\frac{dy}{ds}\,ds,$$

$$\int_{E_t} Q\,dy(t) = \int_{E_s} Q\frac{dy}{ds}\,ds.$$

Hence the conclusion.

If $$F(z)-F(z_0) = \int_{z_0}^{z} f(z)\,dz,$$

taken along l, exists everywhere on l as a complex Lebesgue integral, then $F(z)$ will be called the indefinite integral of $f(z)$, taken along l.

Theorem 5.—*The indefinite integral* $F(z)$ *of a function* $f(z)$, *taken along* l, *has a finite differential coefficient along* * l, *equal to* $f(z)$, *everywhere on* l *except possibly in a set of points of measure zero.*

Proof.—By Theorem 4,

$$F(z) = F(z_0) + \int_0^s f(z)\frac{dz}{ds}\,ds,$$

if $$z_0 = x(t_0) + iy(t_0).$$

Hence $$\frac{dF(z)}{ds} = f(z)\frac{dz}{ds},$$

and is finite almost everywhere in $(O \leqslant s \leqslant S)$. Consequently everywhere on l, except possibly in a set of points of measure zero,

$$\frac{dF(z)}{dz} \text{ (along } l) = \frac{dF(z)}{ds} \cdot \frac{ds}{dz}$$
$$= f(z).$$

(*b*) *Expression of* $\int_{E(l)} f(z)\,dz$ *as an integral along a continuous arc.*

To express $\int_{E(l)} f(z)\,dz$ as an integral of $f(z)$ along an arc, by means of which the inverse operation of integration over $E(l)$ will be investigated, we require two preliminary theorems.

Let $G(l)$ be a fixed measurable set of points on l. Let $E(l)$ be that component which consists of all points of $G(l)$ on the arc corresponding to (t_0, t). The variation of $E(l)$ with t, as t increases from t_0 to T, we shall refer to as the simple variation of $E(l)$ in $G(l)$ with respect to t. Consider the curve Ω, traced out in the w-plane by the point

$$w = \pm m(E_x) \pm im(E_y) = m_0[E(l)],$$

* By the differential coefficient $\frac{dF(z)}{dz}$ along l we mean

$$\lim_{h \to 0} \frac{F(z+h) - F(z)}{h},$$

where $h \to 0$ along l.

when $E(l)$ varies simply in $G(l)$ with respect to t; where the positive or negative signs in $\pm m(E_x)$ are taken, according as $x(t)$ is a non-diminishing or non-increasing function of t in (t_0, T), and the positive or negative signs in $\pm im(E_y)$ are taken, according as $y(t)$ is a non-diminishing or non-increasing function of t in (t_0, T).

The curve Ω is a simple curve, for the sets $E(l)$ and E^s are measurable for every value of t as t increases from t_0 to T, and $m_0[E(l)]$ is a continuous function of $m(E_s)$. From theorem 1 it follows that there is a one-to-one correspondence between $m_0[E(l)]$ and $m(E_s)$. Hence the curve $w=m_0[E(l)]$, which can be defined by means of the parameter $m(E_s)$, is a simple curve.

Theorem 6.—*As $E(l)$ varies simply with respect to t in a measurable set of points $G(l)$, there corresponds to every measurable set of points e_z in $G(l)$ a measurable set of points e_w on the curve Ω and conversely, and the measures of the measurable sets e_z and e_w are equal.*

Proof.—I. First suppose that e_z is a measurable set of points in $G(l)$. A set e_w on Ω corresponds to e_z.

Let $\Delta_n(e_z)$ denote a set of non-overlapping sets of points $\delta_r(e_z)$ in $G(l)$, where every set $\delta_r(e_z)$ consists of all points common to $G(l)$ and an arc $\delta_r(z)$ of l, and $\Delta_n(e_z)$ is such that the points of e_z are common to all the sets of a sequence of sets $\Delta_n(e_z)$, each of which sets contains the next. On the curve Ω there corresponds to $\Delta_n(e_z)$ a set $\Delta_n(e_w)$ of non-overlapping arcs * $\delta_r(e_w)$, where $\delta_r(e_w)$ corresponds to $\delta_r(e_z)$, and $\Delta_n(e_w)$ is such that the points of e_w are common to all the sets of a sequence of sets $\Delta_n(e_w)$, each of which sets contains the next.

Let ce_z be the set of points consisting of all points of $G(l)$ which are not points of e_z, and let ce_w be the set of points on Ω, which corresponds to ce_z. Let $\Delta_n(ce_z)$ denote a set of non-overlapping sets of points $\delta_r(ce_z)$ in $G(l)$, where every set $\delta_r(ce_z)$ consists of all points common to $G(l)$ and an arc $\delta_r(z_r)$ of l, and $\Delta_n(ce_z)$ is such that the points of ce_z are common to all the sets of a sequence of sets $\Delta_n(ce_z)$, each of which sets contains the next. On Ω there corresponds to $\Delta_n(ce_z)$ a set $\Delta_n(ce_w)$ of non-overlapping arcs $\delta_r(ce_w)$, where $\delta_r(ce_w)$ corresponds to $\delta_r(ce_z)$, and $\Delta_n(ce_w)$ is such that the points of ce_w are common

* Arcs consisting of single points are included, and may be coincident.

to all the sets of a sequence of sets $\Delta_n(ce_w)$, each of which sets contains the next.

We have

$$\left.\begin{aligned} \mathrm{M}[\Delta_n(e_z)] &= \mathrm{M}[\Delta_n(e_w)] \\ \text{and} \qquad \mathrm{M}[\Delta_n(ce_z)] &= \mathrm{M}[\Delta_n(ce_w)], \end{aligned}\right\} \quad . \quad . \quad . \quad . \quad (1)$$

where $\mathrm{M}[\Delta_n(e_z)]$ is the sum of the measures of all the sets $\delta_r(e_z)$ of $\Delta_n(e_z)$, and $\mathrm{M}[\Delta_n(e_w)]$, $\mathrm{M}[\Delta_n(ce_z)]$, and $\mathrm{M}[\Delta_n(ce_w)]$ are similarly defined.

Since e_z is measurable,

$$\lim_{n\to\infty} \mathrm{M}[\Delta_n(e_z)] + \lim_{n\to\infty} \mathrm{M}[\Delta_n(ce_z)] = m(e_z) + m(ce_z)$$
$$= m[\mathrm{G}(l)],$$

which is the measure of Ω.

Hence, by (1),

$$\lim_{n\to\infty} \mathrm{M}[\Delta_n(e_w)] + \lim_{n\to\infty} \mathrm{M}[\Delta_n(ce_w)]$$

is equal to the measure of Ω,

so that
$$m(e_w) = \lim_{n\to\infty} \mathrm{M}[\Delta_n(e_w)]$$
$$= m(e_z), \quad \text{by (1).}$$

II.—The conclusion, when e_w is by hypothesis a measurable set of points on Ω, and e_z is the set in $\mathrm{G}(l)$ corresponding to e , follows in a similar manner.

We suppose here that $\Delta_n'(e_w)$ is a set of arcs $\delta_r'(e_w)$, without common points, on the curve Ω, where $\Delta_n'(e_w)$ is such that the points of e_w are common to all the sets of a sequence of sets $\Delta_n'(e_w)$, each of which sets contains the next. In $\mathrm{G}(l)$ there corresponds to $\Delta_n'(e_w)$ a set $\Delta_n'(e_z)$ of non-overlapping sets of points $\delta_r'(e_z)$, where $\delta_r'(e_z)$ corresponds to $\delta_r'(e_w)$, and $\Delta_n'(e_z)$ is such that the points of e_z are common to all the sets of a sequence of sets $\Delta_n'(e_z)$, each of which sets contains the next. If C_{ew} be the set of points on Ω consisting of all points of this curve, which are not points of e_w, let $\mathrm{C}e_z$ be the set in $\mathrm{G}(l)$, which corresponds to $\mathrm{C}e_w$. Let $\Delta_n'(\mathrm{C}e_w)$ be a set of arcs $\delta_r'(\mathrm{C}e_w)$ on Ω, without common points, where $\Delta_n'(\mathrm{C}e_w)$ is such that the points of $\mathrm{C}e_n$ are common to all the sets of a sequence of sets $\Delta'_n(\mathrm{C}e_w)$, each of which sets contains the next. In $\mathrm{G}(l)$ there corresponds to $\Delta_n'(\mathrm{C}e_w)$

a set $\Delta_n'(\mathrm{Ce}_z)$ of non-overlapping sets of points $\delta_r'(\mathrm{Ce}_z)$, where $\delta_r'(\mathrm{Ce}_z)$ corresponds to $\delta_r'(\mathrm{Ce}_w)$, and $\Delta_n'(\mathrm{Ce}_z)$ is such that the points of Ce_z are common to all the sets of a sequence of sets $\Delta_n'(\mathrm{Ce}_z)$, each of which sets contains the next.

As before,

$$\mathrm{M}[\Delta_n'(e_w)]=\mathrm{M}[\Delta_n'(e_z)]$$

and

$$\mathrm{M}[\Delta'_n(\mathrm{Ce}_w)]=\mathrm{M}[\Delta_n'(\mathrm{Ce}_z)],$$

and the conclusion follows exactly as in case I.

Theorem 7.—As $\mathrm{E}(l)$ *varies simply with respect to* t *in a measurable set of points* $\mathrm{G}(l)$, *there is a one-to-one correspondence between the points of* $\mathrm{G}(l)$ *and those of the curve* Ω, *except possibly for a set of points of measure zero.*

Proof.—$\mathrm{G}(l)$ consists at most of arcs $\delta_n z$ of non-zero measure and of sets of points e_r of measure zero, where e_r consists of all points common to $\mathrm{G}(l)$ and an arc $\Delta_r z$ of l, $\delta_n z$ and $\Delta_r z$ being such that, as the point z passes along l, z passes alternately through an arc $\delta_n z$ and an arc $\Delta_r z$.

On the curve Ω there corresponds to $\delta_n z$ an arc $\delta_n w$ of non-zero measure, and to e_r a point w_r. Since the point z passes alternately through an arc $\delta_n z$ and an arc $\Delta_r z$ in its passage along l, the points w_r are end-points of the arcs $\delta_n w$, and are common points to successive arcs $\delta_n w$. As none of the measures of $\delta_n w$ are zero, the points w_r are finite in number or enumerably infinite, and therefore form a set of measure zero. Hence, by theorem 6, the sum of the measures of all the sets e_r is zero. There is a one-to-one correspondence between the points of $\delta_n z$ and of $\delta_n w$, except possibly between the end-points of $\delta_n z$ and of $\delta_n w$, which belong to the sets e_r and the points w_r respectively.

The theorem is proved.

We can clearly deduce now the following theorem :—

Theorem 8.—If $f(z)$ *is measurable in* $\mathrm{G}(l)$, *then*

$$\int_{\mathrm{E}(l)} f(z)\,dz=\int_0^w \mathrm{F}(w)\,dw,$$

taken along Ω, *where* $f(z)=\mathrm{F}(w)$, *if either of these integrals exists.*

4. Generalized Differentiation.

(*a*) Let $\phi\{E(l)\}$ be a function of $E(l)$, where $E(l)$ consists of all points of the measurable set $G(l)$, which lie on the arc corresponding to (t_0, t). The generalized differential coefficient $D\phi\{E(l)\}$ of $\phi\{E(l)\}$ with respect to $E(l)$ will be defined by

$$D\phi\{E(l)\} = \frac{d\psi(w)}{dw} \quad \text{(along } \Omega\text{)},$$

where $\phi\{E(l)\} = \psi(w)$, if the latter differential coefficient exists.

If $$\phi\{E(l)\} = \int_{E(l)} f(z)\,dz$$

exists for all the sets $E(l)$ in $G(l)$, then $\phi\{E(l)\}$ will be called the generalized indefinite integral of $f(z)$ over $E(l)$.

We note that $f(z)$ in $G(l)$ is itself a function of $E(l)$ and may have a generalized differential coefficient at a point where it has not a differential coefficient with respect to z.

Theorem 9.—*Suppose that $E(l)$ varies simply with respect to t in a measurable set of points $G(l)$. Then the generalized indefinite integral*

$$\phi\{E(l)\} = \int_{E(l)} f(z)\,dz$$

of the measurable function $f(z)$, taken over $E(l)$, has a finite generalized differential coefficient with respect to $E(l)$, equal to $f(z)$, for all values of z in $G(l)$, except possibly for points z of a set of measure zero.

Proof.—By theorem 8,

$$\phi\{E(l)\} = \int_0^w F(w)\,dw,$$

taken along Ω, where $f(z) = F(w)$. Hence, by theorems 5 and 6, the conclusion follows.

(*b*) *Generalized Taylor Series.*

Let G(L) be a measurable set of points on the curve L, where L is defined by the segment $(t_0 \leqslant t \leqslant t_N)$ and consists of N arcs l_r, for each of which $x(t)$ and $y(t)$ are monotonic functions of t. E(L) denotes the set consisting of all

points of G(L) on the arc corresponding to (t_0, t). Suppose that E(L) consists of ρ components $E(l_r)$, where $E(l_r)$ is the set consisting of all points of E(L) on the arc l_r. We define a curve $\overline{\Omega}$ in the w-plane by

$$w = \sum_{r=1}^{\rho} m_0[E(l_r)] = m_0[E(L)],$$

where $$m_0[E(l_r)] = \pm m(E_{r,x}) \pm im(E_{r,y})$$

as defined in section 3 (*b*) for curves l, $E_{r,x}$ and $E_{r,y}$ being the sets of points corresponding to $E(l_r)$ on the x- and y-segments respectively.

For a position $e(L)$ of E(L)

$$D\phi\{e(L)\} = \lim. \frac{\phi\{E(L)\} - \phi\{e(L)\}}{m_0[E(L)] - m_0[e(L)]},$$

when $m_0[E(L)] \to m_0[e(L)]$, if this limit exists and is the same for both directions in which E(L) passes into the position $e(L)$.

$Ee(L)$ will be used to denote the set of points in E(L) which are not points of $e(L)$, or the set of points in $e(L)$ which are not points of E(L), according as E(L) contains $e(L)$ or is contained in $e(L)$.

Theorem 10.—*Let* $\phi\{E(L)\}$ *and all its generalized differential coefficients* $D^n\phi\{E(L)\}$ *be one-valued continuous functions of* E(L) *in the measurable set* G(L). *If*

$$\lim_{n\to\infty} \int_{Ee(L)} [D^n\phi\{E(L)\}]\, dz^n = 0,$$

where $e(L)$ *is one of the sets* E(L), *then*

$$\phi\{E(L)\} = \sum_{n=0}^{\infty} \frac{D^n\phi\{e(L)\}}{n!} \{m_0[E(L)] - m_0[e(L)]\}^n.$$

Proof.—

Since $$\phi\{E(L)\} = \psi(w)$$

and $$D^n\phi\{E(L)\} = \psi^{(n)}(w) \qquad (\text{along } \overline{\Omega}),$$

are continuous on $\overline{\Omega}$, the Lebesgue integrals

$$\int_a^w (w-\tau)^n \psi^{(n)}(\tau)\, d\tau$$

($n=0, 1, 2, \ldots n, \ldots$), taken along $\overline{\Omega}$, where $a=m_0[e(\mathrm{L})]$, exist also as Riemann integrals *, and are equal to them respectively. Hence

$$\phi\{\mathrm{E}(\mathrm{L})\} = \frac{d}{dw}\int_a^w \psi(\tau)\,d\tau$$

(the integration and differentiation being along $\overline{\Omega}$)

$$= \sum_{n=0}^{p-1} \frac{\psi^{(n)}(a)}{n\,!}(w-a)^n + \frac{1}{p\,!}\frac{d}{dw}\int_a^w (w-\tau)^p \psi^{(p)}(\tau)\,d\tau$$

(on integrating $\int_a^w \psi(\tau)\,d\tau$ by parts p times)

$$= \sum_{n=0}^{p-1} \frac{\psi^{(n)}(a)}{n\,!}(w-a)^n + \int_a^w \psi^{(p)}(\tau)\,d\tau^p$$

(on integrating $\int_a^w (w-\tau)^p \psi^{(p)}(\tau)\,d\tau$ by parts p times).

The conclusion follows by theorem 8.

XLIV. *Notices respecting New Books.*

Reports on Progress in Physics.—Vol. II. Published by the Physical Society (London) and printed at the University Press, Cambridge, 1935. [Pp. iv+371.] (Price to Non-Fellows of the Society 21*s.* net., to Fellows 12*s.* 6*d.* net.)

This is the second volume of the series of annual reports which was started last year. It consists of 371 pp. dealing with the contents of 1284 papers which were either published during the year 1935 or have a bearing on such publications. It is possible to do little but mention the contents and the editors responsible for them, viz.:—General Physics (A. Ferguson); Quantum Theory (G. Temple); Atomic Physics (N. Feather); Geophysical Prospecting (E. Lancaster-Jones); Radio exploration of upper Atmospheric ionization (E. V. Appleton); Sound (E. G. Richardson); Heat (J. H. Awbery); Electric and Magnetic Measurements (L. Hartshorn); The Charge on the Electron (H. R. Robinson);

* Although $\overline{\Omega}$ may cross itself, the theory of integration along simple curves applies here, since $\overline{\Omega}$ consists of a finite number of such curves. The complex Riemann integral is fully discussed in Watson's 'Complex Integration and Cauchy's Theorem.'

Electron Tubes (G. I. Finch); X-rays (G. W. C. Kaye); Spectroscopy (H. Dingle); and Optics (T. Smith).

When we consider that the work discussed in this Report is mainly for the single year (1935) it gives an idea of the amazingly detailed advance that is being made in many branches of physics.

The following quotations (picked out almost at random) will serve to illustrate the usefulness of the various discussions:—"Within the short space of twenty years the spectra of practically all the elements have been elucidated, yielding information on the electronic configurations of the atoms. The spectra of over 150 diatomic molecules have already been analyzed, but hitherto the progress made with spectra of polyatomic molecules has been disappointingly slow." (G. B. B. Sutherland.)

"In connection with the specific heats of gases it is surprising to note that the specific heat of argon has never been measured above 25° C. Heuse measured it from −180° to room temperature, and found a linear *decrease* of 5 per cent. Since it is assumed in the explosion method that its value at 2000° C. is the theoretic value, there seems good reason for an immediate experimental investigation at some elevated temperature." (J. H. Awbery.)

With regard to general editing, some more uniformity should be introduced in connexion with "references." The various contributions are usually divided into sections. Some editors give the references at the end of their group of sections and number continuously for the whole *group*. Some collect the references at the end but start the enumeration afresh for each *section*. More uniformity is needed in the system that is to be adopted. It is most convenient to a reader if the references for each *section* are gathered together at the end of the section in question, and are numbered accordingly.

Probability and Random Errors. By W. N. Bond. [Pp. 141 and viii.] (Edward Arnold & Co., London. Price 10*s.* 6*d.*)

This book is intended for the experimenter whose knowledge of mathematical methods is limited. The writer does not set out a number of rules of thumb to be used automatically, however, but discusses fundamental ideas in detail, so that the reader may understand completely the principles he applies.

The early chapters deal with problems in probability, and serve to introduce the subject of random errors. After a description of the types of error arising in observations, methods of estimating errors and Chauvenet's criterion for the rejection of data are discussed. The methods to be adopted when combining the results of different observations are then

considered at some length, and the concluding chapters include the problems of correlation and curve fitting.

The book contains many worked-out examples, and is recommended particularly to students of Physics or Chemistry, to whom it should prove invaluable.

The Optical Basis of the Theory of Valency. By R. DE L. KRONIG. [Pp. 237+67 figs.] (Cambridge Series of Physical Chemistry. Price 16*s.* net.)

THIS excellent book, by the author of "Band Spectra and Molecular Structure," is bound to find a ready welcome from all who wish to become acquainted with the subject of molecular structure.

It is not an easy book to read—and this on no account because the writer has not an adequate mastery of pen and subject—but because he has compressed in so brief a space so large a subject. The reader, to understand, must either have been previously so well grounded in the mathematical essentials as to be able to appreciate at a glance the formulæ given, or he must be prepared to look up details in the numerous references which are lavishly put at his disposal.

The aim of the book should be well achieved—to present to the chemist a coherent picture of the progress in knowledge of the nature of chemical valency achieved to so large an extent by the application of purely physical methods.

Such a picture is also required by physicists who may not themselves be working directly on the problem—and to such also will this book be found most useful.

The first few chapters summarize the results, to date, of scattering experiments of X-rays and electrons in terms of molecular configuration. Naturally negative charge distribution and internuclear distances both come into this picture.

Then come chapters on atomic and molecular spectra and their interpretation in terms of molecular structure. The theories of chemical binding associated with the names Heitler and London, Slater and Pauling, Hund and Mullikan are adequately discussed.

There is a final most useful chapter on optical and thermal dissociation.

An exceptionally good feature of this most useful book is the bibliography given at the end of each chapter. There are more than two hundred references to recent literature on the subject.

[*The Editors do not hold themselves responsible for the views expressed by their correspondents.*]

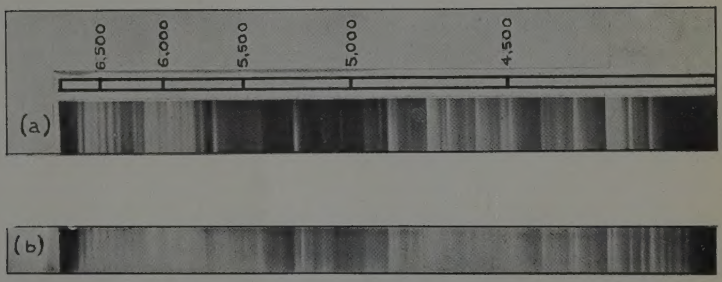

Spectrograms of carbon cold cathode arc in high vacuum.

(*a*) Electrical discharge.
(*b*) Arc.